IMMUNE EVASION AND DISEASE MECHANISMS IN ROSS RIVER VIRUS INFECTION

Ali ZAID, BSc(Hons)

A Thesis submitted for the degree of Doctor of Philosophy (PhD)

Department of Biomedical Sciences

University of Canberra,

August, 22nd 2008

Supervisor: Pr. Suresh Mahalingam

Acknowledgements

I would like to thank my supervisors Pr. Suresh Mahalingam for supervision, guidance and advice and for providing me with Enbrel; Dr. Michael Frese, whose support, knowledge and experience were most appreciated throughout my PhD. I also would like to thank Pr. Andreas Suhrbier (QIMR) for his kind gift of luciferase plasmids, as well as Hilary Warren (Canberra Hospital) for the PK136 hybridomas.

I would like to express my gratitude to all the people who helped me, in particular Dr. Luby Simson for helping me with student affairs as well Drs. Ezequiel Rulli, Cristina Musso, Brett Lidbury, Jasjit Johal and Ruben Ramirez for ever-stimulating interaction inside and outside of the lab; Sandra Thomas and Dr. Michelle Nelson for their time spent reading my thesis, Dr Donna Easton, Dijana Townsend, Jade Podger, and the myriads of students, post-docs and technical staff for assistance and camaraderie.

I am particularly grateful to the dedicated staff at the Postgraduate Research Office, Ms. Cath Raby Jennie Robens, Jennifer Towie Dr. Michelle Fleming and Pr. Sue Thomas and Bill Maher who all helped me throughout my PhD.

Histological sections were performed by Ms. Anne Prins at the Histology Department of the John Curtin School of Medical Research (ANU). The DIG-labelled RRV riboprobe was constructed and optimised by Dr. Cristina Musso. I would like to thank Dr. Jasjit Johal for invaluable help in western blotting and *in situ* hybridisation. I would like to thank Mrs Gillian Nolan and Daniel Ramirez for assistance and maintenance of the animal house.

Finally, I owe a debt of gratitude to my mother, father, siblings and partner who accompanied me from the very beginning.

Abstract

Ross River virus (RRV) is an Alphavirus distributed throughout Australia. It is transmitted by mosquitoes and is known to cause moderate to severe disease symptoms in humans. Along with other alphaviruses such as Sindbis virus and Chikungunya virus, RRV is known to cause arthritic symptoms, characterised by muscle and joint inflammation. Several investigations have established the role of macrophage cells and pro-inflammatory host factors in the development of RRV-induced disease.

In this study, we attempted to determine differences between RRV passaged in mammalian and mosquito cells. There is strong evidence that arthropod-borne viruses are able to display enhanced infectivity when passaged into arthropod cell line. We showed that mosquito cell-derived RRV (mos-RRV) was able to replicate to higher titres than mammalian cell-derived RRV. We also showed that mos-RRV failed to induce Type I IFN-associated antiviral responses.

The second aim of this study was to investigate the role of TNF-α, a pro-inflammatory cytokine implicated in arthritic diseases, in the development of RRV disease. We treated RRV-infected C57BL/6J mice with a commercially available TNF-α inhibitor drug and monitored disease signs. We found that the TNF-α inhibitor does not ameliorate RRV disease (RRVD) symptoms, and that it does not prevent muscle and joint inflammation. We analysed histological sections of muscle and joint tissue of Enbrel-treated and untreated, RRV-infected cells. We also determined and compared host cytokine expression profiles.

Finally, we sought to determine the requirement for natural killer (NK) cells in RRV disease. NK cells have been detected in the synovium of RRV-infected patients since early studies, but their role in disease pathogenesis remains unclear. Using a NK-dysfunctional mouse (C57BL/6J-Lyst^{bg}), we showed that mice lacking a functional NK system are more susceptible to RRV disease than wild-type, C57BL/6J mice. We monitored disease symptoms following RRV infection and assessed muscle and joint inflammation in Lyst^{bg} and C57BL/6J mice.

This thesis examines mechanisms of viral infection and immune evasion employed by RRV, as well as into the role of host cells and cytokines in RRVD pathogenesis disease mechanisms. We showed that a functional NK cell system is required for the regulation of RRV-induced muscle and joint inflammation. Our characterisation of the use of a commercial TNF-α inhibitor in RRV-induced

disease in mice may provide information on the role of TNF-α in viral arthritis, and may help towards developing safe and effective treatment.

Publications

Zaid A, Rulli NE, Johal J, Nelson MA, Mahalingam S (in preparation) "Differential antiviral signaling and infectivity in a macrophage cell line infected with mammalian or mosquito cell-derived Alphavirus" to be submitted in *Journal of Virology*

Zaid A, Rulli NE, Mahalingam S (in preparation) "Enbrel, a TNF-α inhibitor, exacerbates alphavirus-induced myositis in a mouse model" to be submitted in *Arthritis and Rheumatism*

Zaid A*, Tupanceska D*, Rulli NE, Thomas S, Lidbury BA, Mattahei KL, Ramirez RD and Mahalingam S (2007) Ross River virus: an arthrogenic alphavirus of significant importance in the Asia Pacific. In Lal SK, (*editor*) *Emerging Viral Diseases of Southeast Asia*, **4:**94-111 *(* joint 1st authors*)

Rulli NE, Suhrbier A, Hueston L, Heise MT, Tupanceska D**, Zaid A**, Wilmes A, Lidbury BA and Mahalingam S (2005) Ross river virus: molecular and cellular aspects of disease pathogenesis, *Pharmacology and Therapeutics*, **107(3):**329-342

Public presentations

Ali Zaid, Nestor E. Rulli, Jasjit Johal, Reed S. Shabman, Mark T. Heise and Suresh Mahalingam (**2007**) *Differential Induction of Type I Interferon Responses in Macrophages and Dendritic Cells by Mosquito and Mammalian Cell-Derived Alphaviruses*, 4th Australian Virology Group (AVG) conference (2007); Australian Society for Medical Research (ASMR) Young Investigator Forum (2008)

Table of Contents

1. **LITERATURE REVIEW**

Overview……....*p1*

1.1 Ross River virus: an arthrogenic alphavirus.. ……*p3*

1.1.1 History and discovery of RRV …….....*p3*

1.1.2 RRV phylogenetics and genome organization ……...*p3*

1.1.2.1 Alphavirus and RRV taxonomy …….....*p4*

1.1.2.2 Genome oranisation and virion structure …….....*p6*

1.1.3 RRV epidemiology and distribution ……....*p10*

1.2 RRV disease: an inflammatory arthropathy ……...*p12*

1.2.1 Ross River virus disease (RRVD): clinical findings …….……...…...*p12*

1.2.2 RRV pathogenesis and mechanisms of inflammation ……..…...*p13*

1.2.2.1 Cells in RRVD: a focus on macrophages ...……....*p13*

1.2.2.2 Host factors in inflammatory arthritis ……..*p15*

1.2.3 Natural Killer (NK) cells in inflammatory arthropathies ……*p17*

1.3 Cytokines in viral infection ……*p18*

1.3.1 Pro-inflammatory cytokines ……*p18*

1.3.2 Cytokines in inflammation: a focus on TNF-α ……*p19*

1.3.2.1 TNF-α in inflammatory disorders ……*p19*

1.3.2.2 TNF-α signalling pathways …….....*p20*

1.3.2.3 TNF-α inhibition therapies in inflammatory diseases……..*p21*

1.3.2.4 TNF-α in viral infections ……...……....*p22*

1.3.3 Antiviral host response mechanisms: the Interferons …….....*p25*

1.3.3.1 Induction of Type I Interferon signalling pathways …….....*p25*

1.3.3.2 Type I IFN pathway: an overview of Jak/Stat signalling ……....*p28*

1.3.3.3 Interference with host antiviral pathways ……*p30*

1.3.3.4 Cell membrane interactions: a focus on mosquito cell-derived viruses ……*p32*

1.4 Thesis objectives ……...…*p35*

2. MATERIALS AND METHODS

2.1 Cell culture ……..…*p36*

2.2 Virus propagation ……...……*p36*

2.3 Cell treatment ……...……...*p37*

2.4 Monoclonal antibody purification ……...……*p37*

2.5 SDS-PAGE and Western Blotting ……..……*p38*

2.6 Luciferase reporter systems ……..……*p39*

2.7 Mice: Strains, handling and disease score ……..…*p39*

2.8 mRNA extraction and quantitative real-time PCR ……...……*p42*

2.9 Flow cytometry ……..……*p44*

2.10 Differential cell staining ……..……*p44*

2.11 Fluorescence microscopy ……...…….*p45*

2.12 RRV riboprobe preparation and *in situ* hybridisation ……...……*p45*

3. RESULTS PART I: CHARACTERISATION OF MAMMALIAN CELL- AND MOSQUITO CELL-DERIVED ROSS RIVER VIRUS

3.1 Introduction ……*p47*

3.2 Results ……*p48*

3.2.1 mos-RRV replicates to higher titres in RAW264.7 & JAWSII cells *p48*

3.2.2 mam- and mos-RRV replication kinetics in Vero and L929 cells *p49*

3.2.3 mos-RRV displays higher infectivity in RAW264.7 cells as assessed by immunofluorescence …….....*p53*

3.2.4 Infectivity of mam- and mos-RRV in Vero cells ……*p58*

3.2.5 Restoration of mam-RRV phenotype …….……..*p58*

3.2.6 mos-RRV induces lower levels of IFN-β mRNA compared to mam-RRV ……*p62*

` 3.2.7 mos-RRV induces lower activation of antiviral factors ……*p62*

3.2.8 Transcription of IFN-associated genes is reduced following mos-RRV infection ……..……...*p66*

3.3 Discussion ……*p69*

3.3.1 Differential replication kinetics of mam- and mos-RRV infection ...*p70*

3.3.2 Differential infectivity in RAW264.7 and Vero cells……*p71*

3.3.3 Differential induction of Type I IFN by mos-RRV ...……*p72*

3.3.4 Differential activation of transcription factors ……*p73*

3.3.5 Differential Type I IFN-associated promoter transcription ……*p74*

4. RESULTS PART II: IN VIVO RRV STUDIES: TREATMENT OF RRV-INDUCED DISEASE IN MICE WITH ENBREL, A TNF-α INHIBITOR

4.1 Introduction ……*p76*

4.1.1. RRV-induced disease: role of cells and soluble host factors …….*p76*

4.1.2. Cytokines in arthritis: a focus on TNF-α …….....*p78*

4.2 Results …….....*p79*

4.2.1 Effect of Enbrel treatment on RRV disease ……*p79*

4.2.2 Viral titres in tissue of RRV-infected mice ……*p81*

4.2.3 Histological analysis of muscle and joint tissue ……*p81*

4.2.4 Quantitation of inflammatory cell infiltrates ……..*p84*

4.2.5 Differential analysis of host factor expression ……*p92*

4.3 Discussion ……..*p92*

4.3.1 Enbrel treatment in RRV-induced disease ……..*p93*

4.3.2. TNF-α inhibition therapy in rheumatic diseases ……*p94*

4.3.4. Possible mechanisms of RRVD pathogenesis: a role for TNF-α …...*p95*

5 RESULTS PART III: THE ROLE OF NK CELLS IN RRVD PATHOGENESIS

5.1 Introduction ……*p98*

5.2 Results ……*p100*

5.2.1 RRV-induced disease in 20 day-old Lyst^{bg} mice ……..*p100*

5.2.2 Viral replication in muscle and joint tissue ……..*p103*

5.2.3 Histological analysis of RRV-infected muscle and joint tissue ……*p104*

5.2.4 Composition of cellular infiltrates in RRV-infected Lyst^{bg} and C57BL/6J mice …….....…….*p104*

5.2.5 Expression of host factors in RRV-infected Lyst^{bg} & C57BL/6J mice ……..*p110*

5.2.6 Depletion of NK cells using NK1.1 antibody (PK136*)* ***…….....p114***

5.3 Discussion ……***p118***

6 DISCUSSION

6.1 Discussion ……***p123***

6.2 Conclusions ……***p132***

7. BIBLIOGRAPHY ……....*p133*

List of Figures:

Introduction

Figure 1.1 Phylogenetic tree of Alphaviruses based on amino acid sequence comparison

Figure 1.2 Diagram of RRV genome structure.

Figure 1.3 Life cycle of RRV in vertebrate cells

Figure 1.4 Proposed mechanisms of RRV disease pathogenesis.

Figure 1.5 Schematic of Type I IFN signalling pathways.

Figure 1.6 An overview of antiviral pathways and viral evasion mechanisms.

Materials and Methods

Figure 2.1 Maps of the reporter luciferase plasmids used in *in vitro* experiments

Results Part I

Figure 3.1 Viral titres following infection of RAW264.7 (A) and JAWSII (B) cells with mam- and mos-RRV (1.0 MOI)

Figure 3.2 Viral titres following infection of Vero (A) and L929 (B) cells with mam- and mos-RRV (1.0 MOI)

Figure 3.3 Immunofluorescent labelling of RRV in mam- and mos-RRV-infected RAW264.7 cells (A) and Fluorescence cell count (B)

Figure 3.4 Immunofluorescent labelling of RRV in mam- and mos-RRV-infected Vero cells (A) and Fluorescence cell count (B)

Figure 3.5 A single passage of mos-RRV in mammalian Vero cells restores the mam-RRV phenotype following infection of RAW264.7 cells
Figure 3.6 Relative expression of IFN-β in mam- or mos-RRV-infected RAW264.7 (A) and JAWSII (B) cells
Figure 3.7 Western blot analysis of Stat-1 and PKR expression in RAW264.7 cells infected with mam- or mos-RRV at 6 hpi
Figure 3.8 Western blot analysis of nuclear IRF-3 in RAW264.7 cells following mam- or mos-RRV infection at 6 hpi
Figure 3.9 Figure 3.9: Luciferase reporter gene expression following mam- or mos-RRV infection in JAWSII-*pISRE(9-27)Lucter* cells.
Figure 3.10 Figure 3.10: Luciferase reporter gene activity at 6 hpi in RAW264.7-*pIFΔ(-125/+72)Lucter* cells following mam- or mos-RRV infection.

Results Part II

Figure 4.1 RRV disease in RRV-infected and Enbrel-treated (designated RRV-Enbrel) C57BL/6J mice
Figure 4.2 Survival and viral load
Figure 4.3 Histological analysis of muscle tissue of RRV-infected and RRV-Enbrel C57BL/6J mice at 10 dpi
Figure 4.4 Histological analysis of joint synovium of RRV-infected and RRV-Enbrel C57BL/6J mice at 10 dpi
Figure 4.5 Differential leukocyte cell count of muscle and joint tissue in RRV-infected and RRV-Enbrel C57BL/6J mice at 10 dpi
Figure 4.6 Expression of pro-inflammatory cytokines in muscle (A) and joint (B) of RRV-infected and and RRV-Enbrel mice at 10 dpi

Results Part III

Figure 5.1 RRV disease in 20 day-old Lyst^{bg} and C57BL/6J mice
Figure 5.2 Survival plot for RRV infected Lyst^{bg} and C57BL/6J mice
Figure 5.3 RRV titres in tissue of RRV-infected Lyst^{bg} and C57BL/6J mice at 10 dpi
Figure 5.4 *In situ* hybridisation of RRV antigen in the quadriceps muscle of C57BL/6J and Lyst^{bg} mice at 10 dpi
Figure 5.5 *In situ* hybridisation of RRV antigen in the ankle joint of C57BL/6J and Lyst^{bg} mice at 10 dpi
Figure 5.6 Histological sections of RRV-infected muscle in 20 day-old Lyst^{bg} and C57BL/6J mice at 10 dpi
Figure 5.7 Histological sections joint tissue of RRV-infected 20 day-old Lyst^{bg} and C57BL/6J mice at 10 dpi
Figure 5.8 Flow cytometry analysis of cellular infiltrates in the muscle of 20 day-old Lyst^{bg} and C57BL/6J mice at 8 dpi
Figure 5.9 Expression of pro-inflammatory cytokines in muscle and joint of RRV-infected C57BL/6J and Lyst^{bg} mice at 10 dpi
Figure 5.10 Effect of NK cell depletion on RRV disease in 21 day-old C57BL/6J mice using a NK1.1 monoclonal antibody
Figure 5.11 Survival plot of RRV-infected, PK136-treated C57BL/6J mice
Figure 5.12 RRV titres in tissue of RRV-infected, PK136-treated mice at 10 dpi

List of abbreviations

ATCC	American type cell culture collection
BFV	Barmah Forest virus
CARD	Caspase-activated recruitment domain
cDNA	Complementary deoxyribonucleic acid
CEAE	Committee of Experimentation and Animal Ethics
CHIKV	Chikungunya virus
CREB	cAMP-response element-binding protein
DC-SIGN	Dendritic cell-specific ICAM-3 grabbing non-integrin
DEPC	Diethylpyrocarbonate
DHF	Dengue hemorrhagic fever
DMEM	Dulbecco's Minimal Essential Medium
dpi	Days post-infection
dsRNA	Double-stranded RNA
DTT	Dithiothreitol
DV	Dengue virus
EEEV	Eastern equine encephalitis virus
ELISA	Enzyme-linked immunoadsorbent assay
EPA	Epidemic polyarthritis
FCS	Foetal Calf Syndrome
FITC	Fluorescein-isothiocyanate
HCMV	Human cytomegalovirus
HIV	Human immunodeficiency virus
HKG	Housekeeping gene
HLH	Haemophagocytic lymphohistiocytosis
HPF	High power field
hpi	Hours post-infection
IFN	Interferon
IL	Interleukin
IPC	IFN-producing dendritic cells
IRF	Interferon regulatory factor
ISGF	Interferon –stimulated gene factor
ISRE	Interferon-stimulated response element
IU	International units
Jak-Stat	Janus Kinase/Signal transduction and activator of transcription
KUNV	Kunjin virus
LB	Luria broth
LPS	Lipopolysaccharide

mam-RRV	Mammalian cell-derived Ross River virus
MAS	Macrophage activation syndrome
MAVS	Mitochondrial antiviral signalling
MAYV	Mayaro virus
MCMV	Murine cytomegalovirus
MCP-1	Monocyte chemotactic protein-1
MIP-1α	Macrophage inflammatory protein-1α
MDA-5	Melanoma differentiation-associated gene-5
mos-RRV	Mosquito cell-derived Ross River virus
mRNA	Messenger-RNA
MV	Measles virus
MyD88	Myeloid differentiation factor-88
NBT/BCIP	Nitro-blue tetrazolium chloride/5-bromo-4-chloro-3'-indolyphosphate p-toluidine salt
NF-κB	Nuclear factor kappa-B
NK	Natural killer
nSP	Non-structural protein
NSW	New South Wales
ONNV	O'Nyong-Nyong virus
OPD	*o*-Phenylenediamine dihydrochloride
PBS	Phosphate buffer saline
PCR	Polymerase chain reaction
pDC	Plasmacytoid dendritic cells
PFU	Plaque forming units
PKR	RNA-dependent protein kinase
poly(I:C)	Polyinosine-polycytidylic acid
PVDF	Polyvinylidene difluoride
QIMR	Queensland Institute Medical Research
QLD	Queensland
RA	Rheumatoid arthritis
RANTES	Regulated upon activation and T cell-expressed and secreted
RIG-1	Retinoic acid-inducible gene-I
RNA	Ribonucleic acid
RPMI 1640	Roswell Park Memorial Institute, medium 1640
RRV	Ross River virus
RRVD	Ross River virus disease
RSV	Respiratory syncytial virus
RT	Room Temperature
RT-PCR	Reverse Transcription-Polymerase Chain Reaction
RVFV	Rift Valley Fever virus

SD	Subdomain
SDS-PAGE	Sodium-dodecyl sulphate polyacrylamide gel electropohoresis
SDV	Sleeping Disease virus
SESV	Southern elephant seal virus
SFV	Semliki Forest Virus
SFV	Semliki Forest virus
SINV	Sindbis virus
SP	Structural protein
SPDV	Salmon Pancreas Disease virus
TBS	Tris- buffer saline
TICAM-1	TIR-containing adaptor molecule
TIR	Toll-interleukin-1 receptor
TLR	Toll-like receptor
TNF-α	Tumour necrosis factor alpha
TYK	Tyrosine kinase
UV	Ultraviolet
VAF	Virus-activated factor
VEEV	Venezuelan equine encephalitis virus
VV	Vaccinia virus
WA	Western Australia
WEEV	Western equine encephalitis virus
WNV	West Nile virus

1. Introduction

OVERVIEW

The *ar*throp*od-bo*rne viruses (*arbo*viruses) include members of several virus families, such as the *Togaviridae*, *Flaviviridae*, and *Bunyaviridae*. They are maintained in nature by a continuous cycle of transmission between hematophagous arthropod vectors (such as mosquitoes or ticks) and susceptible vertebrate hosts (Gubler, 2001). Infectious diseases transmitted by arthropod vectors such as mosquitoes and ticks have become more important in some countries where vector survival is inherently dependent on climatic conditions (Gubler et al., 2001). Over the past three decades and on several continents, large outbreaks of epidemics caused by arboviruses such as Chikungunya, Dengue, West Nile and Ross River viruses have caused interest in these pathogens and their vectors. A number of arboviral infections can cause considerable pain and discomfort, and their disease symptoms are often associated with inflammatory conditions ranging from arthritis, fever and rash to encephalitis and haemorrhagic symptoms. Additionally, the high incidence of arbovirus infection constitutes a serious public health threat in several countries where public health monitoring is deficient (LaBeaud, 2008). Because of the close correlation between tenuous vector control strategies and vector borne diseases management, arboviruses have affected millions of animals and humans worldwide, thus increasing the size and diversity of viral reservoirs and maintaining transmission cycles of infection (Gubler, 2001).

Alphaviruses, members of the *Togaviridae* family, are found on every continent, including Antarctic regions. For example, the elephant seal from the Antarctic Territories of Macquarie Island has been shown to carry a louse-borne alphavirus, the southern elephant seal virus (SESV), showing that geographic distribution of arboviruses in not restricted to temperate areas (La Linn et al., 2001; Linn et al., 2001). The genus *Alphavirus* encompasses more than 24 species belonging to seven distinct clades (Weaver et al., 2005). **Table 1.1** provides a list of all known alphaviruses, and outlines known human pathogens. Both animals and humans can serve as hosts for alphaviruses, which are generally transmitted by mosquitoes, although ticks and other arthropods have been found to be efficient vectors (Strauss and Strauss, 1994; Johnston and Peters, 1996; Linn et al., 2001). Alphaviral infection in humans can result in conditions ranging from asymptomatic viremia to lethal encephalitis. A phylogenetic tree based on amino acid sequence analysis of 16 common alphaviruses is shown in **Figure 1.1**. Alphaviruses have been classified as New World and Old

World alphaviruses on the basis of their geographic distribution. New World alphaviruses include North and South American viruses such as Eastern equine encephalitis (EEEV), Western equine encephalitis (WEEV) and Venezuelan equine encephalitis (VEEV) viruses. With some exceptions, New World alphaviruses are known to target the central nervous system, EEEV being the most virulent neurotropic virus, exhibiting a 33% death rate in humans (Weaver et al., 1999). While infection in humans is considered rare, EEEV caused the death of large number of horses in the United States during several sporadic outbreaks. Up to 90% of EEEV-infected horses develop acute, and sometimes fatal symptoms, while survivors often bear severe neurological sequelae (Weaver et al., 1999). VEEV epidemics are sporadic and affect horses primarily, as shown in significant outbreaks in 1969-1970 in the United States, and in 1995 in Colombia and Venezuela (Howard et al., 1988; Weaver et al., 1996). However, VEEV was recognised as a human pathogen following the infection of up to 100,000 people in South America, resulting in approximately 300 deaths (Brault et al., 2001).

In contrast, Old World alphaviruses, such as Chikungunya (CHIKV), Sindbis (SINV) and Ross River (RRV) are associated with outbreaks of infectious arthritis/arthralgia in South America, Europe, Africa, Asia, and Australia. Typical symptoms of Old World alphaviruses include fever, rash, headache, myalgia and arthralgia. The African O'nyong-nyong epidemic in the 1960's affected at least two million people (Williams et al., 1965), while an emergence of Ross River virus in the South Pacific in 1979 caused 50,000 cases of infectious polyarthritis in the Fiji Islands (Aaskov et al., 1981; Harley et al., 2001) and a 2006 Chikungunya outbreak on the island of La Réunion affected more than 250,000 people (Laharyia and Pradhan, 2006; Renault et al., 2007). Persistence as well as immune evasion mechanisms have been suggested as potential disease mechanisms following infection with Old World alphaviruses, while macrophage-driven skeletal tissue inflammation is being increasingly recognised as the principal cause for pathogenesis.

1.1 Ross River virus (RRV): an Arthrogenic Alphavirus

1.1.1 History and discovery of Ross River virus

Symptoms known today as those of RRV disease (RRVD) were first reported in Australia in 1928, in the regional areas of Hay and Narrandera in south-western New South Wales. They were described as "unusual" arthritic symptoms (Nimmo, 1928) that, despite the absence of serological evidence, correlate with today's accepted aetiology of RRVD (Harley *et al.,* 2001). In the 1940s, large numbers of RRVD cases in the Asia-Pacific region, including Fiji Islands and Australia, from the Murray Valley through to northern Queensland and the Northern Territory, led to the description of a disease with symptoms that included incapacitating joint pain and occasional rash, followed by a convalescence period (Harris, 1944; Sibree, 1944; Goswell, 1946). This disease was termed epidemic polyarthritis (EPA) and similarities with other arthrogenic diseases were described (Dowling, 1946).

The aetiological agent of RRVD was isolated from a pool of *Aedes vigilax* mosquitoes by Doherty and colleagues near the Ross River, Townsville. However, RRV had not yet been identified as the causative agent of the disease (Doherty et al., 1963). In 1972, Doherty isolated RRV in humans with EPA by passaging patient serum into mouse brains (Doherty et al., 1972). In 1979, more than 60,000 people were affected by the largest known outbreak of RRVD, both in Australia and Pacific Islands including Fiji. RRV is now believed to have been imported from Australia into Fiji by an infected, viremic tourist (Harley et al., 2001). In 1985, Aaskov and colleagues isolated RRV directly from a patient who showed typical signs of EPA, and helped define the pathology of RRVD as a viral, epidemic arthropathy (Aaskov et al., 1985).

1.1.2 RRV phylogenetics and genome organization

1.1.2.1. Alphavirus and RRV taxonomy

RRV is an Alphavirus and a member of the arthropod-borne *Togaviridae* family and is classified as part of the Semliki Forest (SF) clade. Barmah Forest virus (BFV) and RRV are the only two known alphaviruses endemic to Australia. Alphaviruses are maintained through a natural arthropod-dependent transmission cycle where vertebrates, either marine or terrestrial, act as hosts (Powers et

al., 2001). RRV has been isolated in several South Pacific islands such as Fiji, American Samoa and Cook Islands (Fauquet et al., 2005; Luers et al., 2005; Weaver et al., 2005).

Alphaviruses are distributed throughout the inhabited world as well as in remote areas such as the Antarctic territories. They are typically classified as Old World (Europe, Africa, Eurasia, Oceania) or New World viruses (North and South America) depending on their geographic distribution (Powers et al., 2001; Weaver et al., 2005). Old World alphavirus, such as RRV, Sindbis (SIN), Semliki Forest (SF), Mayaro (MAY), O'Nyong-Nyong (ONN), Barmah Forest (BF) and Chikungunya (CHIK) viruses are typically found in a wide range of vertebrate hosts and reservoirs, while New World viruses such as Western equine encephalitis (WEEV), Eastern equine encephalitis (EEEV) and Venezuelan equine encephalitis viruses (VEEV) are associated with equine hosts (Strauss and Strauss, 1994).

Besides terrestrial mammals and birds, alphaviruses have been identified in aquatic animals such as Salmon Pancreas Disease virus in salmon (SPDV) and Sleeping Disease virus in trout (SDV) (Weston et al., 2002). Alphaviruses are believed to have speciated to Old and New World viruses from an ancestor virus. Phylogenetic studies of alphaviruses based on sequence homology analysis showed that two New World alphaviruses, EEEV and WEEV, are recombinant strains of an ancestral Sindbis virus strain (Hahn et al., 1988; Luers et al., 2005). Non-structural protein sequence homology has been observed between alphaviruses and plant viruses such as Tobamoviruses and Tobromoviruses and some studies have suggested the possibility of ancestral plant virus (Bell et al., 1984; Luers et al., 2005; Weaver et al., 2005).

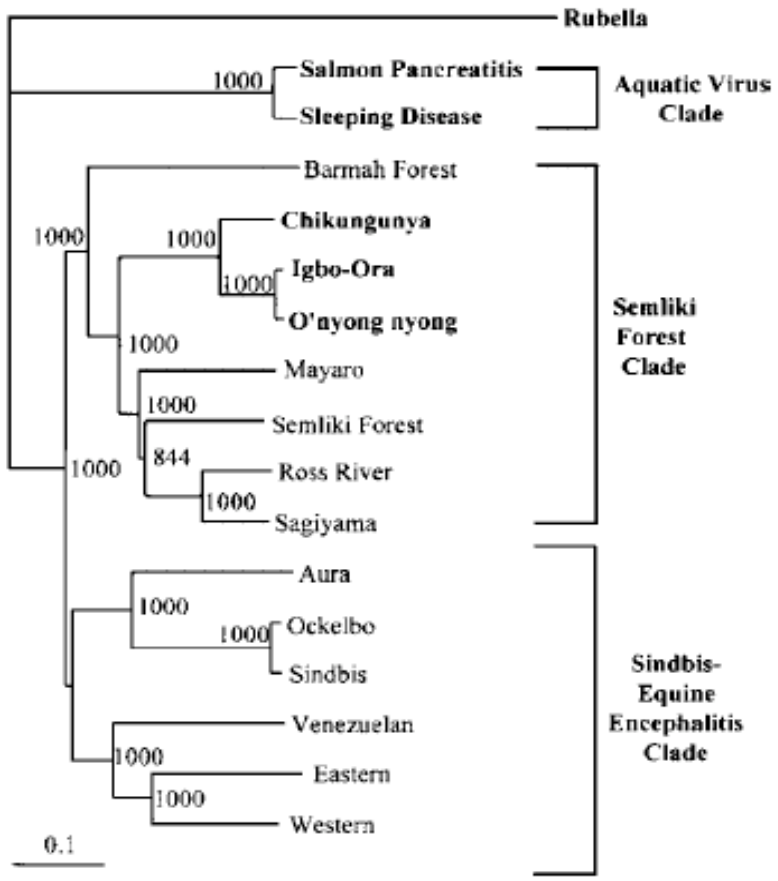

Figure 1.1: Phylogenetic tree of *Alphaviruses* based on amino acid sequence comparison. RRV is a member of the Semliki Forest (SF) clade, which includes Old World viruses such as Chikungunya and O'nyong nyong viruses. The related but distinct Sindbis-Equine Encephalitis clade comprises New World viruses among which equine encephalitis viruses (VEEV, EEEV, WEEV) can be found (Luers et al., 2005). Bootstrap values are indicated in the phylogram.

RRV is a geographically and serologically distinct species of alphavirus and member of the Semliki Forest clade. Several clusters of RRV subtypes were found in different distribution areas, with sequence diverging as much as 2.6% (Russell, 2002). Barmah Forest virus, the only other Australian alphavirus, is not as closely related to RRV as some other members of the SF clade are, such as SINV or Sagiyama virus (Harley et al., 2001; Russell, 2002). However, BFV causes a disease similar to RRV and is thought to cause 10% of all cases of EPA in Australia each year (Russell, 2002; Rulli et al., 2007). .

1.1.2.2 Genome organisation and virion structure

RRV is a single-stranded, positive sense RNA virus, encoding an 11.7 kb genome. The virus consists of an icosahedral nucleocapsid 40 nm in diameter, which is surrounded by a 4.8 nm-thick lipid bilayer, with an overall size of approximately 71 nm (Strauss and Strauss, 1994; Tellinghuisen et al., 1999). The genome encodes two distinct regions of structural (SP) and non-structural (nSP) proteins (Faragher et al., 1988). The non-structural protein nSP1 encodes for a minus-strand transcription initiation protein, the nSP2 for a helicase, while nSP3 is believed to be involved in RNA synthesis and nSP4 the virus's polymerase enzyme (Strauss and Strauss, 1994). Non-structural proteins are involved in transcriptional processes, while structural proteins are involved in capsid and virion structure. Non-structural proteins (nSP) of alphaviruses like SINV and SFV have been shown to interfere with host cell transcription mechanisms. Preliminary studies investigating an nSP-mutant, small plaque variant of RRV suggest that non-structural proteins may have a similar role in RRV (Mahalingam and Lidbury, personal communication). **Figure 1.2** shows the genome organisation and virion structure of RRV. The glycoprotein envelope is constituted of E1 and E2 proteins, which form heterodimers assembled as 80 trimeric spikes on the virus's surface (Strauss and Strauss, 1994; Mukhopadhyay et al., 2006).

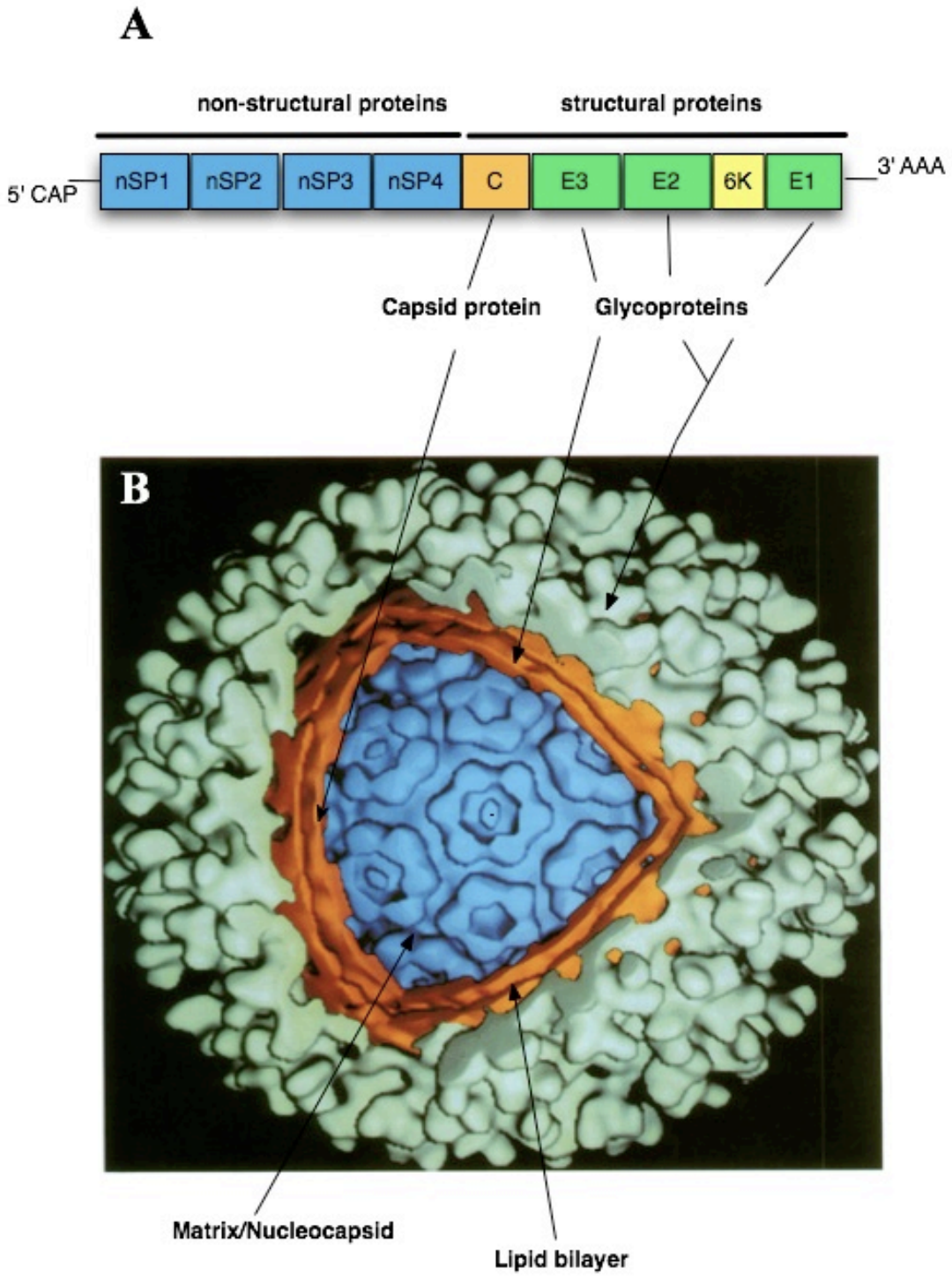

Figure 1.2: A) Diagram of RRV genome structure. A positive sense, non-segemnted, 11.7 kb RNA genome is transcribed into two subgenomic mRNA species for non-structural and structural proteins. The RRV genome encodes five structural proteins, C, E1, E2, E3 and 6K (envelope and capsid) and four non-structural (RNA synthesis and polymerases) nSP1-nSP4 proteins (Strauss and Strauss, 1994). **(B) Rendered 3D reconstruction following cryo-electron microscopy of the RRV virion** (Strauss and Strauss, 1994). The glycoprotein envelope is embedded in the host cell lipid bilayer, which surrounds the matrix and nucleocapsid. Viral genome and subgenomic mRNA species are contained within the matrix/nucleocapsid complex.

Glycoproteins are encoded by structural protein genes E1, E2, E3 and 6K. The function of E3 is not fully understood, but studies in other alphaviruses suggest it is likely to associate with other glycoproteins within the virion's envelope (Strauss and Strauss, 1994; Cheng et al., 1995; Melton et al., 2002). Based on studies with Sindbis virus (SINV), E3 is thought to be located in the lattice structure formed by E1 and E2, and suggests a structural role in capsid structure (Paredes et al., 1998). The authors suggest that, in light of comparative studies between several alphavirus structures, the E3 protein of RRV may have the same function. The 6K protein has been shown to function as an ion channel (Melton et al., 2002). The protein is thought to be required for viral persistence in macrophages, as 6K-deletion RRV mutants could not survive in these cells beyond 6 days post-infection (S. Mahalingam, personal communication).

Glycoproteins such as E2 are involved in the early processes of virus-host cell interaction and modifications to the amino acid sequence can affect viral entry and replication of some viruses. For example, a single amino acid change in the structure of the E2 protein of SINV, was found to determine the neurovirulence and disease outcome in mice (Johnston et al., 2001). The nucleocapsid protein is encoded by gene C (32 kDa), while non-structural proteins are encoded by subgenomic mRNA sequences, which are highly conserved among several Alphaviruses (Dalgarno and Marshall, 1999). RRV replication, illustrated in **Figure 1.3**, is believed to conform to mechanisms of alphavirus replication observed with SINV and SFV. Firstly, the non-segmented, positive RNA strand is transcribed to a complementary negative strand, while the non-structural region undergoes translation into non-segmented polyproteins. These polyproteins are then cleaved into nSP1, nSP2, nSP3 and nSP4 (Strauss and Strauss, 1994). Secondly, the complementary, negative RNA strand encoding structural proteins is transcribed to a subgenomic mRNA strand, which is in turn translated to a non-segemented polyprotein strand. This is followed by successive proteolytic cleavage processes resulting in the mature forms of C, 6K, E1, E2 and E3 proteins (White and Fenner, 1994).

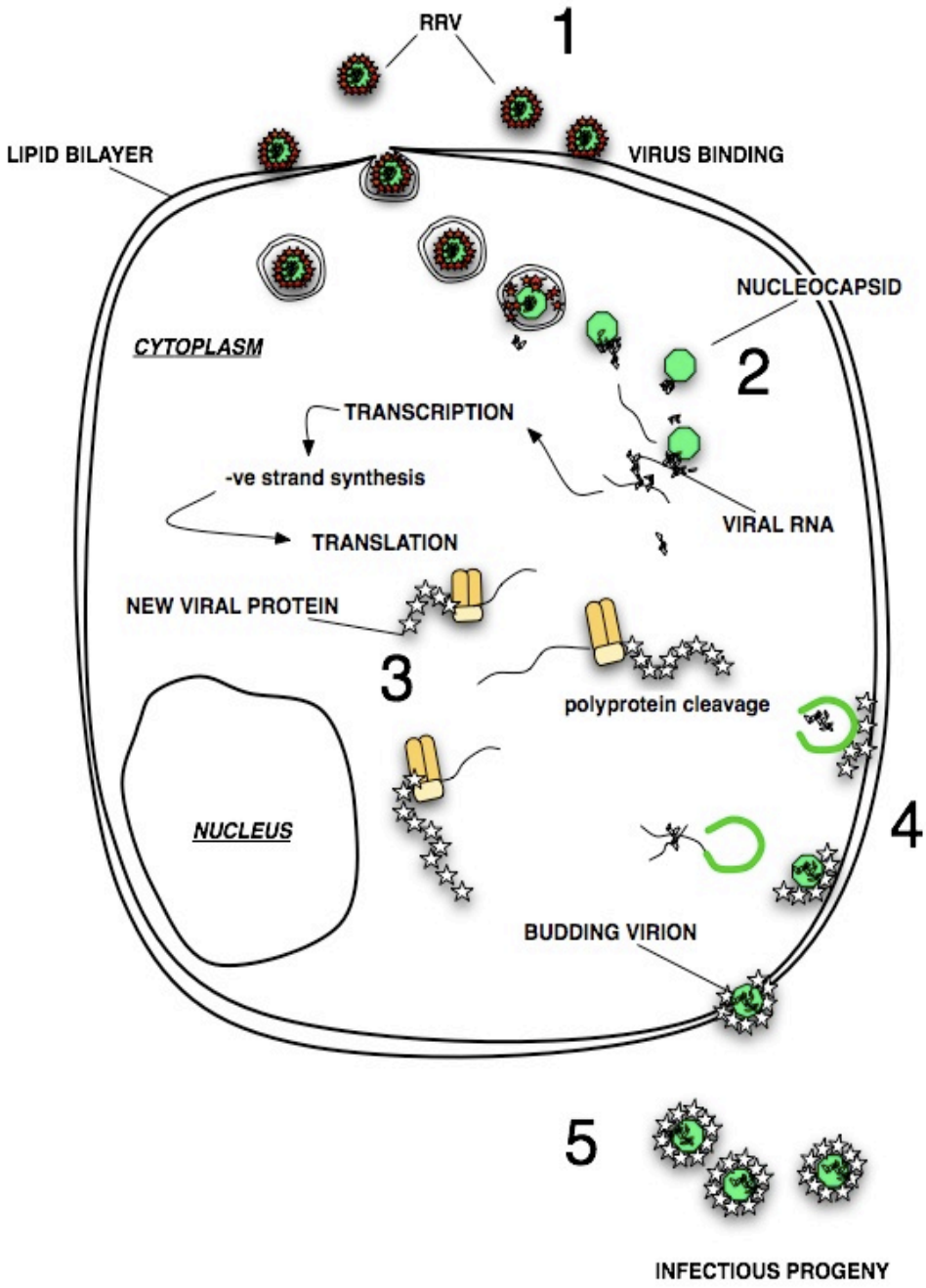

Figure 1.3: Life cycle of RRV in vertebrate cells. RRV is believed to bind host cell carbohydrate attachment complexes (eg. cell surface integrins, complex carbohydrates). The viral envelope fuses with the membrane **(1)** and the virion is incorporated by endocytosis. In the cytosol, the nucleocapsid is released, along with viral RNA **(2)**. The non-segmented RNA strand is successively transcribed into subgenomic mRNA strands, that are in turn translated by host cell ribosomes into protein precursors **(3)**, which are later cleaved to generate mature proteins. Assembly and packaging of the new virion occurs beneath the cell membrane **(4)**, allowing the budding of new, infectious progeny RRV into the extracellular milieu **(5)**.

1.1.3 RRV Epidemiology and Distribution

Over 35 species of mosquitoes have been shown to carry RRV, while 104 species of birds have been identified as potential carriers, suggesting that avian migration routes may be a critical factor in the geographical dissemination of many alphaviruses (Strauss and Strauss, 1994; Russell, 2002). RRV has been isolated from mosquito species such as *Culex annulirostris*, *Aedes vigilax* and *Anopheles annulipes*, and has been reported in horses, dogs, flying foxes and humans (Azuolas et al., 2003; Kay et al., 2007).

While the reservoir host range spans across several higher vertebrates, terrestrial mammals, in particular marsupials such as kangaroos and wallabies were found to be a major host involved in horizontal transmission of Alphaviruses such as RRV (Harley et al., 2001). In a study aimed at assessing RRV exposure in the wild, up to 33% of wallabies and wallaroos caught around urban areas tested positive for anti-RRV antibodies, suggesting a strong role for marsupials as reservoir hosts for RRV and potentially for BFV (Old and Deane, 2005).

RRV has been found in the South Pacific as far as Fiji, the Cook Islands, and American Samoa, as well as in Papua New Guinea, Timor and the Solomon Islands (Russell, 2002; Tupanceska et al., 2007). In Australia, RRV has been detected in all states and territories, with the highest incidences found in New South Wales (NSW), Western Australia (WA) and northern Queensland (QLD). Incidence rates over 700 cases per 100,000 people were reported in the 1993 outbreaks in south-western NSW, while between 600 and 700/100,000 cases were notified in WA and South Australia outbreaks of 1996-97 (Russell, 2002).

RRV has been increasingly reported in the vicinity of large coastal urban centres such as Brisbane and Sydney, and patterns of RRV clusters in northern QLD have been the subject of several studies (Brokenshire et al., 2000; Old and Deane, 2005; Hu et al., 2007; Kay et al., 2007). The incidence of RRV linked to floods or heavy rain events that facilitate vector expansion across vast area of Australia (Tong et al., 1998; Tong, 2004).

Up to 7000 Australians are affected by RRV each year and given the debilitating nature of the disease, prevention and amelioration of disease symptoms are needed (Rulli et al., 2007). Despite the availability and efficacy of anti-inflammatory drugs and corticosteroid therapy, shown to be a safe treatment for RRV-induced arthritis, the idea of a vaccine is also being considered and motivated by increasing occurrences of RRV infections in and around urban areas in Australia (Mylonas et al., 2004; Kay et al., 2007).

1.2. RRV disease, an inflammatory arthropathy

1.2.1. RRVD pathogenesis: clinical findings

The onset of RRVD symptoms has been reported to occur within 7 to 10 days of infection, generally afflicting the carpal and metacarpal joints as well as larger joints such as the elbows and knees (Dalgarno and Marshall, 1999). The extent of joint pain has often been described as moderate to significant, sometimes incapacitating the patient and significantly restricting movement (Bielefeldt-Ohmann and Barclay, 1998). Over 50% of RRV-infected adults exhibit a range of symptoms including rash, fever, arthralgia, myalgia, lethargy and anorexia (Bielefeldt-Ohmann and Barclay, 1998). Children generally seem to be spared from the disease manifestations and it is not clear why this is the case. Children are suspected of producing less of the arthrogenic cytokines (TNF-α and IFN-γ), and it is possible that children are less susceptible to a range of immunopathological and autoimmune phenomena (rheumatoid arthritis, glandular fever, etc.) that depend on these cytokines (Ordemann et al., 2002).

Arthritic symptoms usually persist for up to 6 weeks before progressively diminishing, suggesting that co-morbid conditions may be involved in persisting illnesses experienced by some patients (Yu and Aaskov, 1994; Mylonas et al., 2002). A number of studies aimed at characterising the duration of RRV disease symptoms have found 3 to 12 months of symptom manifestation (Fraser, 1986; Mylonas et al., 2002). A comprehensive study on the socio-economic impact of RRV infection in Australia by Mylonas and co-workers estimated the cost incurred from consultations, treatment and loss of productivity at AU$1018 per person, based on average income and sick leave (Mylonas et al., 2002). However loss of productivity is believed to cost significantly more in cases of persistent illness. RRV is also the most prevalent form of EPA in indigenous Australian communities, although cases often go unreported. Aboriginal people showed higher seroprevalence (between 60 and 81% in some rural communities), compared to a much lower range (8-43%) in non-aboriginal people residing in endemic areas (Russell, 2002).

To this day, there is no RRV vaccine available, despite several attempts at designing a vaccine (binary ethylenimine or BEI) (Yu and Aaskov, 1994). More recently, Kistner and colleagues

reported developing a formaldehyde-inactivated RRV vaccine for humans, which is currently undergoing clinical trials (Yu and Aaskov, 1994; Kistner et al., 2007).

A wide array of Aboriginal medicinal plants were the subject of a study by Semple and colleagues which showed that fruit, wood and leaf extracts of *phylliraeoides* var. *microcarpa* (Pittosporaceae) effectively reduced *in vitro* RRV infectivity by 25% (Semple et al., 1998) while other plant extract were found to have antiviral activity against human cytomegalovirus (HCMV). Some of these plants are known to have been used by Aboriginal Australians to alleviate arthritic symptoms. However, non-steroidal anti-inflammatory drugs such as paracetamol and aspirin remain the treatment of choice for RRV-induced symptoms, since they alleviate the arthritic symptoms and lead to very little side-effects (Mylonas et al., 2002; Suhrbier and Linn, 2004). New therapies that target specific host factors (e.g. monocyte chemotactic protein, MCP-1), which mediate cell recruitment leading to arthritic symptoms are currently being developed (Rulli et al., 2008, in press).

1.2.2. RRVD pathogenesis and mechanisms of inflammation

1.2.2.1. Cells in RRVD: a focus on macrophages

The first comprehensive clinical studies of RRV disease in humans, conducted by Fraser and co-workers demonstrated that the disease was characterised by extensive monocyte and macrophage infiltrations in the joint tissue of EPA patients, during the early stages of the disease (Clarris et al., 1975; Fraser et al., 1981; Fraser et al., 1983). Infiltrating macrophages were positive for RRV antigen by immunofluorescence assay as early as 1 day following the onset of symptoms (Fraser et al., 1981). A small number of T lymphocytes were reported as part of the cellular infiltrates, whereas no B-lymphocytes were present. Inflammatory arthropathies such as RA are characterised by the recruitment of T cells, B cells, macrophages as well as mast cells to the synovium. However, histological examinations of RRV-infected synovium revealed massive infiltration of macrophages (Fraser, 1986; Soden et al., 2000; Weyand, 2000).

Several studies highlight the role of macrophages in joint inflammation in RRVD, as well as the presence of RRV antigen in synovial effusions of EPA patients (Fraser and Becker, 1984; Linn et al., 1996; Soden et al., 2000). An early study reported that RRV-infected cultures of primary human synovial cells released virulent RRV at 35 days post-infection (dpi), initiating several studies on

RRV persistence (Journeaux et al., 1987). In a more recent study ,the authors were able to detect RRV viral RNA by RT-PCR in joint tissue of EPA patients up to 5 weeks after the onset of the disease symptoms (Soden et al., 2000; Way et al., 2002).

From the above studies, it became apparent that RRV was able to persist in an inflammatory environment that is deemed particulary hostile to viral replication. Macrophages were considered likely to principal effector cell, since they were found in large numbers in the synovium of RRV-infected patients, and were unable to effectively clear RRV from the host. Interestingly, fibroblasts expressing attachment molecule a1b1-integrin were found to be permissive to RRV, and RRV-infected fibroblasts secreted a number of macrophage-attracting chemokines (macrophage chemotactic protein-1, MCP-1; macrophage inflammatory protein-1α , MIP-1α) (Mateo et al., 2000). In addition, tissue macrophages are considered as a major source of MCP-1 following RRV infection *in vivo* (Lidbury et al., 2008). It is likely that macrophages respond to strong chemokine signalling by RRV-infected fibroblasts and macrophages in the joint, resulting in massive cellular infiltration into the synovium (Mateo et al., 2000; Linn et al., 2005; Lidbury et al., 2008).

The use of animal models, in particular mice, have led to a better understanding of RRV tropism, disease mechanisms and kinetics *in vivo*. Early experimental work in mice found the presence of monocytes in the brain of RRV-infected mice, accompanied by cortical thinning of the brain as well as muscle necrosis (Mims et al., 1973). Other studies have reported the presence of macrophages in the muscle tissue of RRV-infected mice, suggesting a strong link between muscle disease and macrophage infiltration (Seay et al., 1981; Seay and Wolinsky, 1983).

Macrophages have been found to be the major effector cell in RRVD pathogenesis in mice. Lidbury and Hapel showed that macrophage infiltration was responsible for the extensive muscle damage in a mouse model of RRV disease (Lidbury et al., 2000b). In line with earlier findings of RRV persistence in joints of EPA patients, *in vitro* studies by Way and co-workers have shown that RRV could persist in a macrophage cell line. They showed that RRV could be detected by immunofluorescence and Reverse Transcription-Polymerase Chain Reaction (RT-PCR) in a macrophage cell line infected with RRV (Way et al., 2002). The RRV-E2 protein could be detected in macrophages (*in vitro*) after 62 days post-infection (dpi), even after apparent clearance of the virus, which was undetectable between 39 and 62 dpi. (Way et al., 2002). Immunofluorescence assays showed that viral clearance and stress-induced responses could trigger a relapse of RRV

replication *in vitro* and macrophages were found to remain persistently infected up to 2 months after relapse events (Way et al., 2002).

In summary, macrophages have been identified as an important effector cell in RRV disease. They are permissive to RRV infection *in vitro*, RRV-infected synovial cells have been shown to produce large amounts of macrophage chemoattractants and macrophages are the dominant infiltrating cell in the synovium of EPA patients. Joint inflammation, particularly in viral arthritis, is the consequence of immune cell-mediated tissue damage in response to infection. In RRVD, macrophages have been identified as the main effector cells in a mouse model of RRV disease (Lidbury et al., 2000b; Lidbury et al., 2008).

1.2.2.2 Host factors in inflammatory arthritis

Mechanisms other than macrophages such as the complement system have been found to contribute to the severity of RRVD. For example, Morrisson and co-workers observed reduced muscle damage in RRV-infected C3 deficient mice (Morrisson et al., 2007a). The extent of RRVD-induced myofibre damage was significantly reduced in RRV-infected C3 -/- mice compared to wild-type, infected mice. This study found that the absence of the major complement system precursor (C3) prevented macrophage-induced muscle damage, suggesting that the complement system may be a part of the immunoregulatory processes in RRVD pathogenesis. The complement cascade represents an evolutionarily conserved component of the innate immune system that is involved in direct pathogen clearance, as well as the regulation of other elements of the innate and adaptive immune systems (Carroll, 2004). Complement has been identified as an important component in the pathology of various inflammatory disorders (Markiewski and Lambris, 2007; Heise and Morrison, 2008).

A recent study by Lidbury and coworkers showed that RRVD pathogenesis in mice was due to macrophages and macrophage-derived factors, such as MCP-1, tumor necrosis factor-α (TNF-α) and interleukin-1β (IL-1β (Lidbury et al., 2008). The authors showed that the depletion of macrophages reduced the expression of the pro-inflammatory cytokines TNF-α, MCP-1, IL-1β, MIP-1α and interferon-γ (IFN-γ) in the muscle and synovial tissue of RRV-infected mice. Macrophage-depleted mice showed less severe disease symptoms following RRV infection compared to undepleted, RRV-infected mice (Lidbury et al., 2008).

More recently, the role of pro-inflammatory host factors in RRVD pathogenesis was further investigated by Rulli (2007). RRV-infected mice treated with Bindarit, an MCP-1 inhibitor, showed reduced disease symptoms compared to untreated, RRV-infected mice (Rulli, 2007). Bindarit is known to inhibit MCP-1 and TNF-α *in vivo*, and has been found to ameliorate disease in experimental animal models of adjuvant-induced arthritis, acute pancreatitis and lupus nephritis (Zoja et al., 1998; Guglielmotti et al., 2002; Bhatia et al., 2005). These cytokines are therefore important in the development of RRVD and other inflammatory conditions and they may provide a clue to new treatments.

RRVD has many similarities with non-viral arthritides, such as Rheumatoid Arthritis (RA). RA is an autoimmune, chronic inflammatory disease that affects more than 2 million people in the United States alone, and the exact mechanism of disease is still unclear (Gabriel et al., 1999). Like RRVD, RA has been characterised as an inflammatory arthropathy where massive cellular infiltration results in chronic skeletal tissue damage, in particular cartilage and bone (Weyand, 2000; Gravallese, 2002). Experimental RA has provided invaluable insight into the cellular and physiological mechanisms behind autoimmune joint inflammation and damage and parallels have since been drawn between the effector phases in RA and viral arthritides such as RRVD.

1.2.3 Natural Killer (NK) cells in inflammatory arthropathies

Early studies in RRV-infected EPA patients revealed the presence of Natural Killer (NK) cells in the synovium, suggesting their possible involvement in joint and, perhaps, muscle damage (Aaskov and Dalglish, 1981; Aaskov et al., 1986). NK cells are a distinct type of immune cell; they have lymphocytic morphology yet belong to a granulocytic cell lineage (Hamerman et al., 2005). NK cells are thus considered as the interface between the innate and adaptive immune systems, being able to coordinate cytokine response signals as well as killing infected cells and tumour cells (Chan et al., 2006; Lanier, 2008).

The interest in the role of NK cells in RRV-induced joint inflammation is triggered by the observation that these cells contribute to RA (Dobloug et al., 1982; Villanueva et al., 2005). Recent studies suggest that during RA, the activation of specific pathways following receptor-dependent interaction between synoviocytes and NK cells plays an immuno-modulatory role in inflammation

(Chan et al., 2008). The authors, who collected synoviocytes and NK cells from RA patients, found that synoviocytes enhanced NK cell proliferation and pro-inflammatory cytokine production. Another study conducted on a cohort of patients with conditions including RA and psoriatic arthritis reported high levels of infiltrating NK cells that are able to interact with monocytes and initiate inflammatory processes (Dalbeth et al., 2004). The same authors had previously identified a subset of NK cell, termed $CD56^{bright}$ NK cells, that were the predominant subset found in synovial tissue during inflammation (Dalbeth and Callan, 2002).

Several murine models of experimental arthritis were used to understand the role of NK cells in arthritis *in vivo*. Most relevant to NK cell physiology is a mouse strain with an autosomal recessive mutation which causes mice to produce NK cells with deficient cytotoxic activity. The Beige, or Chediak-Higashi mouse, whose NK cells lack lysosomal trafficking regulators involved in the release of cytotoxic compounds, has been used in a number of studies to assess the role of NK cells in several disease models (Brandt and Swank, 1976; Roder, 1979). For instance, experimental, antigen-induced rheumatoid arthritis in Beige mice was shown to cause more severe symptoms associated with cartilage and synovial tissue damage than in their wild-type congeners (Schalkwijk et al., 1988; Schalkwijk et al., 1990). This suggests that an arthritic inflammatory response is likely to be regulated, rather than exerted by NK cells, and that other cells such as macrophages are more likely to be the primary effector of tissue damage. Macrophage activation syndrome (MAS), an abnormal inflammatory condition associated with RA is characterised by depressed NK cell activity and aberrant macrophage and T cell responses (Villanueva et al., 2005). Such imbalance, albeit rare, causes severe complications in RA patients such as phagocytic lymphohistocytosis (HLH), characterised by an abnormal mononuclear phagocyte system, which can lead to death (Ravelli, 2002; Villanueva et al., 2005).

NK cells appear to play an important role in viral infection, as they have been found to mediate antiviral responses against Murine cytomegalovirus (MCMV) and Influenza viruses, as well as enhance cytotoxicity against HIV-infected CD4+ cells and SINV-infected cells (Biron et al., 1999). The role of NK cells in RRVD has not been characterised in the mouse model, however a recent study was able to examine the role and requirement for lymphocytes in RRVD using RAG-/- mice, which are deficient in T and B-lymphocytes (Morrisson et al., 2007b). The authors found that the ablation of lymphocyte function observed in RAG -/- mice did not affect the severity of RRVD. They also argue that, since the absence of lymphocytes did not result in the amelioration of RRVD

symptoms, granulocytes such as macrophages are most likely to be the main effector cell (Morrisson et al., 2007b). This supports the idea that macrophages are the main effector cell in RRV disease, however, the role of NK cells in RRVD pathogenesis remains unclear.

1.3 Cytokines in viral infection

1.3.1 Pro-inflammatory cytokines

Cytokines are plenipotent and pleiotropic immune molecules, which bind to specific cell surface receptors and induce intracellular signalling pathways . Cytokines are key to viral pathogenesis and, according to the type of systemic response they promote, are classified as pro-inflammatory or anti-inflammatory cytokines. Pro-inflammatory cytokines such as interleukin (IL)-Iβ, IL-2, IL-6, IL-8 and IFN-γ promote the proliferation and survival of cells capable of generating an inflammatory response, such as macrophages (Dinarello, 2007; Schett, 2008). Macrophages are often responsible for the tissue damage in inflammatory diseases. In the subsequent sections of this chapter, the role of TNF-α in inflammatory disease and viral infection will be discussed. In addition, the antiviral interferon system will be covered, along with aspects of interferon-induced antiviral mechanisms and early antiviral responses. Strategies of immune evasion used by some RNA viruses will be covered, with a focus on interference with interferon-associated pathways and interferon avoidance observed in arthropod cell-derived viruses.

1.3.2. Cytokines in inflammation: a focus on TNF-α

Inflammatory arthropathies are strongly regulated by a range of soluble host factors known as cytokines. Cytokines such as tumour necrosis factor-a (TNF-α), interleukin-1b (IL-Iβ), interleukin-6 (IL-6) and chemokines such as MCP-1 and RANTES have been shown to play an important role in the development of aberrant responses *in vivo* resulting in arthritic symptoms (Lewthwaite et al., 1995; Lechner et al., 1997; Lawlor et al., 2001; Hata et al., 2004). In 1975, Carswell and colleagues identified an endotoxin-induced serum factor in the Calmette-Guerin vaccine preparation that caused necrosis of tumours, and named it tumor-necrosis factor (Carswell et al., 1975) The authors tested the tumorigenic properties of TNF-α on various cell lines and paved the way for further studies, leading to the isolation and cloning of human TNF-α in 1984 (Chen and Goeddel, 2002).

1.3.2.1 TNF-α in inflammatory disorders

TNF-α is a pluripotent cytokine involved in processes such as apoptosis and antimicrobial defence. It is produced mainly by macrophages and T cells and is thought to be an important regulator of immune responses (Bradley, 2008). TNF-α is widely recognised as a key cytokine involved in cell survival, differentiation and apoptosis within lymphoid, mammary and neuronal tissue, and belongs to a large family of motif-associated ligands and receptors (Ware, 2003). However, over the last two decades, TNF-α has emerged as a key mediator implicated in a range of severe inflammatory conditions. Most importantly, TNF-α is considered as an essential requirement for septic shock, a potentially lethal condition that occurs following bacterial infections (van der Poll and Opal, 2008). TNF-α has been found at high levels in the blood of animals and patients with systemic inflammation and is believed to induce the secretion of cytokines able to affect the structure of the surrounding tissue (Dinarello, 1997).

In a recent study by Zhao and colleagues, TNF-α was found to promote chemokine expression in synoviocytes obtained from RA patients. The study shows that TNF-α enhanced the expression of sphingolisin-1-phosphate receptors in synoviocytes from RA patients, resulting in the secretion of chemokines and pro-inflammatory factors into the synovium (Zhao et al., 2008). TNF-α was also found to play an important role in tissue remodelling in an experimental model of lung inflammation (Mazzon and Cuzzocrea, 2007). Two studies by Mazzon and co-workers found that TNF-α increased the permeability of tight junctions in the lung epithelial tissue, resulting in acute lung inflammation and respiratory dysfunction (Mazzon and Cuzzocrea, 2007; Mazzon et al., 2008). TNF-α has been implicated as a major pro-inflammatory factor contributing to disease in a variety of conditions, including inflammatory bowel disease, respiratory (asthma, chronic bronchitis), cardiovascular (myocarditis and allograft rejection) and renal disease (glomerulonephritis and transplant rejection) (Bradley, 2008). This has led to abundant studies on the effect of TNF-α inhibition, or blockade, in inflammatory diseases regulated by TNF-α.

1.3.2.2 TNF-α signalling pathways

TNF-α occurs in two forms: a membrane-bound form (*mem*TNF-α), which is the main isotype, and a soluble form (*s*TNF-α) (Wajant et al., 2003; Ware, 2003). *mem*TNF-α is cleaved and converted to the soluble form by the TNF-α converting enzyme (TACE), which releases TNF-α into the extracellular milieu (Blobel, 1997; Bradley, 2008).

TNF-α exerts its action by binding to its receptors, TNFR1 and TNFR2. Two distinct forms of TNF receptors are found in mammals: TNFR1 is expressed constitutively in a broad range of cells and tissues, whereas TNFR2 is primarily expressed on immune cells (Wajant et al., 2003; Ware, 2003). It also appears that TNFR1 and TNFR2 differ in their signalling mechanisms. TNFR1 has been associated with general TNF-α signalling, namely pro-inflammatory responses, cell survival and apoptosis (Wajant et al., 2003). In contrast, TNFR2 is thought to regulate lymphoid system-associated responses, and its function is still being characterised (Chen and Goeddel, 2002).

TNF-α induces several intracellular signalling cascades, each involved in the different roles of TNF-α described earlier. However, most relevant to inflammatory responses is the TNF-α/ Nuclear factor kappa-B (NF-κB) pathway. NF-κB is a transcription factor involved in a number of signalling pathways, and is considered as an essential regulator of TNF-α signalling and high levels of this protein have been associated with inflammatory conditions such as asthma, septic shock and cancer (Baldwin, 2001; Hayden and Ghosh, 2008). Interestingly, high levels of NF-κB expression in the synovium have been identified as a characteristic feature of RA and osteoarthritis (OA) (Marok et al., 1996). Similarly, in an animal model of RA, a study showed that exogenous administration of NF-κB protected synovial cells from TNF-α-induced damage (Miagkov et al., 1998).

1.3.2.3 TNF-α inhibition therapies in inflammatory diseases

Studies on the effect of TNF-α blockade have provided invaluable insight into the roles of TNF-α and associated factors in inflammatory disease. Some studies used monoclonal antibodies that neutralise TNF-α, while others used transgenic mice that overexpressed TNF-α in disease models of arthritis and Crohn's disease (Keffer et al., 1991; Bondeson et al., 2006; Hayward et al., 2007; Bradley, 2008).

The first of many anti-TNF-α biological agents, Enbrel (Etanercept®), was found to be safe and effective and was approved for use as a therapeutic for RA, Crohn's disease and psoriatic arthritis by the United States Federal Food and Drug Administration in 1998 (Feldmann and Maini, 2001). Enbrel has been tested in randomised, large cohort trials with the findings that anti-TNF-α therapy is beneficial to RA patients and consistently helps reducing disease symptoms in RA and other arthritic conditions, such as psoriatic arthritis and spondylarthritis (Elliott et al., 1993; Feldmann and Maini, 2001).

Enbrel has been widely used for the last 10 years as an RA therapeutic and has been found to be generally more effective than alternative therapeutic methotrexate (Bathon et al., 2000; Rigby, 2007). However, the fact that these drugs do not completely abrogate the disease means that factors other than TNF-α may also be involved in the development of arthritis. A study on collagen-II-induced arthritis in mice showed that IL-I α/β blockade reduced inflammation and prevented bone and cartilage damage, whereas TNF-α blockade could only suppress inflammation and failed to protect mice from tissue damage (Joosten et al., 1999).

Recent findings have helped reinforce the paradigm by which the inhibition of TNF-α-associated pathways reduces inflammation and tissue destruction. As mentioned earlier in this section, the release of TNF-α depends on the action of the TNF-α-converting enzyme (TACE), and inhibition of TACE during inflammation has provided new insights into anti-TNF-α therapy (Blobel, 1997). Zhang and co-workers reported the reduction of TNF-α secretion in the synovium of RA patients using a TACE inhibitor, TMI-1 (Zhang et al., 2004). In addition, symptoms of experimental arthritis in mice were found to be dramatically reduced following administration of TMI-1. The development of TACE inhibitors is justified by the crucial need of orally-administred medication for the treatment of RA and other inflammatory conditions (Moss et al., 2008).

1.3.2.4 TNF-α in viral infections

In viral infections, TNF-α is responsible for triggering antiviral pathways, in synergy with IFN-γ, leading to apoptosis in order to limit the replication and spread of the virus. However, some viruses are known to circumvent these processes (Herbein and O'Brien, 2000; Bradley, 2008). Herpes simplex, Vaccinia and Hepatitis B viruses have been reported to inhibit TNF-α-mediated

cytotoxicity or apoptosis, in some cases via the use of virally encoded host protein antagonists (Herbein and O'Brien, 2000). TNF-α has also been implicated in the pathogenesis of viral diseases such as Dengue Haemorragic Fever (DHF) and Influenza A respiratory infection. Wang and co-workers have observed high levels of TNF-α in the serum of DHF patients, and considered TNF-α as an effective marker for DHF diagnosis (Wang et al., 2007). Similarly, Influenza A and Sendai virus infections were found to induce chemokine secretion in lung epithelial cell lines. However, pre-treatment with TNF-α resulted in an enhanced chemokines production following viral infection, suggesting that TNF-α, among other pro-inflammatory factors, can exacerbate inflammatory responses following viral infection (Veckman et al., 2006).

Viral-induced inflammation of the central nervous system was also found to be mediated by TNF-α-dependent signalling. Camelo and colleagues reported that wild-type mice were more susceptible to neurotropic Rabies virus infection than mice lacking the the p55-TNFR receptor, suggesting that signalling pathways induced by TNF-α may be useful as therapeutic targets for treating inflammatory disorders (Camelo et al., 2000).

The ability of TNF-α to influence effector cell function in inflammatory diseases is another important aspect of TNF-α signalling. TNF-α was found to drive macrophages towards a pro-inflammatory state during murine experimental arthritis and is considered to be an active host factor in lentivirus-induced arthritis, thus suggesting a potential pivotal role in viral arthropathies such as RRVD (Lechner et al., 1997; Takasugi et al., 2006; Williams et al., 2007). Interestingly, Lidbury and colleagues recently investigated the role of pro-inflammatory cytokines in the RRVD mouse model and identified TNF-α as an important factor in the disease (Lidbury et al., 2008). This study also found that TNF-α inhibition using a monoclonal, anti-TNF-α antibody, resulted in ameliorated symptoms in RRV-infected mice, based on clinical score data only.

Several studies report the use of commercially available anti-TNF-α compounds (eg. Enbrel®, Infliximab®) in non-viral arthritis mouse models showing amelioration of inflammatory symptoms (Mageed et al., 1998; Gosselin and Martinez, 2004; Grounds and Torrisi, 2004; Hodgetts et al., 2006). However, the Lidbury et al., study did not report sufficient data to assess the role of TNF-α inhibition in RRVD pathogenesis *in vivo*. Based on human and mouse findings to date, an illustration of the proposed model of RRVD pathogenesis is shown in **Figure 1.4.** It is hypothesised that RRV-infected synovial tissue cells generate large amounts of pro-inflammatory cytokines,

which result in the recruitment of macrophages into the synovium. RRV-infected macrophages are believed to produce pro-inflammatory cytokines, resulting in IFN-γ-dependent activation by infiltrating T lymphocytes and NK cells. Once activated, large numbers of macrophages accumulate in the synovium and release cytotoxic compounds (TNF-α, nitric oxide) causing tissue damage.

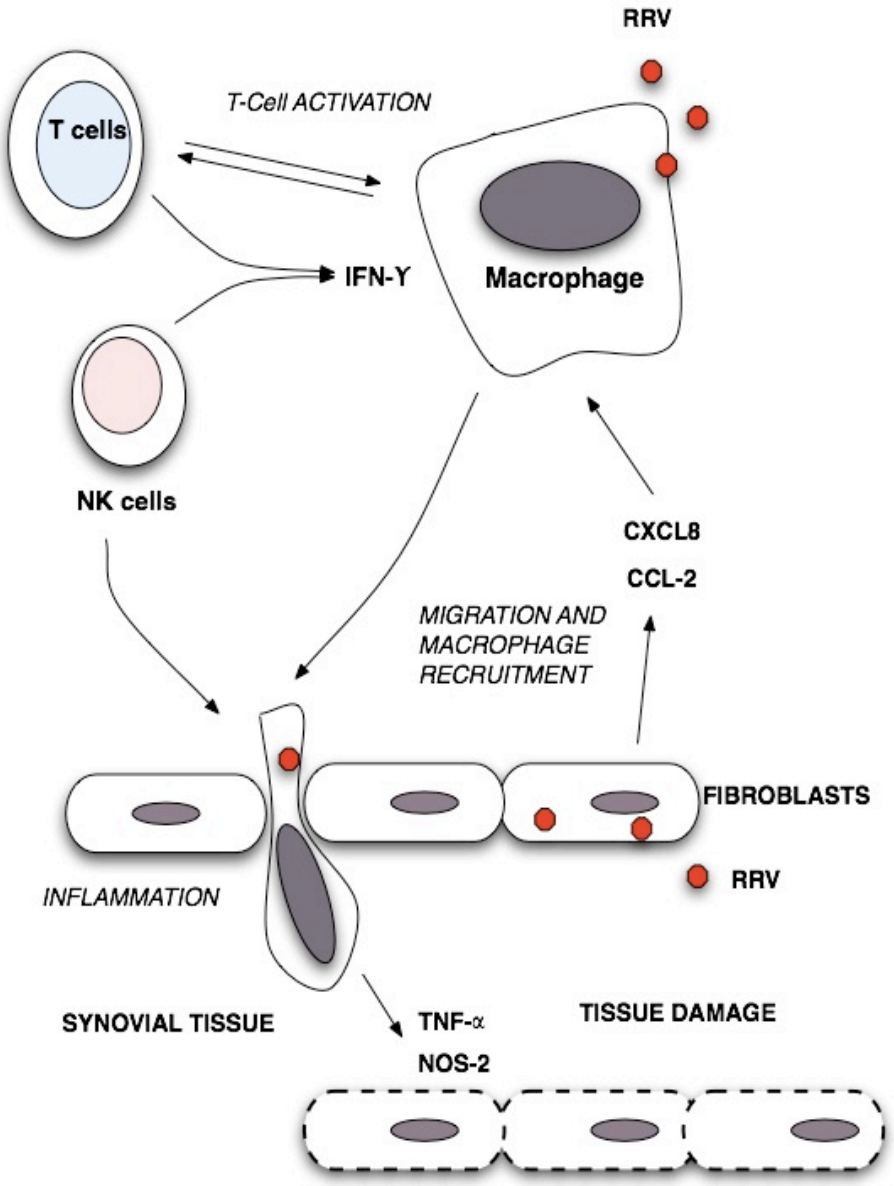

Figure 1.4: Proposed mechanisms of RRV disease pathogenesis. RRV-infected fibroblasts secrete chemokines (CCL-2/MCP-1, CXCL8/IL-8), to which macrophages respond to by migrating in large numbers towards the skeletal and synovial tissue. T cells and NK cells are activated by RRV-infected macrophages and produce large amounts of IFN-γ, which amplifies the inflammatory response. It is possible that activated infiltrating macrophages release TNF-α in the synovium, resulting in tissue damage.

1.3.3. Antiviral host response mechanisms: The Interferons

Interferons (IFN) are the most widely studied and characterised antiviral host factors, and have been at the forefront of antiviral therapies for several diseases. From the 1970's onward, large-scale studies involving the infection of human leukocytes with virus to generate interferons contributed to the first clinical trials of human interferon treatment, which later established itself as a new therapeutic paradigm with the advent of industrial protein purification (Pestka, 2007). After 50 years of interferon research, several transduction pathways and mechanisms of induction have been elucidated. The interferon system now comprises 10 mammalian types, 7 of which are found in humans, that are subdivided into two main groups, Type I and Type II interferons.

This section will focus on Type I interferons, of which IFN-α and IFN-β are the most widely characterised members. However the role played by Type II IFN (IFN-γ) in viral infections and disease pathogenesis is worth noting. IFN-γ is mainly involved in the regulation of adaptive immune responses, is required for the activation of T helper (T_h) lymphocytes, and is also involved in viral clearance (Bach et al., 1997; Burdeinick-Kerr and Griffin, 2005).

1.3.3.1 Induction of Type I Interferon signalling pathways

Plasmacytoid dendritic cells (pDC) (also known as professional Type I IFN-producing dendritic cells, or IPC) have been shown to produce large amounts of Type I IFNs upon viral stimulation. Such large amounts of IFNs are believed to promote large-scale local activation of B cells, T cells NK cells and myeloid dendritic cells (Liu, 2005). Type I IFN induction, in particular IFN-β induction, is believed to be triggered mostly by viral double-stranded RNA (dsRNA). A number of cytoplasmic proteins have been shown to detect dsRNA and trigger signalling cascades leading to the transcription of the IFN-β gene. Upon detecting dsRNA, RNA-dependent protein kinase (PKR) recruits initiation factor eIF-2a, which inhibits nucleotide exchange during viral transcription. Most importantly, PKR has been shown to activate NF-κB and interferon regulatory factor-3 (IRF-3). When activated, NF-κB and IRF-3 both translocate to the nucleus and bind to their respective target sequences - PRDII and PRDIII-I - located on the IFN-β gene promoter, resulting in IFN-β gene transcription followed by mRNA synthesis (Pestka, 2000). PKR was found to be essential in

resistance of cells to infection with West Nile virus (WNV) and Sindbis virus (SINV) *in vitro* (Ryman et al., 2005; Samuel et al., 2006).

It is worth noting the role played by interferon regulatory factors (IRFs) in mediating dsRNA-induced antiviral signals leading to Type I IFN induction. IRFs are the 'signal interface' between the cytoplasm where the signal is initiated, and the nucleus where they translocate and bind target or 'consensus' DNA sequences (Paun and Pitha, 2007). All IRFs are able to bind to interferon-stimulated responses element sequences (ISRE), that are present upstream of IFN gene promoter sequences and are involved in IFN receptor-associated pathways, known as Janus Kinase/Signal Transduction and Activator of Transcription (Jak-Stat) pathways. Studies have shown that IRF-3 and IRF-7 could both bind ISRE following Sendai virus infection with the collaboration of co-activators cAMP-response element-binding protein (CREB) and virus-activated factor (VAF), and subsequently result in Type I IFN gene transcription (Ning et al., 2005; Paun and Pitha, 2007). Further confirming the critical role of IRFs in host immune response, Honda and co-workers have identified IRF-7 as the most important IRF for Type I IFN- and MyD88-dependent responses in dendritic cells *in vitro* following viral infection using IRF-7-deficient mice. The authors suggest that IRF-7 may also control CD8+, or T-cell dependent mechanisms during viral infection (Honda et al., 2005; Hiscott, 2007).

Recognition of dsRNA has been considered as a primary event in the induction of Type I IFN since the discovery of receptors able to 'sense' pathogens. Toll-like receptors (TLRs) are members of the interleukin-1 receptor family, and so far 10 species have been identified in mice and humans (Akira et al., 2001; Vogel et al., 2003). TLR3 is an intracellular, endosomal dsRNA-specific receptor; TLR4 is a receptor for bacterial lipopolysaccharide (LPS) and the ssRNA-specific TLR7 have elicited substantial interest due to their strong links with type I IFN mechanisms and their role in antiviral responses (Hoshino, 1999; Heil et al., 2004; Kariko, 2004; Lund, 2004).

TLRs are genetically conserved, membrane-spanning receptors whose cytoplasmic or Toll-interleukin-1 receptor (TIR) domains are flanked by molecular adaptors, that transduce signal cascades upon extracellular ligand binding (Vogel et al., 2003). TLRs can induce IFN-α/β via several pathways involving molecular adaptors such as *my*eloid *d*ifferentiation factor-*88* (MyD88)

or *TI*R-*c*ontaining *a*daptor *m*olecule (TICAM-1, which is an IFN-α/β inducer) (Fitzgerald et al., 2003; Jiang et al., 2004). Factors such as interferon-regulatory factors (IRFs) are also involved in downstream cascades following TLR activation and their induction depends on a range of TIR-associated molecular adaptors. For instance, TICAM-1 has been identified as a requirement for TLR3 and TLR4-mediated IRF-3 and NF-κB induction (Oshiumi et al., 2003; Funami et al., 2008).

More recently, an antiviral signalling pathway consisting of the helicases *r*etinoic acid-*i*nducible *g*ene-*I* (RIG-I) and *m*elanoma *d*ifferentiation-*a*ssociated gene-*5* (MDA-5) was characterised. Initial studies revealed that polyinosine-polycytidylic acid (poly(I:C)), a synthetic dsRNA analogue, could be detected by the cytoplasmic helicases later identified as RIG-I/MDA-5, and confirmed their crucial role in viral infection (Kato et al., 2005; Kato et al., 2006). Upon binding of viral RNA to RIG-I, a caspase-activated recruitment domain (CARD) is activated and transduces signal to a mitochondrial-signalling complex known as mitochondrial antiviral signalling (MAVS). MAVS induces both NF-κB and IRF-3 activation pathways, which promote antiviral gene transcription (Seth et al., 2006). MDA-5 is believed to employ similar mechanisms for different isoforms of RNA strands.

It was found that RIG-I and MDA-5 differentially recognise RNA viruses and that RIG-I was essential to type I IFN induction, namely through the activation of IRF-3 and NF-κB (Yoneyama et al., 2004; Kato et al., 2006). The 5' triphosphate cap found on single-stranded RNA viruses was found to be the specific binding motif for RIG-I, while MDA-5 was involved in the detection of viruses lacking the 5' triphosphate end (such as Picornaviridae) as well as *in vitro*-transcribed RNA (Hornung et al., 2006; Pichlmair et al., 2006).

1.3.3.2 Type I IFN pathway: an overview of Jak/Stat signaling

Type I IFNs share a common IFN receptor which is composed of two 110kDa subunits (IFNAR1 and IFNAR2) that span the plasma membrane and are constituted of a ligand binding (extracellular) domain, a transmembrane portion and an adaptor-binding (cytoplasmic) domain (Pestka, 2000; Samuel, 2001). The extracellular domain is composed of four subdomains (SD), two of which (SD1 and SD3) are dedicated to ligand interaction, while SD2 and SD4 fulfil structural and adaptor binding functions (de Weerd et al., 2007). The C-terminal or intracellular domain of the Type I IFN

receptor is flanked by adaptor molecules such as the tyrosine kinase TYK2 and JAK1, a member of the Janus kinase family (Platanias and Fish, 1999; Cutrone and Langer, 2001).

Figure 1.5 summarises the mechanisms of Type I IFN induction and signal transduction pathways discussed in this section. Both Type I and Type II IFNs engage their respective transmembrane receptors, which in turn transduce signals via molecular adaptors bound to the receptor's cytoplasmic carboxy (C)-terminal portion. Upon engagement of the IFN receptor by Type I IFNs, the adaptor kinases are activated through conformational modifications and they in turn induce the phosphorylation of Tyr^{466} and Tyr^{481} residues on *s*ignal *t*ransducers and *a*ctivators of *t*ranscription STAT-1 and STAT-2 which dimerise in the cytoplasm and allow the recruitment of p48, a transcription factor (David, 2002; de Weerd et al., 2007). The resulting complex, termed interferon-stimulated gene factor 3 (ISGF3), translocates to the nucleus to bind a consensus DNA sequence known as interferon-stimulated regulatory element (ISRE). The bound transcription factor induces ISRE promoter initiation and early response gene activation (Haque et al., 2000). Type I IFNR activation can also lead to a Type-II IFN-associated STAT-1 homodimer, which translocates to the nucleus to bind the IFN-γ-activated sequence (GAS) or the IFN-γ-response region (GRR) (David, 2002).

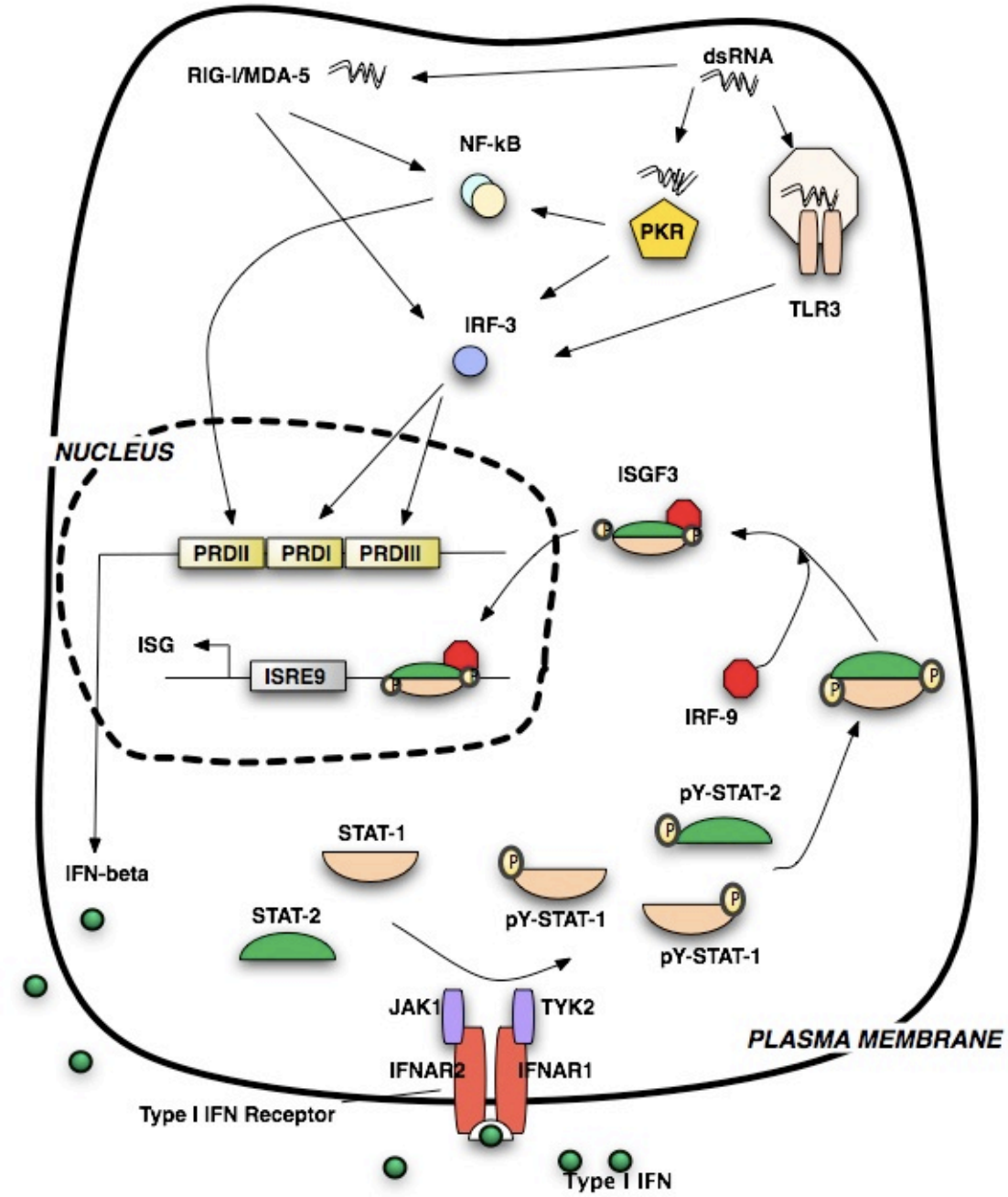

Figure 1.5: Schematic of Type I IFN signalling pathways. Induction of Type I IFN by double-stranded RNA (dsRNA) **(Top)** and Jak/Stat signalling pathway mechanisms of Type I IFN receptor induction **(Bottom)**. Viral, dsRNA is detected by cytoplasmic proteins PKR, TLR-3 and the RIG-I/MDA-5 complex, which in turn activate NF-κB and/or IRF-3. Translocation of NF-κB and IRF-3 to the nucleus and binding to specific consensus sites results in the transcription of IFN-β gene and secretion of IFN-β into the extracellular milieu. The bottom of the diagram describes the Jak/Stat signalling pathway following binding of IFN-α/β to the Type I IFN receptor. Receptor engagement induces phosphorylation of Janus kinases Jak1 and Tyk2, which in turn recruit and phosphorylate STAT-1 and STAT-2. Activated STATs associate as heterodimers (STAT-1/STAT-2) and recruit IRF-9, to form the ISGF-3 complex. ISGF-3 translocates to the nucleus and binds an interferon-stimulated response element (ISRE), resulting in the expression of interferon-stimulated genes (ISGs).

1.3.3.3 Interference with host antiviral pathways

As described earlier, viral infections induce a number of antiviral defence mechanisms aimed at inhibiting viral replication, however some viruses have evolved to circumvent these responses. Some RNA viruses are believed to have benefited from structural changes allowing them either to remain undetected by the host immune system or to interfere with viral genome recognition systems. Retroviruses such as HIV are known to elude T cell immune surveillance by concealing their genome within the host cell nucleus (Levy, 1993). Other viruses that cannot conceal their presence in the midst of their host's genome employ alternative means of evasion.

Vaccinia virus (VV), for example, is known to interfere with the PKR system, through the action of two viral proteins, E3L and E3K. These proteins were found to inhibit the phosphorylation of eIF-2a, subsequently inhibiting PKR activity following VV infection (Davies et al., 1993). Similarly, Epstein-Barr virus SM protein was found to actively bind PKR and inhibit its activity, a feature considered common across Herpesviruses (Poppers et al., 2003). Paramyxoviruses such as Measles (MV) and Respiratory Syncytial viruses (RSV), have also been reported to circumvent Type I IFN responses by avoiding STAT-1 and STAT-2- signalling mechanisms (Young et al., 2000; Gotoh et al., 2002). Interestingly, it was found that with members of the *Bunyaviridae* and *Flaviridae* family, modulation of IFN response was mediated by non-structural proteins, like NS in Rift Valley Fever virus (RVFV) or NS2A in Kunjin virus (KUNV), both of which are arthropod-borne viruses (Billecocq et al., 2004; Liu et al., 2004). HIV virus has also been found to interact with antiviral responses. Bour and colleagues identified the Vpu protein, which binds to the CD4 receptor on T helper lymphocytes, as a specific NF-κB inhibitor and suggest that Vpu contributes to the modulation of NF-κB-dependent cytokine signalling (Bour et al., 2001). A summary of mechanisms of viral interference with host immune response pathways is displayed in **Figure 1.6**.

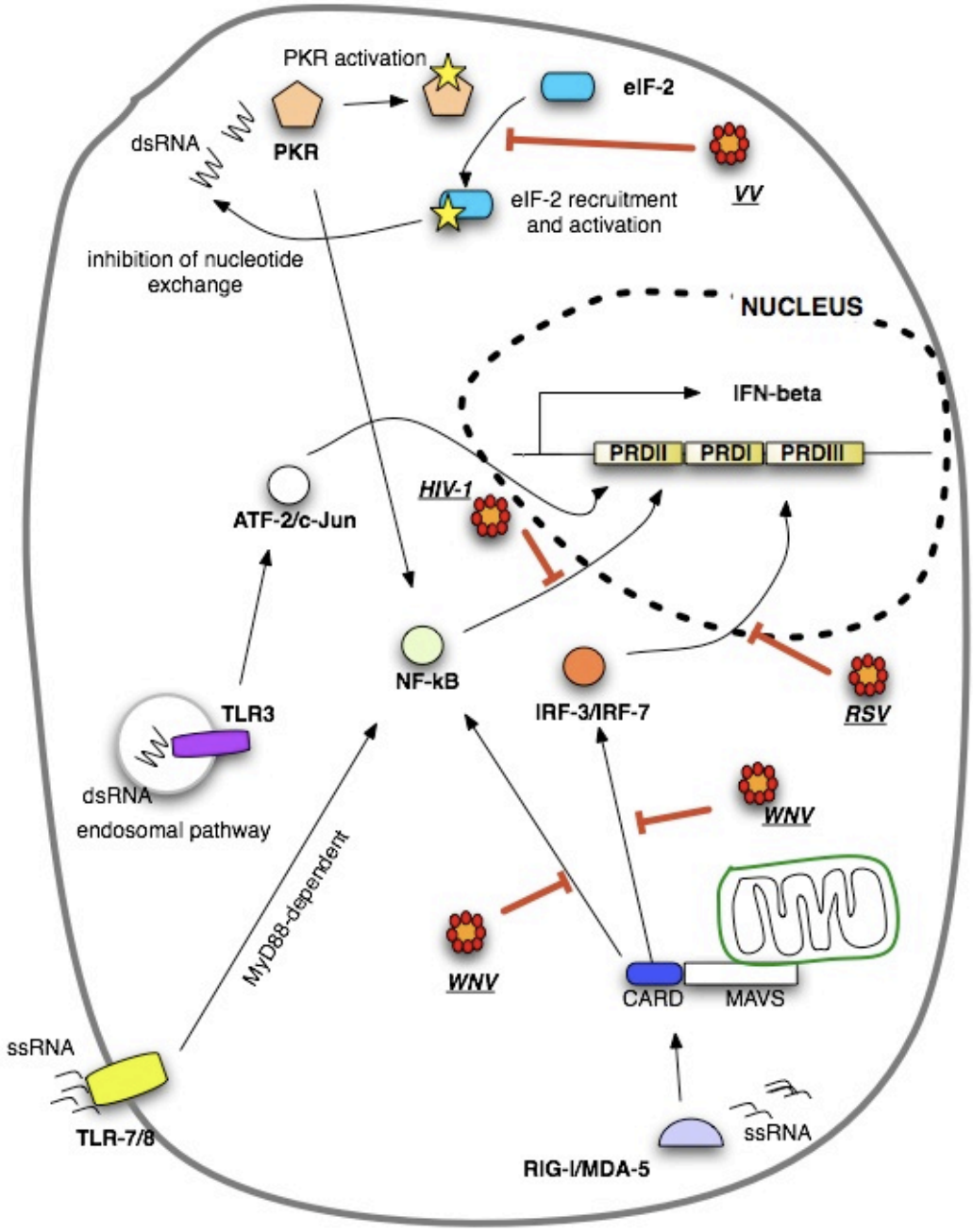

Figure 1.6: An overview of antiviral pathways and viral evasion mechanisms. The PKR system involves the activation of eIF-2a, which inhibits viral genome transcription. The eIF2-a recruitment process was found to be inhibited by Vaccinia virus (VV). The RIG-I/MDA-5 pathway recognises ssRNA and relays a signal through mitochondrial activation system MAVS. Adjacent activation domains (CARD) promote activation of IRFs and NF-κB, which stimulate Type I IFN gene expression. West Nile virus (WNV), Human Immunodeficiency virus-1 (HIV-1) and Respiratory Syncytial virus (RSV) have been found to interfere with NF-κB and IRF activation processes, preventing Type I IFN induction. The TLR system recognises ssRNA (TLR3) and dsRNA (TLR7/8) leading to the activation of transcription factors NF-κB and ATF-2/c-Jun, resulting in the induction of an 'antiviral state'.

Alphaviruses are also known for their capabilities to evade the host's immune system. The Kunjin strain of West Nile virus (WNV), found in the Asia-Pacific region, was found to interfere with Type I IFN signalling via its non-strutural protein, NS2A (Liu et al., 2004). Interestingly, WNV was shown to delay the induction of transcription factor IRF-3 and subsequent RIG-I mediated antiviral responses (Fredericksen and Gale, 2006). This 'delayed' IRF pattern was also observed by Scherbik and co-workers, who found IRF-I and IRF-7 activation to be delayed, and suggested that WNV downregulates the expression of some ISGs (Scherbik et al., 2007). The E glycoprotein of WNV, and arthropod-derived glycoprotein envelopes, were shown by Arjona and colleagues to inhibit dsRNA-induced responses independently of TLR-3 (Arjona et al., 2007). This accords with other findings that mosquito cell-derived RRV suppresses Type I IFN responses in primary myeloid dendritic cells, although the mechanisms are, as yet, unknown (Shabman et al., 2007).

1.3.3.4 Cell membrane interactions: a focus on mosquito cell-derived viruses

The ability of several arthropod-borne viruses to circumvent host immune responses raises questions about the role of the vector, in the acquisition of specific vector-derived cell membrane attributes. Some studies support the idea that during transmission of the virus from arthropod to mammalian host, some vector components such as saliva in mosquitoes can interfere with host immune responses (Limesand et al., 2000; Limesand et al., 2003; Schneider et al., 2004). One of these studies reports that Sindbis virus (SINV), an alphavirus, was shown to down-regulate the expression of type I and type II interferons when inoculated in the presence of mosquito salivary gland extract (Schneider et al., 2004).

However, other factors such as membrane structure and glycoprotein composition are believed to confer mosquito-cell derived viruses immunosuppressive properties. The surface of mammalian cells is composed of complex glycans and carbohydrate moieties, whereas the mosquito cell membrane is mostly constituted of mannose glycans. Several studies suggest that high mannosylated, mosquito-cell derived virus particles show better binding and entry efficiency than the mammalian cell-derived virus. For example, the macrophage mannose receptor was found to enhance binding and entry of DENV, and anti-MR antibodies were found to prevent DENV infection (Miller et al., 2008).

Lozach and co-workers showed that Dengue virus (DV) derived from mosquito cells is able to infect mouse dendritic cells via a specific receptor known as dendritic cell-specific ICAM-3 grabbing non-integrin (DC-SIGN) (Lozach et al., 2005). These observations corroborated earlier observations by Klimstra and colleagues that the presence of DC-SIGN resulted in differences in infectivity between mammalian and mosquito-cell derived DV (Klimstra et al., 2003). It has also been reported that several viruses, such as HIV, HCV, and CMV can use DC-SIGN as entry portal, which results, in some cases, in a decreased antiviral response (van Kooyk and Geijtenbeek, 2003; van Kooyk et al., 2004). However, some studies showing enhanced entry SINV and WNV via DC-SIGN suggest that arthropod-borne viruses, including alphaviruses, are likely to benefit from characteristics derived from mosquito cell membranes (Klimstra et al., 2003; Davis et al., 2006).

A recent study showed that mosquito cell-derived RRV could infect murine myeloid dendritic cells (mDCs) more efficiently than mammalian cell-derived RRV (Shabman et al., 2007). The authors investigated the differences in type I IFN induction of mDCs infected by either mammalian or mosquito cell-derived RRV, and found that the latter failed to induce a significant IFN response. The ability for mosquito-derived RRV to induce type I IFN was restored following one passage in mammalian cells, suggesting that components of the mosquito cell-derived membrane could be responsible for the differential induction observed (Shabman et al., 2007). Additionally, the authors observed a similar effect with the alphaviruses Barmah Forest (BFV) and Venezuelian Equine Encephalitis viruses (VEEV) and suggest a determining role for N-linked glycans located on glycoprotein moieties in hampering Type I IFN induction in mDCs (Shabman et al., 2007).

The establishment of a mouse model of RRV disease has enabled researchers to pinpoint specific mechanisms leading to disease symptoms, such as the role of macrophages in joint inflammation and the involvement of host factors in the elaboration of immune responses leading to symptoms. Recent findings suggest that RRV employs a complex network of cellular and soluble components to induce disease and to interact with the host's immune system. Differences in infectivity of RRV have been found between strains grown in mammalian and mosquito cells, suggesting a strong correlation between host-derived cell membrane, entry mechanisms and, possibly, immune evasion (Shabman et al., 2007). However more studies are required to determine the precise nature of virus-host interaction and the role it plays in disease pathogenesis. There is currently no vaccine or specific cure for RRVD and the exact nature of cellular and physiological mechanisms in RRV-induced arthritis remain unclear.

1.4 Thesis objectives

The first aim of this study was to investigate the differences in infectivity between mammalian cell (Vero)- and mosquito cell (C6/36)-derived RRV, (mam- and mos-RRV respectively) in selected cell lines. The ability of both mam- and mos-RRV to induce Type I interferons in IFN-producing cells was also examined. The expression of Type I IFN-associated transcription factors involved in antiviral responses following infection with mam- or mos-RRV was also examined.

The second aim of this study was to investigate the role of TNF-α inhibition in RRVD pathogenesis by treating RRV-infected mice with a TNF-α inhibitor drug, Enbrel. Clinical signs of disease and weight change were analysed and the extent of muscle and joint inflammation compared between treated and untreated RRV-infected mice by histological analysis. The differences in expression of host factors in muscle and joint tissue were also investigated.

The third and final aim of this study was to investigate the role of and requirement for NK cells in RRVD pathogenesis. By adapting the wild-type, mouse model of RRV disease to a NK-dysfunctional strain, $Lyst^{bg}$ or Beige, we assessed the differences in disease development between wild-type and $Lyst^{bg}$ mice. Disease progression and the extent of tissue inflammation were compared between RRV-infected $Lyst^{bg}$ and wild type mice. Differential expression of host factors in the muscle and joint tissue was also compared between RRV-infected $Lyst^{bg}$ and wild type mice.

2. Materials and Methods

2.1 Cell culture

RAW264.7 (ATCC#TIB-71) were cultured in RPMI 1640® (Gibco) containing 10% Foetal Calf Serum (FCS) (Cambrex) accordingly to ATCC methodolgy. JAWSII cells (ATCC# CRL-11904) were cultured in RPMI 1640 supplemented with 10 ng/mL recombinant mouse GM-CSF (R&D) and 10% FCS and grown in a humidified 37°C incubator supplied with 5% $CO_{2.}$. Vero (ATCC# CCL-81) and L929 cells (ATCC# CCL-1) were cultured in Dulbecco's Minimal Essential Medium (DMEM) (Gibco®) containing 5% Newborn Calf Serum (Cambrex, Australia). Cells were maintained in a humidified 37°C incubator supplied with 5% CO_2 and were subcultured using 0.25% Trypsin (Sigma). C6/36 cells, derived from *Aedes albopictus* (ATCC# CCL-1660) were cultured in RPMI 1640 containing 10% FCS and maintained in a humidified incubator at 29°C and supplied with 5% $CO_{2.}$ All bovine serum used was heat-inactivated at 56°C for 30 minutes.

2.2 Virus propagation, purification and titration

Ross River virus (RRV) was generated from the T48 (RRV-T48) infectious plasmid clone following electroporation in mammalian (Vero) or mosquito (C6/36) cells. Confluent cell monolayers of Vero or C6/36 cells were inoculated with 10^5 PFU RRV-T48 and the virus was allowed to adsorb for 90 minutes. Cells were supplied with culture medium (DMEM, 10% FCS) and were incubated for 48-72 hours, or until cytopathic effect (CPE) was detected. The supernatant was collected and virus purified by ultracentrifugation over a 20% sucrose cushion at 120,000 x g in a Hitachi CPW900X ultracentrifuge (Hitachi). Purifed virus was resuspended in PBS, aliquoted and titrated by plaque assay, as described below. For RRV plaque assays, monolayers of Vero cells were grown in 24-well plates overnight and inoculated with 10-fold serial dilutions of mam-RRV or mos-RRV and allowed to adsorb for 2 hours at 37°C in the presence of serum-free DMEM medium. The inoculum was then replaced by a semi-solid agar medium (0.2% agarose in DMEM + 10% FCS) and the plates were incubated for 48-72 hours. The semi-solid medium was aspirated, and the monolayers stained using 0.01 % crystal violet. Plaques were counted and titres were determined in plaque forming units per mL (PFU/mL). In experiments describing the use of mam-RRV and mos-RRV (Chapter 3), mam-RRV refers to RRV propagated in Vero (mammalian) cells, while mos-RRV refers to RRV propagated in C6/36 (mosquito) cells.

2.3 Cell treatment

Where indicated, mouse recombinant IFN-α and IFN-β (R&D) were used in stimulation experiments at concentrations of 1, 10, 100 or 1000 IU/mL. Cells were washed with PBS before addition of either IFN-α or IFN-β in serum-free RPMI 1640 (Gibco). Cells were incubated for 3 hours before the stimulant culture medium was removed and virus was added in fresh RPMI 1640 supplemented with 5% FCS. Poly(I:C) (Sigma) was used as a single strand RNA control at concentrations of 250 ng/mL. Vero cells were stimulated with poly(I:C) 3 hours prior to infection with either mam- or mos-RRV, following the same process as described for the IFN-α and IFN-β stimulation experiments.

2.4 Monoclonal antibody purification

Anti-mouse NK1.1 monoclonal antibody (IgG_2a,k) was harvested from PK136 hybridoma clones (generously provided by Hilary Warren, Cancer Research Unit, Canberra Hospital). Briefly, hybridomas were cultured in serum-free hybridoma PHFM II medium (Gibco) for 6 days when the supernatants were collected. The supernatant was then dyalised against a phosphate buffer saline (PBS; pH 7.9) with light stirring and multiple buffer changes. Antibodies were then titrated by direct ELISA, using a rabbit anti-mouse IgG-HRP (hydrogen peroxidase conjugate; Sigma A9044) as capture antibody. Briefly, PK136 antibodies were serially diluted and adsorbed overnight at 4ºC on an ELISA plate with carbonate coating buffer (0.1M Na_2CO3, 0.1 $MNaHCO_3$). The plate was washed with washing buffer (PBS, 0.5% Tween20) The detection antibody was serially diluted and incubated for 1h at 37ºC. *o*-Phenylenediamine dihydrochloride (FAST-OPD; Sigma) was added to each well and the colour substrate was allowed to develop for 30 minutes at 25°C. Absorbances were read in an ELISA plate-reader (BioRad) at 450 nm.

2.5 SDS-PAGE and Western Blotting

Protein extracts from infected cells were analysed by sodium-dodecyl sulphate polyacrylamide gel electropohoresis (SDS-PAGE), based on the method described by Laemmli (Laemmli, 1970). RRV-infected RAW264.7 cells were washed with PBS and scraped off the flask, then spun to a pellet by

centrifugation for 5 minutes at 300 x g. The pellet was resuspended in commercial cell lysis buffer (Pierce) and nuclear and cytoplasmic fractions were separated using NE-PER, a nuclear protein extraction kit (Pierce). Protein fractions were quantitated by Bradford Reagent (BioRad) assay to ensure equal protein loading and heat-denatured (5 minutes at 95°C) in a reducing loading 4X SDS buffer (0.25 M Tris pH 6.8, 20% SDS, glycerol, bromophenol blue and b-mercaptoethanol). Samples were loaded on a 12% SDS-PAGE gel cassette (Bio-Rad) and run in SDS running buffer (196mM glycine, 50 mM Tris-CHl, 0.1% SDS, pH 8.3) for 2 hours at 120 volts. Protein was transferred from the gel onto a Hybond® polyvinylidene difluoride (PVDF) membrane (Amersham Biosciences) in a Mini Trans-Blot transfer cassette (Bio-Rad). Proteins were transferred for 2 hours at 160V in cold transfer buffer (0.025 M Tris, 0.192 M Glycine, 30% Methanol). The PVDF membrane was blocked in ECL Blocking Agent (GE Healthcare) (2% in Tris-buffered saline (TBS) with 0.01% Tween20 (TBS-T)) for 1 hour at RT. Primary antibody (anti-IRF-3 (Santa Cruz), anti-G3PDH (Trevigen), anti-PKR-PhosphoDetect™ ($pThr^{451}$) (Calbiochem), anti-pStat-1 (Santa Cruz)) were applied where indicated at optimised concentrations in blocking agent overnight at 4°C. Primary antibody was washed off with TBS-T, and the membrane incubated with secondary antibody (anti-rabbit-HRP-IgG or anti-mouse-HRP-IgG conjugates, Sigma) in TBS-T for 1 hour at RT.

The membrane was washed in TBS-T then incubated in ECL Chemiluminescent Detection System (GE Healthcare), according to manufacturer's instructions. The membrane was exposed to ECL Hyperfilm (GE Healthcare) in a Kodak Exposure cassette and developed in Kodak Developer and Fixer reagents (Kodak). Photographs were taken using a Transwhite Illuminator and a Bio-Rad Gel Doc camera system (Bio-Rad) and processed using Quantity One software (Bio-Rad).

2.6 Reporter Luciferase Systems

Reporter luciferase plasmid constructs pIFΔ(-125/+72)Lucter and pISRE(9-27)Lucter (generously donated by A.Prof A. Suhrbier, QIMR) were used in experiments involving transient transfection of RAW264.7 cells and JAWSII cells. **Figure 2.1** shows the plasmid maps of these reporter luciferase constructs.

Briefly, plasmids were transformed by heat-shock into XL-1 Blue MRF' Supercompetent cells (Stratagene; #200230) as per manufacturer's instructions. Cells were cultured in selective Ampicillin (100mg/mL) LB medium (Oxoid) and transformant colonies were grown at 37°C in a shaking incubator for 16-20 hours. Cells were collected and streaked onto LB (Amp) plates for colony screening. Colonies were picked and plasmid was extracted and purified using a Maxi-Prep Kit (Promega) according to manufacturer's instructions. The recovered plasmids were digested using *EcoRI* restriction enzyme (Roche Diagnostics), following the manufacturer's instructions, and plasmid digest sizes were verified by agarose gel electrophoresis. Plasmid integrity and concentration were assessed by agarose gel electrophoresis and spectrophotometry. JAWSII and RAW264.7 cells were transfected using a GeneJammer transfection reagent (Stratagene). JAWSII cells were co-transfected with 2 mg of pISRE(9-27)Lucter and pCMV-βGal (Promega) plasmids, whereas RAW264.7 cells were co-transfected with pIFΔ(-125/+72)Lucter and pCMV-βGal plasmids according to the manufacturer's instructions. For reporter assays, cells were harvested at each time point and processed for measurement of luciferase activity (Luciferase Reporter Assay Kit, Promega) and b-galactosidase activity as an internal control (β-galactosidase Reporter Assay Kit, Promega) according to the manufacturer's instructions. Luciferase activity was read on a Ascent Luminoskan (Pathtech) and b-galactosidase activity was measured on a UV-Visible microplate reader at 495 nm (Bio-Rad) as per the manufacturer's instructions.

2.7 Mice: Strains, handling and disease score

In vivo RRV experiments were performed using 20 to 21 day-old mice of the C57BL/6J and Beige or Lyst^{bg} (C57BL/6J-Lyst^{bg}/Arc) background purchased from the Animal Resources Facility (WA, Australia). Mice were inoculated subcutaneously in the axillary

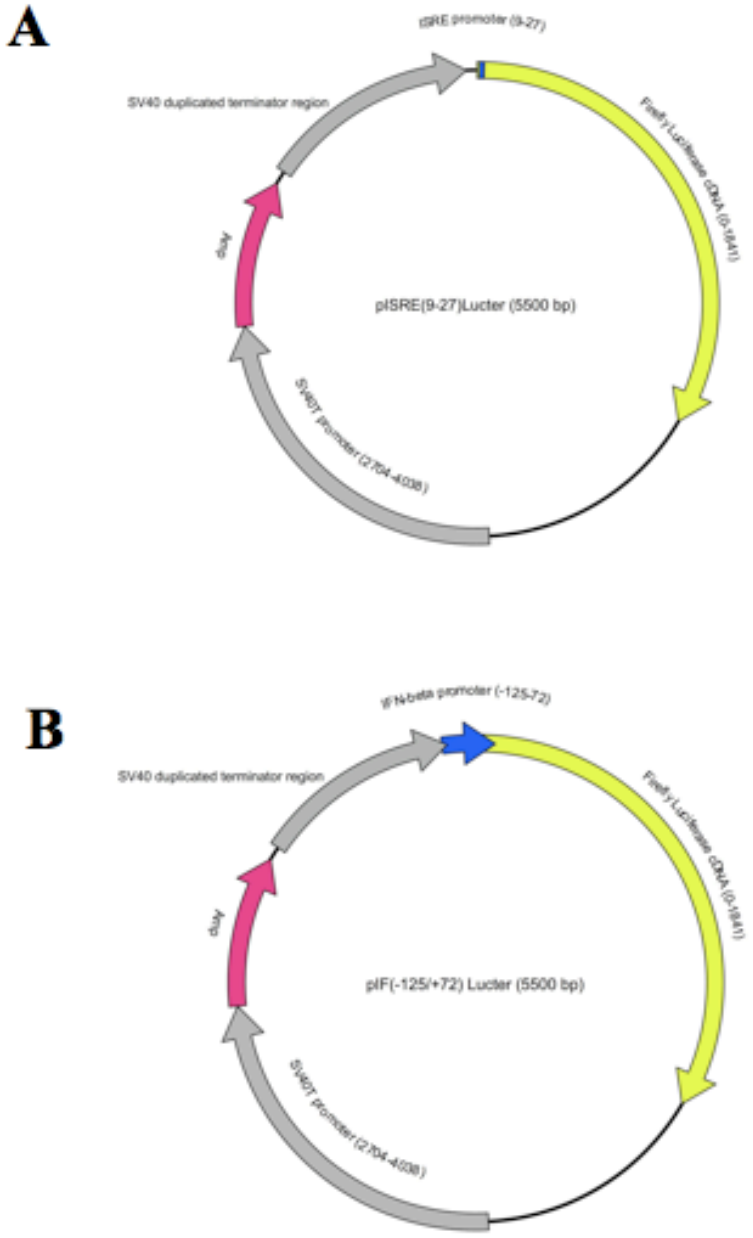

Figure 2.1: Maps of the reporter luciferase plasmids used in *in vitro* experiments (kind gift from Assoc.Pr. Andreas Suhrbier, QIMR). **(A)** pISRE(9-27)Lucter and **(B)** pIFΔ(-125/+72)Lucter plasmid constructs were transfected in JAWSII and RAW264.7 cells, respectively, to determine ISRE or IFN-β promoter activation following infection with RRV. Luciferase activity was normalised to β-galactosidase expression read in a luminometer.

area with 10^3 PFU of purified RRV (T48 strain) in 100 ml PBS (pH 7.2) and monitored daily for weight change and clinical score progression (See **Table 2.1**). Control mice were injected with 100 ml diluent (PBS) alone. All mice were kept in a rodent facility under the approval of the Animal Ethics Committee (CAEC#06-14).

Table 2.1: Descriptive clinical score for Ross River virus disease. Symptoms observed in 20-21 day-old C57BL/6J mice infected with 10^3 PFU of RRV T48 subcutaneously.

SCORE	Disease Symptoms and Signs
0	No symptoms
1	Mild symptoms - ruffled fur
2	Mild disease - lethargy, sunken eyes
3	Moderate disease - hind limb dragging, mild paresis
4	Severe disease - moderate to advances paresis
5	Death

In the Enbrel studies, mice were inoculated with 400 μg/g bodyweight Enbrel (in sterile double distilled (dd) H_2O) intraperitoneally on days 1, 3, 5, 7, 9, 11, 13, 15 and 17 days post-infection. Enbrel-treated, uninfected control mice received identical treatment frequency and dosage.

In NK1.1/PK136 depletion studies, mice were inoculated intraperitoneally with 200 μg of the monoclonal PK136 antibody one day prior to infection. After RRV inoculation, the antibody solution was administered every 2 days via the intraperitoneal route. Mice were euthanised upon disease manifestation or where indicated by CO_2 asphyxiation following anaesthesia using Methoxyflurane. Muscle and joint samples were collected and processed for measurement of viral titres, RNA extraction, flow cytometry, histology and *in-situ* hybridisation where indicated. For viral titres, tissue was snap frozen then homogenised in 100 μL PBS. Samples for RNA extraction were frozen in RNAwiz RNA extraction reagent (Ambion), then processed as described in Section ***2.8***. For histology and *in situ* hybridisation, tissue was fixed as described in Section ***2.12*** and processed at the Histology Facilities at the ANU.

2.8 mRNA extraction and quantitative real-time PCR

RNA extraction was performed on RRV-infected cells and tissues to determine host factor expression profiles at selected timepoints. Infected cells were collected by scraping, then centrifuged and the supernatant discarded. The pellet was resuspended in 500 μL RNAwiz extraction reagent (Ambion). Tissue collected from mice was minced and homogenised in 500 mL RNAwiz, and RNA recovered following manufacturer's instructions. RNA concentration was quantified on a UV-VIS Spectrophotometer (Hitachi) at 260 nm and purity (>1.8) determined by OD_{260}/OD_{280}. RNA was transcribed to cDNA using M-MLV Reverse Transcriptase (RT) (Sigma). Briefly, for each sample 5 μg total RNA was transcribed in a RT mix consisting of 10X RT buffer (Sigma), 25 mM deoxynucleotides triphosphate (dNTP) (Promega), 10 mM Oligo $d(T)_{15}$ (Promega), 20 U RNAsin ribonuclease inhibitor (Promega) and diethylpyrocarbonate (DEPC)-treated water (0.01%). RNA was incubated for 10 minutes at 37°C with dNTPs and Oligo $d(T)_{15}$ followed by the addition of RT and incubated for 1 hour at 72°C in an Eppendorf Master Cycler™ (Eppendorf®, Germany).

Recovered cDNA was quantified by spectrophotometry (as described above) and optimised at 150 ng/mL for quantitative real-time PCR. Reactions were performed using Roche MasterMix™ SYBR I (Roche Molecular Biochemicals) and analysed with a Corbett Rotorgene™ 3000 (Corbett Life Sciences, Australia). Primer assay kits designed for real-time PCR were purchased from QIAGEN. Amplicon lengths and target sequence size are shown in **Table 2.2.** Comparative quantitation of mRNA levels and statistical significance analyses were performed using the Relative Expression Software Tool (REST™-RG, Version 3©) (Pfaffl et al., 2002). Cytokine and host factor expression levels were normalised against housekeeping gene (HKG) levels using a pairwise fixed reallocation randomisation test. HKGs were selected using a gene normalisation panel (Quantace) and Bestkeeper© (Version 1.0) (Pfaffl et al., 2004). The data was then tabulated and plotted using the GraphPad© Prism software version 4.0b (GraphPad Software Inc.).

Table 2.2 : List of Quantitect Assay primers used in quantitative real-time PCR. The Medline accession ID number is given for the gene transcript recognised by the primers, including transcript and amplicon length.

Gene name	Transcript ID	Transcript length (bp)	Amplicon length (bp)
HPRT	NM013556	1349	168
GAPDH	NM008084	1243	100
IFN-α	NM010503	573	111
IFN-β	NM010510	770	119
IFN-γ	NM008337	1207	168
IL-10	NM010548	1314	103
IL-15	NM008357	1250	93
CCL-2/MCP-1	NM011333	806	118
CCL-3/MIP-1a	NM011337	804	107
CCL-5/RANTES	NM013653	579	107
NOS-2	NM010927	3990	118
TNF-α	NM013693	1619	112
CXCL10/IP-10	NM021274	1063	92

2.9 Flow cytometry

Muscle tissue was collected from infected and control Lyst^{bg} mice and prepared for flow cytometry analysis. Briefly, muscle tissue was ground and minced with scissors in digestion buffer (RPMI 1640, 10% FCS, 1 mg/mL DNase I (Sigma), 1 mg/mL Collagenase A/Dispase (Roche Molecular Biochemicals) and incubated at 37ºC with vigorous shaking for 2 hours. Digests were flushed through a sterile mesh strainer (BD Biosciences) in RPMI with 10% FCS, then centrifuged at 1,200 rpm and resuspended for counting. Cells were resuspended in staining buffer (PBS, pH 7.9; 0.5% bovine serum albumin; 0.02% NaN_3) and labelled with fluorochrome-conjugated anti-mouse CD11b or Pan-NK (DX5) antibodies (R&D). Labelling was allowed for 30 min on ice, then cells

were washed and fixed in 0.5% paraformaldehyde. Cells were analysed through a FACScalibur (Beckman-Coulter) flow cytometer and data was generated using CellQuest Pro. All samples were processed at the Flow Cytometry facilities at the John Curtin School of Medical Research (ANU).

2.10 Differential cell staining

Differential leukocyte staining was performed on muscle and joint tissue homogenates of mice showing disease following RRV infection. Samples were collected the day symptoms were most representative of RRVD. Briefly, muscle and joint tissue was collected and incubated in digestion buffer (See Section ***2.9*****),** minced and placed in a shaking incubator for 2 hours at 37°C. Excess tissue debris was excluded by straining (BD Bioscience) and cell suspensions were applied onto a microscope slide. Cells were air-dried, then fixed in methanol for 10 minutes. Slides were then dipped in May-Grumwald stain for 5 minutes, then in Giemsa counterstain for 15 minutes. Cells were finally washed in water for 10 minutes. Glass coverslips were mounted using Eukitt medium (Carl Zeiss, Germany). Cells were counted (at least 100 per high power field (HPF; 400x magnification)) using a Compudiff 200X counter (Molek Scientific Equipment, Sweden) and ratios expressed as percent HPF.

Fluorescence Microscopy

For *in vitro* immunofluorescence microscopy, cells were seeded onto coverslips in 24-well plates (Iwaki). After infection, cells were fixed using warm 0.5% paraformaldehyde in PBS for 10 minutes, then washed with PBS three times for 5 minutes each. Cells were then washed with ddH_2O and primary anti-RRV polyclonal antibody from hyperimmune ascitic fluid (ATCC# VR373) was applied at an optimised dilution (1:750) in PBS with 5% goat serum (Sigma). The antibody was incubated for 45 minutes at RT, then washed three times with PBS/Triton (0.05%) (Sigma). A fluorescein-isothiocyanate (FITC)-labelled secondary antibody (AlexaFluor®488, Invitrogen) was applied (1:2000, in PBS/5% goat serum) and incubated for 45 minutes at RT. The secondary antibody was washed off with PBS/Triton X-100 (0.05%) and cells incubated with 4',6-diamidino-2-phenylindole (DAPI) nuclear stain (Sigma) for 1 minute. Slides were washed with PBS, then deionized water and mounted with Fluoromount-G (Southern Biotech) onto microscope slides. Images were taken on a Nikon Eclipse TE300 microscope, equipped with a SPOT Xplorer XS 1.4MP Monochrome camera (Diagnostic Instruments Inc.) and controlled by a Lambda 10-2

(Sutter instrument) wheel shutter controller. Data was acquired using Spot software (Diagnostic Instruments Inc.).

2.12 RRV Riboprobe preparation and In-Situ Hybridisation

A riboprobe targeting a conserved portion of the E2 glycoprotein sequence of RRV T48 genome was constructed to detect viral RNA in muscle and joint tissue of RRV-infected mice by *in situ* hybridisation. Briefly, total RNA was isolated from purified RRV T48 and primers were designed (Sigma Genosys) to amplify a 441 bp fragment (nucleotides 7311 – 7450) flanked by *EcoRI* and *HindIII* restriction sites. The fragment was then inserted into a pSPT18 vector plasmid (Boehringer Mannheim) alongside an *Sp6* promoter site. The plasmid was linearised by digestion with *EcoRI* and/or *HindIII* to generate E2-specific forward and reverse strands, while the integrity of the insert was verified by agarose gel electrophoresis. Bands were excised from the gel and bands containing the insert of interest were purified using the ultra-free MC purification kit (Millipore). The sequence-specific region was then reverse transcribed using an RNA polymerase *Sp6* (Roche Molecular Biochemicals) and subsequently labelled with digoxigenin (DIG) using a DIG-labelling kit (Roche Molecular Biochemicals).

The 441-bp forward sense probe (5'-CAAGATGAAGATCGTAGGCGTG-3') was generated by PCR using Proof Start DNA polymerase (Qiagen) and verifed by agarose gel electrophoresis. Prior to quantification and optimisation, the probe was concentrated by lithium chloride (4M LiCl) precipitation. Probe quantities were determined by southern hybridisation to allow the use of optimal working dilutions. Briefly 0.1 to 1 ng probe were fixed by dot-blotting on a Hybond N+ charged membrane (Amersham) using a UV crosslinker for 2 min at 1800kJ (UVP-CL1000), and detected according to the manufacturer's instructions (Roche Molecular Biochemicals). Muscle and joint samples from mice were fixed in 3.5% formaldehyde in DEPC-PBS, imbedded in paraffin and cut to 4 mm-thick sections onto silane-coated slides. Tissue sections were deparaffinised with Xylene for 10 min, then dehydrated in decreasing concentrations of ethanol in DEPC-H_2O (100%, 90%, 70%). Slides were washed in DEPC-PBS and DEPC-H_2O, then rinsed in 0.1M triethanolamine (Sigma). After the addition of 50 mM dithiothreitol (DTT), slides were incubated for 30 min at RT. Sections were treated with Proteinase K (Fluka) (2 and 5 mg/mL) and incubated for 60 minutes at 60ºC.

Slides were washed and incubated with DIG-labelled RRV probe, baked at 94ºC for 5 minutes then incubated overnight at 60ºC in a XTRON HI 2002 hybridisation oven (Bartelt Instruments),

following manufacturer's instructions (Roche Molecular Biochemicals). A secondary, alkaline phosphatase-labelled anti-DIG F'*ab* fragment antibody (Roche Molecular Biochemicals) was used to detect the probe in muscle and joint tissue sections and subsequently developed using NBT/ BCIP reagent overnight at 4ºC (Roche Molecular Biochemicals) according to the manufacturer's instructions. After 3 final washes in maleic acid buffer (0.1 M maleic acid, 150 mM NaCl, pH 7.5, in DEPC-H_2O), slides were counterstained in Fast Green stain (0.01% in 90% ethanol) and mounted using an aqueous-based mounting medium (Sigma) and dried prior to microscopical analysis.

3.1 Introduction

RRV is transmitted by mosquitoes, and was shown to target and replicate to high titres in salivary gland endothelium; mosquitoes are known to inject saliva in the host's bloodstream as a blood-thinning agent, before feeding on blood (Harley et al., 2001). Several arboviruses have been the subject of studies aimed at characterising the differences in immune cell responses following infection with mammalian- or mosquito-cell membrane-derived virus. For example, modifications to the E and NS proteins of Dengue virus (DV) were observed following serial passages into mammalian and mosquito cells (Chen et al., 2003). The study by Chen and co-workers showed that nucleotide and amino acid sequences are subject to modifications following several passages in Vero (mammalian) or C6/36 (mosquito) cells. The study concludes that passages in C6/36 cells have a stabilising effect on DV genome, suggesting that traits such as infectivity and virulence may be associated to this phenomenon, which may well have evolutionary implications (Chen et al., 2003).

The manner in which mammalian- or mosquito cell-derived viruses interact with host cells has also been the focus of several investigations. Differences in glycoprotein glycosylation between mammalian and mosquito cell membranes have helped identify some key entry mechanisms characteristics of well-characterised arboviruses such as DV. A study reports that DV lacking a glycolsylation site (Asn67) on its envelope protein (E) was unable to replicate in mammalian cells (Mondotte et al., 2007). However, this Asn67 mutant E protein was efficiently produced in mosquito cells, while mammalian cells failed to synthesise this component, thus preventing virion assembly, suggesting important roles for host cells during viral replication.

Studies on glycosylation patterns of mammalian- and mosquito-cell-derived arboviruses allowed the identification of specific attachment receptors. DV was shown to preferentially infect cells expressing C-type lectins, such as DC-SIGN (dendritic cell-specific intercellular adhesion molecule 3-grabbing nonintegrin) and its related liver and lymph-node associated protein, L-SIGN (Tassaneetrithep et al., 2003). Interestingly, cells expressing DC-SIGN are dendritic cells, which are potent mediators of antiviral responses and key regulators of adaptive immune processes, which suggests that viruses using DC-SIGN as receptors must also employ strategies to evade recognition and degradation of their genome by sensitive cells such as DCs (Geijtenbeek and van Kooyk, 2003). Several viruses have been shown to use DC-SIGN/L-SIGN to infect immune cells, such as Hepatitis C virus (HCV), West Nile virus (WNV), Sindbis virus (SV) as well as Human Immunodeficiency

virus (HIV) (Steinman, 2000; Klimstra et al., 2003; Lozach et al., 2003; Tassaneetrithep et al., 2003; Cambi et al., 2004; Davis et al., 2006)

More recently, a study investigating differential infectivity of WNV passaged in mammalian and mosquito cells revealed that mosquito cell-derived WNV failed to induce Type I IFN in plasmacytoid DC. The authors report that while mammalian-derived WNV induced high levels of IFN-α in pDCs, mosquito-derived WNV induced 100-fold less IFN-α, suggesting differential induction based on glycoprotein composition of mosquito cell-derived WNV (Silva et al., 2007).

Subsequently, Shabman and co-workers showed higher infectivity of mos-RRV in murine bone marrow-derived myeloid dendritic cells (mDC) compared to that of mam-RRV. The study also reports that mam-RRV induces a substantial Type I IFN response in mDCs, whereas mos-RRV induce much lower levels (Shabman et al., 2007).

In this chapter, we attempt to characterise the key differences between mam-RRV and mos-RRV in a macrophage cells line, RAW264.7, which has been used extensively in RRV studies *in vitro* (Way et al., 2002) and an immature DC cell line, JAWSII. Differences in viral replication were investigated and the ability of both mam- and mos-RRV to induce a Type I IFN response in RAW264.7 cells was assessed. It was demonstrated that mos-RRV exhibits higher infectivity than mam-RRV in RAW 264.7 and JAWSII cells, and that mos-RRV was unable to induce the expression of transcription factors associated with Type I IFN and antiviral responses in either macrophage or DC cell lines used.

3.2. Results

3.2.1. mos-RRV replicates to higher titres in RAW264.7 and JAWSII cells

The first aim was to investigate the ability of mos-RRV to infect macrophage and dendritic cell lines. RAW264.7 and JAWSII cells were infected with mam- or mos-RRV and titres were recovered from supernatants. Viral titres are shown in **Figure 3.1**. In RAW 264.7 **(Fig 3.1A)** higher titres were recovered from mos-RRV-infected cultures at 4 (1.984±0.254 PFU/mL vs. 1.265±0.323) and 6 (3.982±0.218 vs. 2.671±0.193 PFU/mL) hours post-infection (hpi). By 24 hpi, titres recovered in mam- and mos-RRV-infected cell culture supernatants were similar in both RAW264.7 and JAWSII

cells. The differences in titre were significant at 4 (*p=0.0388*) and 6 hpi (*p=0.0015*), but not at 24 hpi.

In JAWSII cells **(Fig. 3.1B)**, the differences in titres between mam- and mos-RRV infected cultures observed at 4 and 6 hpi were statistically significant (*p=0.0009* and *p=0.0004*, respectively). As observed in RAW264.7 cells, differences in titre were no longer observed by 24 hpi. In both cell lines, the major differences in titre were observed at early time-points, during which RRV is actively replicating. The highest titres recovered from JAWSII cells were at 6 hpi (4.136 ±0.198 PFU/mL) in mos-RRV-infected cultures. It is possible that 24 hpi, a predominant population of first-generation, RAW264.7-membrane-derived RRV virions were recovered from inoculae.

However at 24 hpi, both mam- and mos-RRV titres were higher in RAW264.7 than in JAWSII cultures. At this time point RAW264.7 cell supernatants yielded titres above 5 Log PFU/mL, for both mam- and mos-RRV (5.370±0.192 and 5.652±0.240 PFU/mL, respectively) compared to titres below 4 Log PFU/mL recovered in JAWSII infectious cultures.

Figure 3.1: Viral titres following infection of RAW264.7 (A) and JAWSII (B) cells with mam-RRV and mos-RRV (1.0 MOI). RAW264.7 and JAWSII cells were inoculated with mam- and mos-RRV, and infectious supernatants were collected at 4, 6 and 24 hpi. Viral titres are expressed in plaque-forming unit/mL (PFU/mL), and were determined by plaque assay as described in Section 2; Data is representative of 3 separate experiments.

A

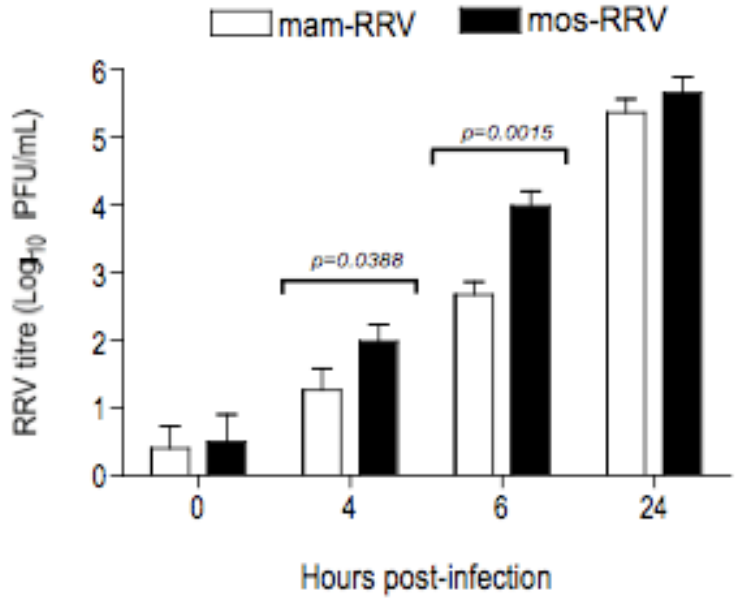
mam-RRV
mos-RRV
RRV titre (Log10 PFU/mL)
p=0.0388
p=0.0015
0
1
2
3
4
5
6
0
4
6
24
Hours post-infection

B

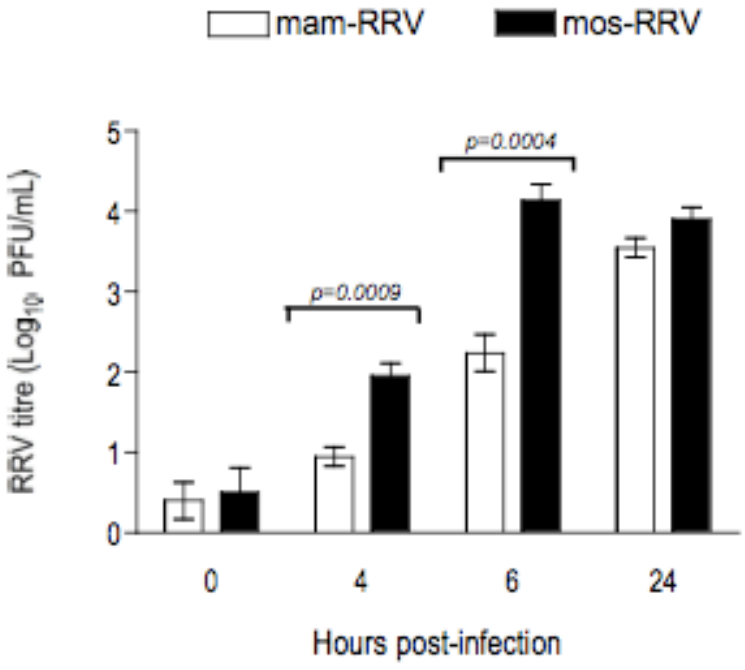
mam-RRV
mos-RRV
RRV titre (Log10 PFU/mL)
p=0.0009
p=0.0004
0
1
2
3
4
5
0
4
6
24
Hours post-infection

Figure 3.2: Viral titres following infection of Vero (A) and L929 (B) cells with mam-RRV and mos-RRV (1.0 MOI). Vero cells were inoculated with mam- and mos-RRV, and infectious supernatants were collected at 4, 6 and 24 hpi. Viral titres were determined by plaque assay; Data is representative of the mean number of plaques (n=5) for each time point. Error bars represent the standard error of the mean (SEM).

A

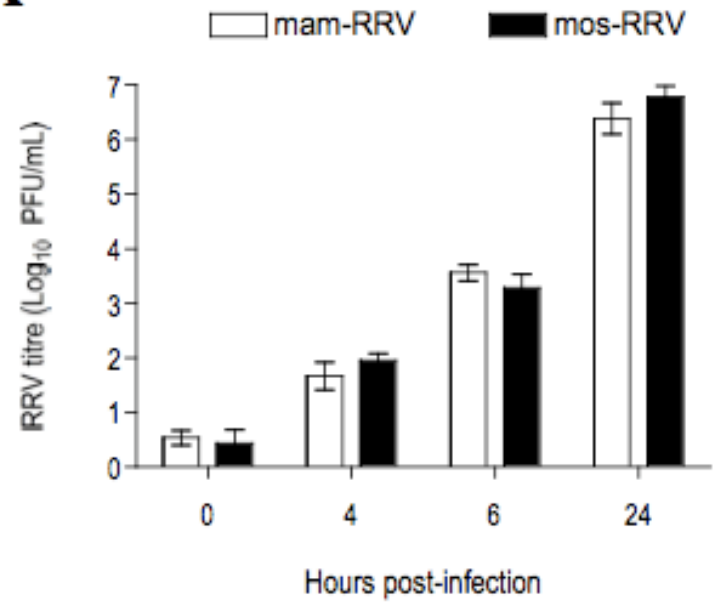
mam-RRV
mos-RRV
RRV titre (Log10 PFU/mL)
0
1
2
3
4
5
6
7
0
4
6
24
Hours post-infection

B

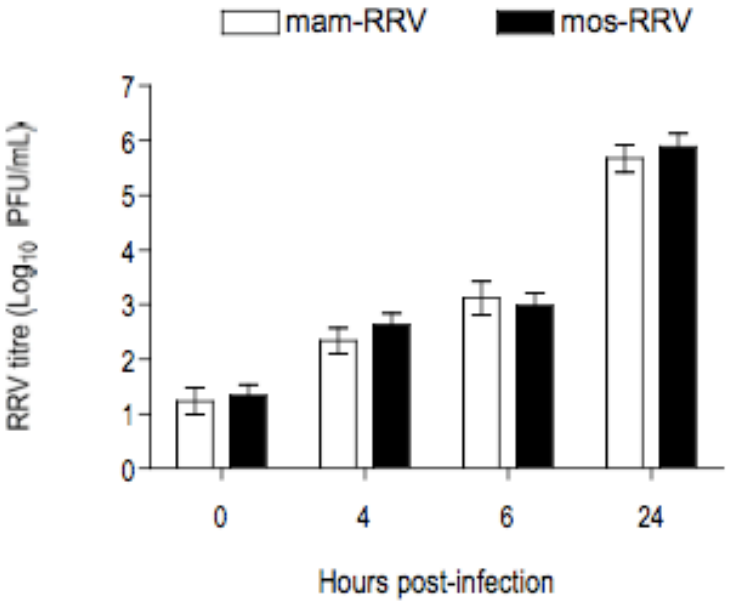
mam-RRV
mos-RRV
RRV titre (Log10 PFU/mL)
0
1
2
3
4
5
6
7
0
4
6
24
Hours post-infection

3.2.2. mam- and mos-RRV replication kinetics in Vero and L929 cells

We have shown that mos-RRV could be recovered at higher titres in macrophage and dendritic cell lines, both of which are potent producers of Type I IFN. This raised the question as to whether a functional Type I IFN system was required for mos-RRV to display higher infectivity. In order to test this hypothesis, we infected Vero and L929 cells with mam- and mos-RRV (1.0 MOI), both of which possess a deficient Type I IFN system. Viral titres recovered from supernatants are displayed in **Figure 3.2.**

No differences in titre were observed between mam- and mos-RRV-infected Vero cells **(Fig 3.2A)** and L929 cells **(Fig 3.2B)**. At all time points, titres recovered in the supernatant showed no significant differences.

3.2.3. mos-RRV displays higher infectivity in RAW264.7 cells as assessed by immunofluorescence

Next, we attempted to determine if there was a difference in infectivity between mam- and mos-RRV when infecting RAW264.7 cells. RAW cells were infected with mam- or mos-RRV at fixed at 12 hpi and RRV antigen was detected by immunofluoresence **(Fig 3.3A)**. Levels of infectivity were determined by counting RRV-positive cells, and differences were assessed for statistical significance **(FIG 3.3B)**. Mos-RRV displayed higher infectivity in RAW 264.7 cells than mam-RRV, with a 2-fold higher positive cell count. This correlates with findings of higher titre recovery in RAW264.7 cells at early timepoints.

Next, we aimed to investigate whether the presence of IFN-β could protect RAW 264.7 cells from infection. Data presented earlier suggested that differences in titre were only observed in type I IFN-potent cells. In addition, we attempted to determine whether the ability of mos-RRV to display higher infectivity could be abrogated by pre-treating RAW264.7 cells with IFN-β. We treated cells with IFN-β at concentrations of 1, 10 and 100 IU/mL 3 hours prior to infection with mam- or mos-RRV. Microscopy images showed that mos-RRV still displayed significantly higher infectivity ($p<0.001$) than mam-RRV in RAW264.7 cells treated with 1 and 10 IU/mL. However, almost no RRV antigen could be detected in cells treated with 100 IU/mL in either mam- or mos-RRV-infected samples.

Figure 3.3: (A) Immunofluorescent labelling of RRV in mam- and mos-RRV-infected RAW264.7 cells (magnification x100). RAW264.7 cells were either infected with mam- or mos-RRV (MOI=1.0), or treated with 1, 10 or 100 IU/mL recombinant murine IFN-β 3h prior to infection and fixed at 12 hpi. Infected cells were labelled (green) with anti-RRV polyclonal antibody while nuclei (blue) were stained using DAPI. Data is representative of 3 separate experiments. **(B) Fluorescence cell count of RAW264.7 cells positive for anti-RRV antibody at 12hpi**. FITC-positive cells were counted on 10 mid-power fields (x 40) in IFN-β-treated (1, 10 and 100 IU/mL) and untreated cells infected with either mam- or mos-RRV (1.0 MOI). Data is representative of 10 mid-power (x40) fields. Statistical significance (* = $p<0.001$) was determined by 2-way ANOVA followed by Bonferroni's post-test.

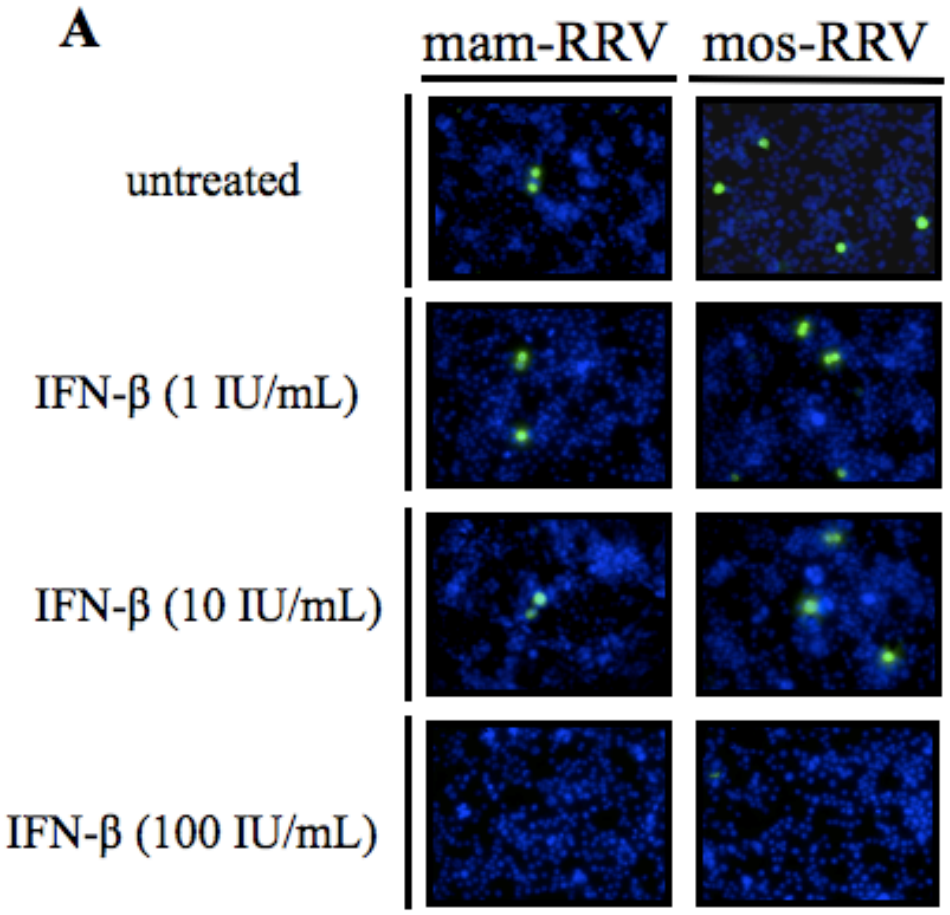
A
mam-RRV
mos-RRV
untreated
IFN-β (1 IU/mL)
IFN-β (10 IU/mL)
IFN-β (100 IU/mL)

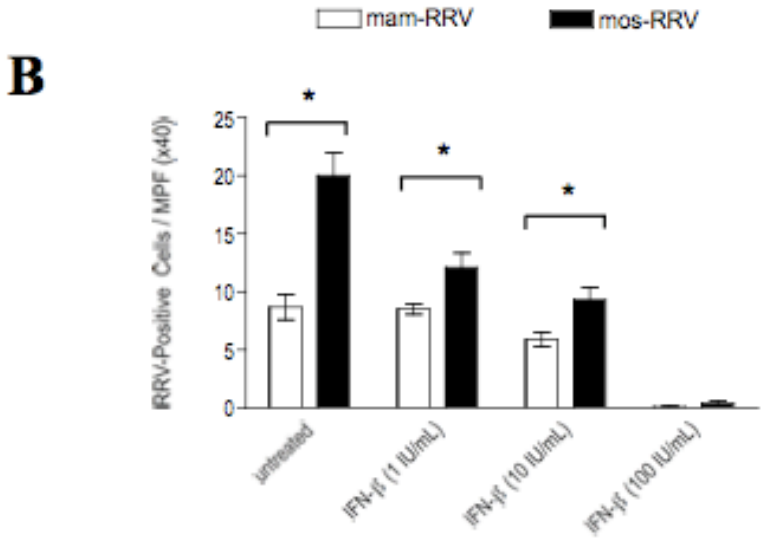
B
mam-RRV
mos-RRV
RRV-Positive Cells / MPF (x40)
25
20
15
10
5
0
*
*
*
untreated
IFN-β (1 IU/mL)
IFN-β (10 IU/mL)
IFN-β (100 IU/mL)

3.2.4. Infectivity of mam- and mos-RRV in Vero cells

Next, based on previous findings showing that mos-RRV exhibits higher infectivity than mam-RRV in RAW264.7 cells, we decided to confirm that, in line with titre data, the two viruses show no significant differences in infectivity in Vero cells.

Firstly, we infected Vero cells with mam- or mos-RRV (1.0 MOI) and fixed cells at 12 hpi. RRV-positive cells were detected by immunofluoresence and counted. **Figure 3.4A** shows immunofluorescence images of mam- and mos-RRV-infected Vero cells and **Figure 3.4B** shows the RRV-positive cell counts.

There was no difference in infectivity between mam- and mos-RRV-infected Vero cells. The number of RRV-positive cells was higher in Vero than in RAW264.7 cell cultures infected with either mam- or mos-RRV.

Secondly, we set out to determine whether Vero cells, which are irresponsive to Type I IFN, can be protected from RRV infection by stimulating elements of the cell's type I IFN system. Vero cells were pre-treated with either IFN-α at 10 IU/mL, or with poly(I:C) (250 ng/mL). Poly(I:C) is a synthetic RNA strand commonly used for its ability to induce antiviral responses initiated by the detection of viral RNA by host cells. Pre-treatment of Vero cells was performed for 3 hours prior to infection with either mam- or mos-RRV. Images of mam- and mos-RRV fluorescence in Vero cells are shown in **Figure 3.4.**

No differences in infectivity were observed between mam- and mos-RRV-infected Vero cells, regardless of IFN-α or poly(I:C) treatment. This is expected as Vero cell are unable to respond to IFN signals and are unable to mount an antiviral response upon infection.

3.2.5 Restoration of mam-RRV phenotype

The difference between mam- and mos-RRV is the cell type in which they were propagated. The cell surface of mosquito cell such as C6/36 is rich in high mannose sugars, while mammalian cells like Vero display a membrane surface covered with

Figure 3.4: A) Immunofluorescent labelling of RRV in mam- and mos-RRV-infected Vero cells (magnification x100). Vero cells were either infected with mam- or mos-RRV (MOI=1.0), or treated with poly(I:C) (250 ng/mL) or recombinant mouse IFN-α (10 IU/mL) 3h prior to infection and fixed at 12 hpi. Infected cells were labelled with anti-RRV polyclonal antibody (green) while nuclei were stained using DAPI (blue). Data is representative of 3 separate experiments. B) **Fluorescence cell count of Vero cells positive for anti-RRV antibody at 12hpi**. FITC-positive cells were counted on 10 mid-power fields (magnification x100) in poly(I:C) (250 ng/mL) or IFN-α-treated (10 IU/mL) and untreated cells infected with either mam- or mos-RRV (1.0 MOI). Data is representative of cells counted over 10 high power (magnification x100) fields.

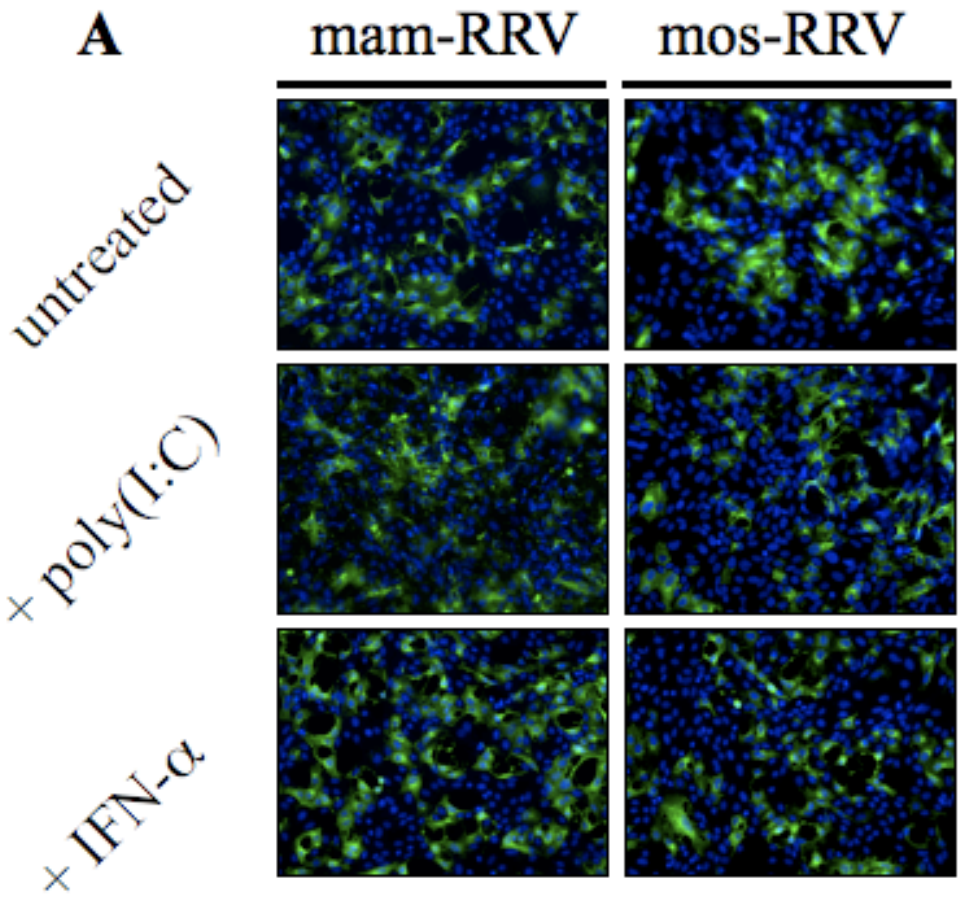
A
mam-RRV
mos-RRV
untreated
+ poly(I:C)
+ IFN-α

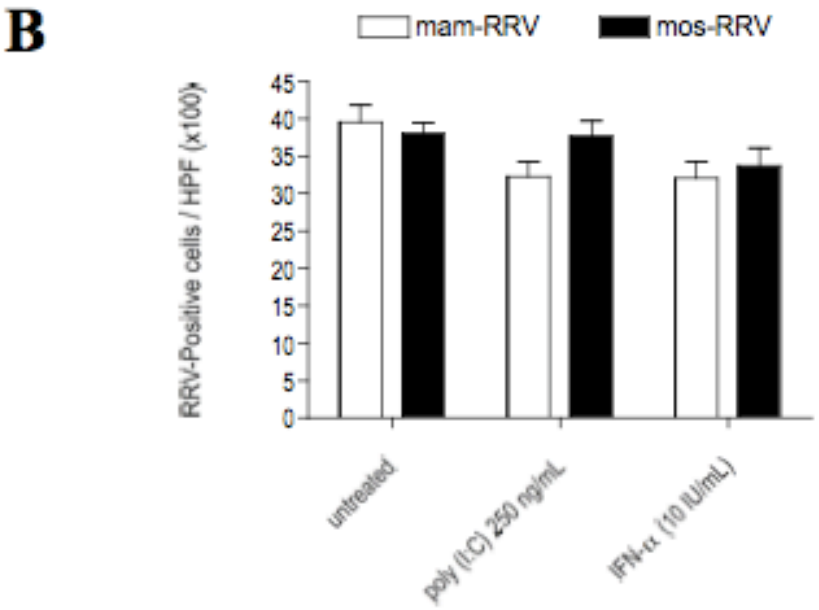
B
mam-RRV
mos-RRV
RRV-Positive cells / HPF (x100)
45
40
35
30
25
20
15
10
5
0
untreated
poly (I:C) 250 ng/mL
IFN-α (10 IU/mL)

complex glycan carbohydrates. In the light of differences in titre and infectivity observed between mam- and mos-RRV, we attempted to determine whether the differences observed between mam- and mos-RRV are due to a genetic mutation, or due to the difference in surface glycosylation acquired from from their respective host cells.

We passaged mos-RRV once in Vero cells and first passage mos-to-mam-RRV was recovered in the supernatant. RAW264.7 cells were infected with mam-RRV, mos-to-mam-RRV and mos-RRV. Titres recovered in supernatants are shown in **Figure 3.5**.

There was no difference between titres of mam-RRV and mos-to-mam-RRV recovered in the supernatants of RAW264.7 cells at 4, 6 and 24 hpi. There was however a strong correlation (R^2= 0.9385; Pearson's correlation coefficient r=0.9688) between average titres, strongly contrasting with differences between mos-to-mam-RRV and mos-RRV titres. In parallel, JAWSII cells were infected with 1st passage mos-to-mam-RRV, which was recovered at similar titres than mam-RRV, showing no differences between parent mam-RRV virus and mos-to-mam-RRV virus titres (data not shown)

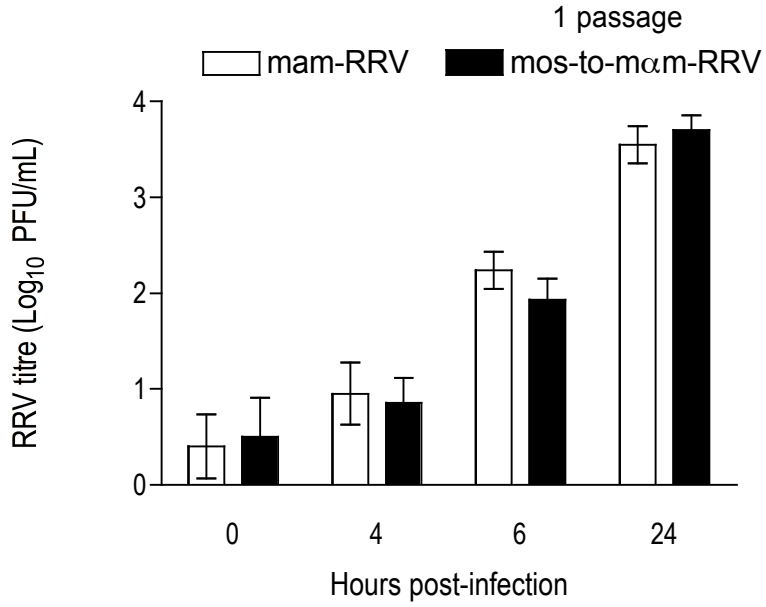

Figure 3.5: A single passage of mos-RRV in mammalian Vero cells restores the mam-RRV phenotype following infection of RAW264.7 cells. Supernatants of RAW264.7 cells infected with mam-RRV or mos-RRV passaged in Vero cells were collected at 4, 6 and 24h.p.i. Viral titres were determined by plaque assay. Data is representative of 3 separate experiments.

3.2.6 mos-RRV induces lower levels of IFN-β mRNA compared to mam-RRV

We showed that mos-RRV could display higher infectivity than mam-RRV in RAW264.7 cells pre-treated with IFN-β. This raised the question as to whether mos-RRV can inhibit or avoid a Type I IFN response. We started by investigating the differences in IFN-β expression in RAW264.7 and JAWSII cells infected with mam- or mos-RRV (MOI=1.0). IFN-β mRNA expression in the abovementioned cells was analysed by reverse transcriptase, real-time, quantitative polymerase chain reaction (RT-PCR). GADPH was used as a housekeeping gene and differences in IFN-β mRNA levels are expressed in "Fold-change" normalised to GADPH expression. The data was analysed using the comparative quantitation software REST (Pfaffl et al., 2002). Expression data was plotted in **Figure 3.6A** for RAW264.7 cells, and in **Figure 3.6B** for JAWSII cells.

In RAW264.7 cells, IFN-β expression was found to be lower in cells infected by mos-RRV at 4 and 6 hpi **(Fig. 3.6A).** Levels of IFN-β mRNA were significantly lower at 4 and 6 hpi, but not at 24 hpi ($p<0.05$). Differences in mRNA expression of up to 5-fold were observed between mos- and mam-RRV at 6 hpi. At 24 hpi, IFN-β mRNA levels were similar in mam- and mos-RRV-infected cells, corroborating viral replication kinetics patterns showing differences at 4 and 6 hpi.
In JAWSII cells, IFN-β was also found to be downregulated at 4 and 6 hpi, but not at 24 hpi **(Fig. 3.6B)**. Mos-RRV induced up to 5-fold less IFN-β in JAWSII cells than mam-RV at 6 hpi ($p<0.05$). At 24 hpi, mam- and mos-RRV induced similar levels of IFN-β expression. Likewise, the absence of differences in IFN-β induction at 24 hpi correlate with earlier observations of titre recovery.

Figure 3.6: Relative expression of IFN-β in mam- or mos-RRV-infected RAW264.7 (A) and JAWSII (B) cells. Cells were collected at 4, 6 and 24 hpi. Differences were analysed by quantitative, real-time PCR and are expressed as fold-change in mRNA level expression, normalised against mock-infected controls. Data is representative of the mean fold change in mRNA levels compared to uninfected controls. Data reflects 3 separate experiments (n=4), and statistical significance (*=$p<0.05$) was analysed by unpaired, two-tailed *t*-test using REST software.

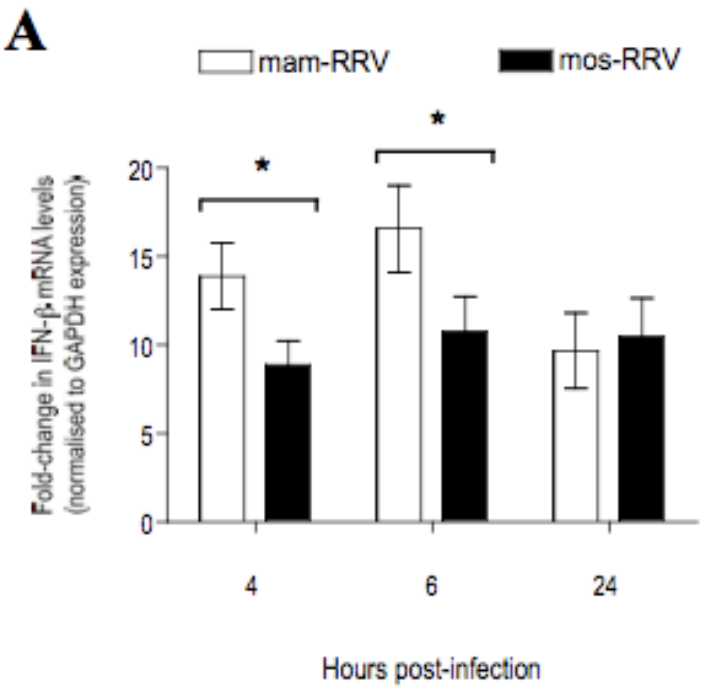
A
mam-RRV
mos-RRV
*
*
Fold-change in IFN-β mRNA levels
(normalised to GAPDH expression)
20
15
10
5
0
4
6
24
Hours post-infection

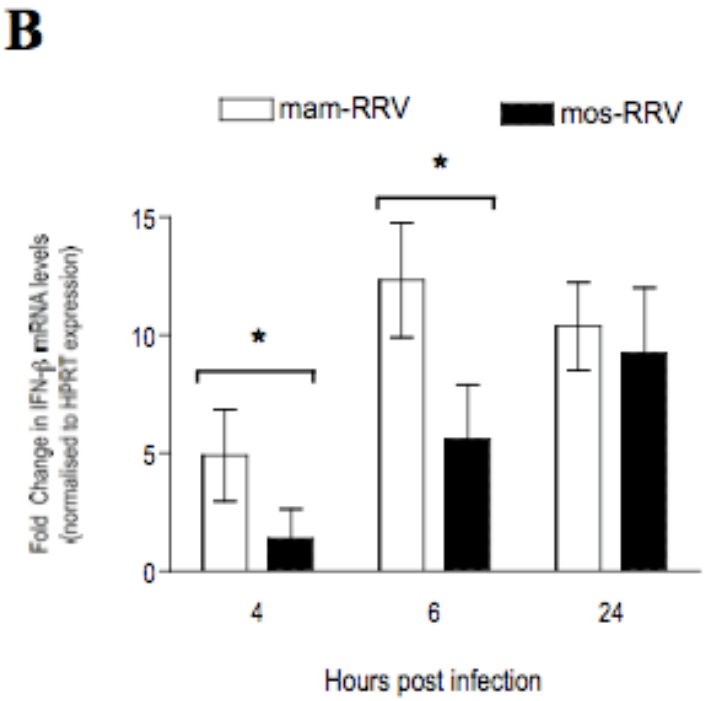
B
mam-RRV
mos-RRV
*
*
Fold Change in IFN-β mRNA levels
(normalised to HPRT expression)
15
10
5
0
4
6
24
Hours post infection

3.2.7 mos-RRV induces lower activation of antiviral transcription factors

Using quantitative RT-PCR, mos-RRV was shown to induce less IFN-β expression than mam-RRV in RAW264.7 and JAWSII cells. This evoked the possibility that mos-RRV may be interfering with components of the Type I IFN signalling pathway, in particular transcription factors involved in IFN-β signalling. We assessed the differences in expression of transcription factors IRF-3 and STAT-1 as well as PKR, a cytoplasmic, RNA-dependent kinase involved in viral RNA recognition and degradation. Since the most significant differences in viral infectivity, replication and IFN-β production were observed at early time points, RAW264.7 cells were infected at 1.0 MOI and harvested at 6 hpi. Total cellular protein was extracted and cytoplasmic and nuclear fractions were separated, then subjected to western blot analysis.

STAT-1 was detected in the cytoplasm using a specific antibody against the activated, phosphorylated form pSTAT-1. Similarly, PKR was detected in the cytoplasm using an antibody raised against the activated PKR protein, phosphorylated at the Threonine 457 residue ($PKR^{(Thr475)}$). Western blots are shown in **Figure 3.7A**, while band intensity was quantitated and expressed as a ratio to G3PDH, housekeeping protein band intensity **(Fig 3.7B)**. IRF-3 was detected in the nucleus. Western blot is shown in **Figure 3.8A**, and band density analysis plotted **in Figure 3.8B**.

In cytoplasmic fractions, the presence of phosphorylated $PKR^{(Thr475)}$ was found to be higher in RAW264.7 cells infected with mam-RRV than in mos-RRV-infected cells at 6 hpi (**Fig 3.7A** and **Fig 3.7B**). Differences in band intensity were statistically significant *($p=0.0128$*). Similarly, yet to a lesser extent, mam-RRV was found to induce higher levels of pStat-1 (*$p=0.0099$*) expression in RAW264.7 cells at 6 hpi, as band intensity was consistently higher in all replicates of mam-RRV-infected cell nuclear extract than in mos-RRV-infected cells (**Fig 3.7A** and **Fig 3.7B**).

RAW264.7 cells infected with mam-RRV expressed more IRF-3 than those infected with mos-RRV, at 6 hpi (**Fig 3.8A** and **Fig 3.8B**). Band density was measured and found to be significantly higher (*$p<0.001$*), at least three-fold, in mam-RRV than in mos-RRV-infected RAW cells. **Figure 3.8C** shows a Coomassie Blue-stained SDS-PAGE gel showing equal loading of mam- and mos-RRV total protein samples.

Figure 3.7: Western Blot analysis of Stat-1 and PKR expression RAW264.7 cells infected with mam- or mos-RRV at 6 hpi. (**A**) Detection of PKR$^{(Thr451)}$ and pStat-1 in cytoplasmic extract of mam- and mos-RRV-infected RAW264.7 cells at 6 hours post-infection. Cells were collected at 6 hpi and cytoplasmic protein was isolated and separated by SDS-PAGE. Cytoplasmic protein was transferred to a PVDF membrane and detected by Western Blotting .G3PDH was detected as a negative control. (**B**) Relative densitometric analysis of PKR$^{(Thr451)}$ and pStat-1 signal, expressed as a density ratio compared to G3PDH expression. Densitometry was performed using QuantityOne software (BioRad). Data is representative of 3 separate experiments.

A

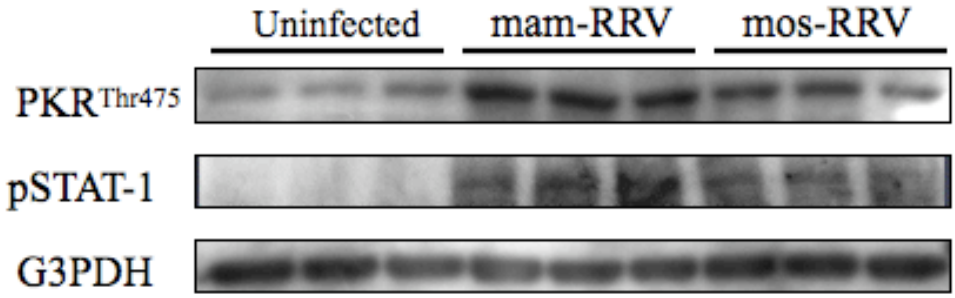
Uninfected
mam-RRV
mos-RRV
PKR Thr475
pSTAT-1
G3PDH

B

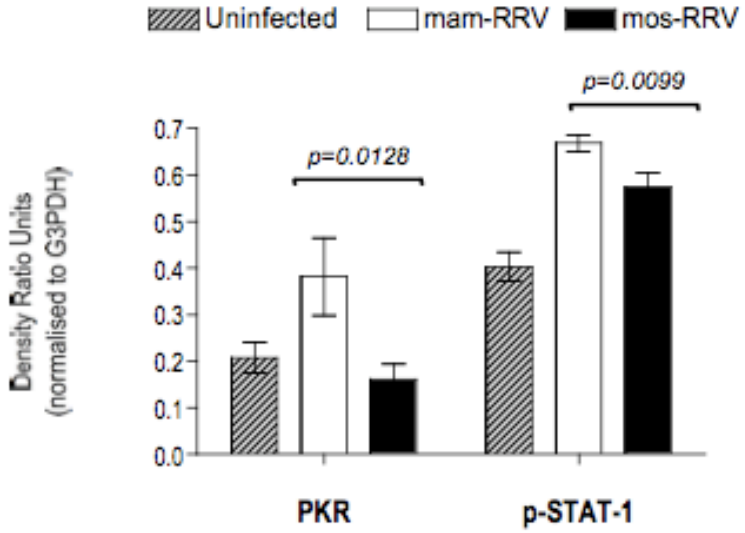
Uninfected
mam-RRV
mos-RRV
Density Ratio Units
(normalised to G3PDH)
0.7
0.6
0.5
0.4
0.3
0.2
0.1
0.0
p=0.0128
p=0.0099
PKR
p-STAT-1

Figure 3.8: Western Blot analysis of nuclear IRF-3 in RAW264.7 cells following mam- or mos-RRV infection at 6 hpi. (**A**) Detection of IRF-3 in nuclear extract of mam- and mos-RRV-infected RAW 264.7 cells at 6 h.p.i. Cells were infected with 1.0 MOI mam- or mos-RRV and colelcted t 6 hpi. Nuclear protein was extracted and spearated by SDS-PAGE. Nuclear proteins were transferred to a PVDF membrane and IRF-3 was detected using a polyclonal anti-IRF-3 antibody. (**B**) Densitometric analysis of IRF-3 band intensity, performed by Gel Doc analysis sfotware Quantity One (BioRad). (**C**) Coomassie Blue stain of the SDS-PAGE gel showing equal protein loading. Data is representative of 3 separate experiments.

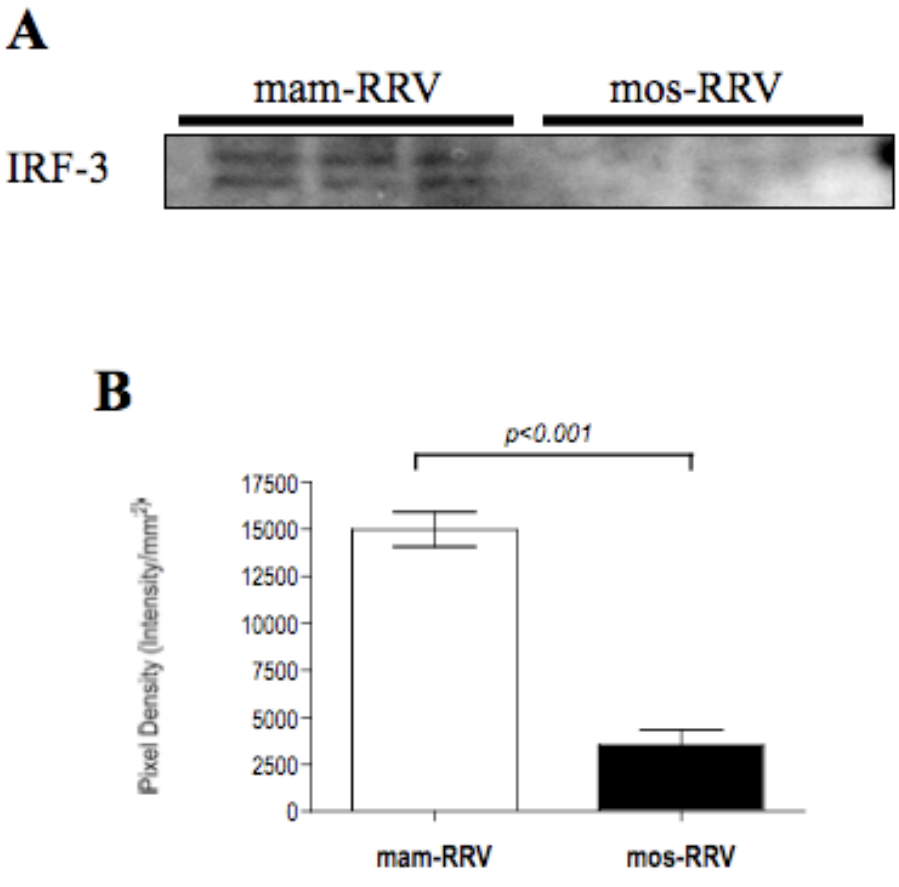
A
mam-RRV
mos-RRV
IRF-3
B
p<0.001
Pixel Density (Intensity/mm²)
17500
15000
12500
10000
7500
5000
2500
0
mam-RRV
mos-RRV
C
mam-RRV
mos-RRV

3.2.8. Transcription of IFN-associated genes is reduced following mos-RRV infection

Western blot analysis revealed that the amount of activated transcription factors was significantly lower in mos-RRV-infected RAW264.7 cells. Previously, RT-PCR data suggested that elements of the Type I IFN signalling pathway could be affected by mos-RRV, which would explain the correlated differences in titre and infectivity observed in RAW264.7 and JAWSII cells.

We attempted to further explore the mechanisms involved in Type I IFN signalling that could be affected, or fails to be induced by mos-RRV, in particular whether transcriptional activity of Type I IFN-associated genes would also be differentially induced. The transcription of IFN-associated genes was assessed in mam- and mos-RRV-infected cells. JAWSII cells were co-transfected with a luciferase reporter plasmid (pISRE(9-27)Lucter) and a control reporter plasmid (pCMV-βGal) encoding the β-Galactosidase gene.

Transfectants were infected with either mam- or mos-RRV (MOI=1.0) or stimulated with 250 ng/ mL LPS (lipopolysaccharide) as a positive control. Cell lysates were collected at 0, 4, 6, and 24 hpi and luminescence as well as β-galactosidase activity were measured as described earlier. Mean luciferase activity (n=4) was plotted in **Figure 3.9**. Mam-RRV was found to induce significantly higher luciferase activity compared to mos-RRV at 4 ($p=0.0087$) and 6 ($p=0.0076$) hpi. At 24 hpi, mam- and mos-RRV induced similar levels of luciferase activity in JAWSII-*pISRE(9-27)Lucter* cells (**Fig. 3.9**).

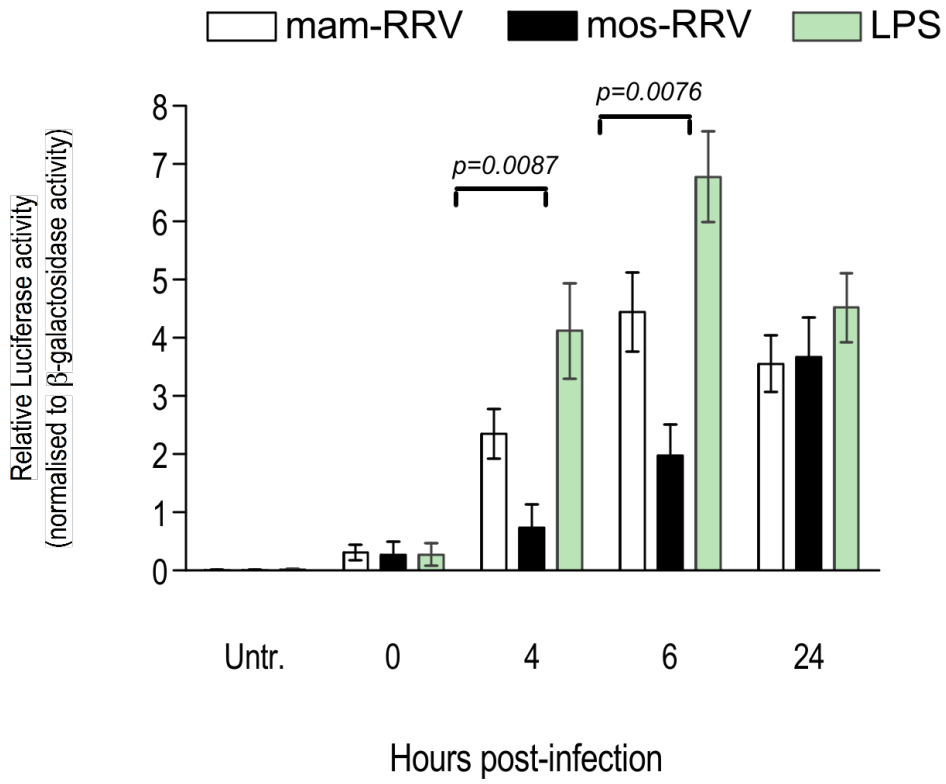

Figure 3.9: Luciferase reporter gene expression following mam- or mos-RRV infection in JAWSII-*pISRE(9-27)Lucter* cells. JAWSII cells were transiently transfected with the pISRE(9-27)Lucter reporter plasmid and infected with 1.0 MOI mam- or mos-RRV. LPS was used at 250 ng/ml as a positive control. Cells were lysed at 0, 4, 6 and 24 hpi and luciferase activity was measured in a luminometer. Data is representative of 3 separate experiments. Statistical significance was assessed by unpaired, two-tailed *t*-test.

We then investigated the differences of early transcriptional induction of the IFN-β promoter in RAW264.7 cells, using the pIFΔ(-125/+72)Lucter reporter plasmid, which carries the -125/+72 consensus sequence of the IFN-β promoter (described in 2.8). RAW264.7 cells were co-transfected with pIFΔ(-125/+72)Lucter and (pCMV-βGal) as described earlier and infected with either mam- or mos-RRV (MOI 1.0). Poly(I:C) was used at 250 ng/mL as a positive control. Mean luciferase activity (n=4) was plotted in **Figure 3.10.** At 6 hpi mam-RRV induced higher luciferase activity than mos-RRV in RAW264.7-*pIFΔ(-125/+72)Lucter* cells. The difference between mam- and mos-RRV-infected cells was statistically significant (*p=0.003*).

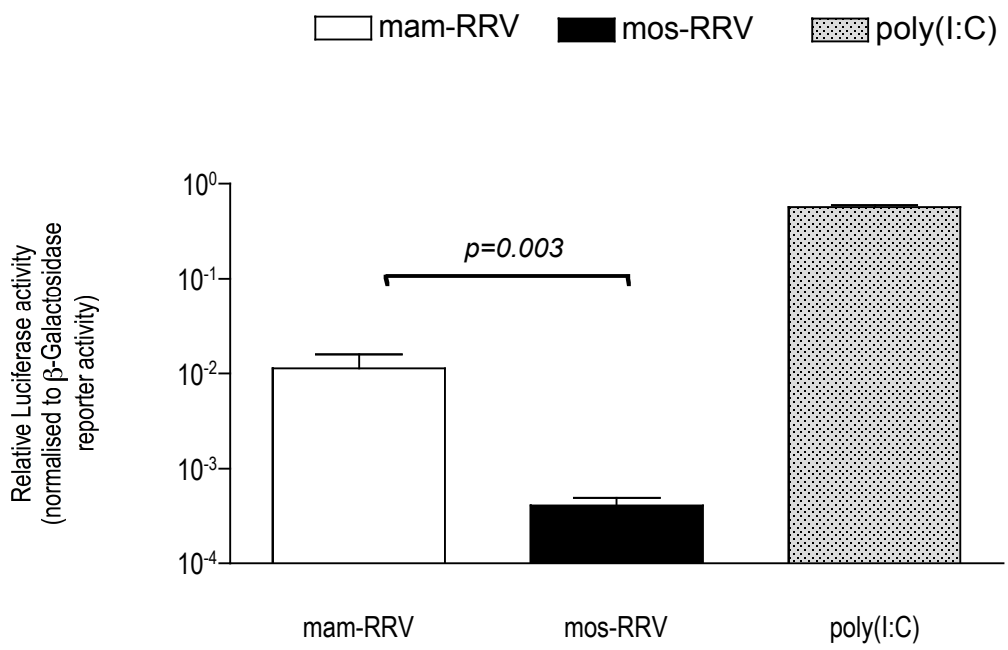

Figure 3.10: Luciferase reporter gene activity at 6 hpi in RAW264.7-*pIFΔ(-125/+72)Lucter* cells following mam- or mos-RRV infection. RAW264.7 cells were transiently transfected with pIFΔ(-125/+72)Lucter reporter plasmid. Transient transfectants were inoculated with 1.0 MOI mam- or mos-RRV or stimulated with 250 ng/mL poly(I:C) and cell were lysed at 6 hpi. Data is representative of 3 separate experiments. Luciferase activity was normalised to β-Galactosidase reporter expression. Statistical significance was assessed by unpaired, two-tailed *t*-test.

3.3. Discussion

Differences in infectivity and antiviral response induction have been observed between viruses derived in mammalian or mosquito cells. Arthropod-borne viruses are thought to exploit such differences, which result in higher infectivity and lower antiviral response signals in immune cells. Studies investigating arboviruses derived from mammalian or mosquito cells have shown that WNV, an arthropod-borne Flavivirus, as well as RRV, induced less Type I IFN in primary dendritic cell cultures (Silva et al., 2007). In the case of RRV, higher levels of infectivity in myeloid DCs were also reported for mosquito cell-derived RRV (Shabman et al., 2007).

3.3.1 Differential replication kinetics of mam- and mos-RRV infection

In this study, we investigated the differences in RRV replication kinetics, levels of infectivity and Type I IFN induction and the expression and activity of associated transcription factors in macrophage (RAW264.7) and dendritic cell lines (JAWSII).

The first important observation made in this study was that mos-RRV was recovered at higher titres in RAW264.7 and JAWSII cells, at early time points following infection (4 and 6 hpi). Differences in titre were statistically significant in both cell lines. At 24 hpi, titres recovered were similar in both mam- and mos-RRV-infected cell supernatants, most likely due to the fact that at 24 hpi, RRV has completed at least one replication cycle through RAW264.7 and JAWSII cells, which are mammalian (murine) cells.

However, the nature of the cells assayed, namely specialised monocytic cells with potent antiviral properties, raised the question as to whether mos-RRV can interfere with, or evade a antiviral response. We thus investigated mam- and mos-RRV replication kinetics in IFN-irresponsive cells, such as Vero and L929 cells. There was no difference in replication between mam- and mos-RRV in either Vero or L929 cells, suggesting that the ability of mos-RRV to replicate to higher titres is dependent on the presence a functional Type I IFN system.

Using immunofluorescence assays, we determined that levels of infectivity were similar in mam- and mos-RRV-infected Vero cells at 12 hpi. We also observed that pre-treatment of Vero cells with either poly(I:C), a synthetic single strand RNA, and recombinant IFN-α, did not protect Vero cells from infection with either viruses. As expected, cells such as Vero that would not normally respond to IFN and IFN-associated signals induced by either viral infection or exogenous stimulation did not provide mos-RRV with the required phenotype for differential infectivity, as was observed in IFN-potent cells. This is in line with findings that mos-RRV and mam-RRV display similar infectivity in mDCs from IFNa/b Receptor deficient mice, suggesting that elements of the Type I IFN signalling pathway are involved in the differential induction of Type I IFN observed with mam- and mos-RRV in IFN potent cell lines such as RAW264.7 and JAWSII cells (Shabman et al., 2007).

We also showed that in order to abrogate such differences, one passage of mos-RRV in mammalian Vero cells was sufficient to restore the initial mam-RRV phenotype. Mos-RRV was passaged once in Vero cells and RAW264.7 cells were infected alongside with original, 1st

passage mam-RRV. No differences in titres were observed at any of the time points, suggesting that the cause of differential replication kinetics are most likely associated with mosquito cell membrane composition, as one passage through a different cell line is unlikely to induce a adaptive mutation. Similar observations were reported in mDCs infected with a mos-RRV that was passaged once in BHK-21 cells which are mammalian, hamster cells (Shabman et al., 2007). These results also lessen the likelihood that such differences are due to a genetic mutation following a passage in mosquito cells, however they do not exclude the possibility of a viral antagonist.

3.3.2 Differential infectivity in RAW264.7 and Vero cells

Based on titre recovery, we hypothesised that higher titre recovery for mos-RRV should correlate with higher infectivity. Using immunofluorescent techniques, we were able to determine the proportion of RRV-infected cells in mam- and mos-RRV-infected samples. First, we attempted to determine differential levels of infectivity in RAW264.7 cells infected with mam- and mos-RRV. RAW264.7 cells showed differential infectivity at 12 hpi, as the differences in RRV-positive cells were 2-fold higher in mos-RRV-infected cells compared to mam-RRV. Similar observations were made in JAWSII cells infected with mam- and mos-RRV.

Secondly, we sought to determine whether mam- and mos-RRV would display differential infectivity in IFN-potent cells that have been stimulated with Type I IFN, to the extent that infectivity would be reduced, or similar between mam- and mos-RRV. We treated RAW264.7 cells with recombinant IFN-β three hours prior to RRV infection. At concentrations of 1 and 10 IU/mL, mos-RRV still displayed higher infectivity than mam-RRV. However, IFN-β was found to substantially inhibit viral infectivity in both mam- and mos-RRV at high concentrations (100 IU/ mL). Such effect is expected since a concentration of 100 IU/mL are beyond true physiological levels of Type I IFN-β involved in antiviral responses *in vivo* (Cantell et al., 1974).

To verify that the differential effect observed in RAW264.7 cells was indeed related to the stimulation of the Type I IFN system in a IFN-potent cell line, we attempted to determine the infectivity of mam- and mos-RRV in IFN-irresponsive Vero cells by immunofluorescence. There was no difference in infectivity between mam- and mos-RRV-infected cells, corroborating titre recovery data presented earlier. Next, to confirm that the differences in infectivity observed in

RAW264.7 cells treated with IFN-β were indeed due to subsequent activation of an IFN pathway, we treated Vero cells with IFN-α, or with poly(I:C), a synthetic dsRNA able to induce Type I IFN-associated antiviral responses (Cheng et al., 2007). As expected, neither the presence of IFN-α or poly(I:C) had a protective effect on mam- or mos-RRV infection. Pre-treatment with IFN-α or poly(I:C) no difference in infectivity between mam- or mos-RRV in Vero cells.

However, these results only suggested that some elements of the type I IFN pathway were needed for differential infectivity to occur, yet do not inform as to which IFN regulators would be involved. We thus formulated the hypothesis that mos-RRV requires a functional Type I IFN system that it can effectively modulate upon entry, resulting in a somewhat less threatening intracellular environment. Such a weakened antiviral state would ultimately render viral replication less detectable, which would explain the higher titres and infectivity observed with mos-RRV.

3.3.3 Differential induction of Type I IFN by mos-RRV

To verify the hypothesis that mos-RRV induces less Type I IFN in interferon-potent cells, we set out to determine how mam- and mos-RRV affected the Type I IFN response in RAW264.7 and JAWSII cells. Using quantitative, real-time PCR analysis, we found that mos-RRV failed to induce the same IFN-β levels as mam-RRV in both RAW264.7 and JAWSII cells. The most significant differences in IFN-β mRNA levels were observed, in both cell lines, at early time points of 4 and 6 hpi. At 24 hpi, similar levels of IFN-β transcripts were detected in mam- and mos-RRV-infected cells. This correlates with findings described earlier that mos-RRV titres are higher than mam-RRV at 4 and 6 hpi, but similar at 24 hpi, after at least one replicative cycle in mammalian cells such as those assayed. This data corroborates earlier findings in mDCs, which reports patterns of lower IFN-β induction by mos-RRV as early as 2 hpi. Having observed that mos-RRV fails to induce Type I IFN levels similar to those induced by mam-RRV, we next sought to determine if elements of the Type I IFN signalling pathway were also affected by mos-RRV.

3.3.4 Differential activation of transcription factors

Having found that levels of IFN-β message RNA were reduced in cells infected with mos-RRV compared to mam-RRV, we attempted to identify some of the components of the Type I IFN

system that could be differentially modulated by mos-RRV infection. We investigated differences in protein expression of Stat-1, a key transcription factor in Type I IFN signalling; IRF-3, an IFN-regulated factor activated upon viral infection, and PKR, an RNA-dependent protein kinase involved in detection and degradation of viral RNA (Maggi et al., 2000; Andersen et al., 2007).

Using western blotting immunodetection we observed that in RAW264.7 cells, mam-RRV induced higher levels of pStat-1, PKR and IRF-3, compared to mos-RRV at 6 hpi. Nuclear extracts were isolated for the detection of IRF-3 because when activated following Type I IFN induction of viral infection, IRF-3 dimerises with either IRF-3 or IRF-7, then translocates to the nucleus to bind target DNA sequences such as IFN-β promoter gene sequences, and drive the expression of Type I IFN-associated genes (Andersen et al., 2007; Hiscott, 2007). In cytoplasmic fractions, we were able to detect phosphorylated forms of both Stat-1 and PKR. In a similar fashion to IRF-3, Stat-1 is phosphorylated in the cytoplasm upon Type I IFN receptor engagement. P-Stat-1 forms homo- or heterodimers with other Stat species then translocates to the nucleus, to bind target DNA sequences, such as the interferon-stimulated response element (ISRE) (Goodbourn et al., 2000; Geiss et al., 2001; David, 2002).
These results suggest that activation levels of some transcription factors involved in downstream activation of Type I IFN-associated genes are reduced following mos-RRV, which partially explains the low levels of IFN-β message detected following mos-RRV infection. However, the apparent down-regulation or lower activation of such transcription factors could be the downstream result of the modulation of another component of the signalling network, and further studies are needed to elucidate this mechanism. Interestingly, IRF-3 has been identified as a requirement for protection against WNV infection, while its related isospecies, IRF-7, considered as a master-regulator of Type I IFN responses, was found to prevent WNV-induced lethal infection (Coccia et al., 1995; Honda et al., 2005; Daffis et al., 2007). Future studies involving the use of IRF-3 or IRF-7 overexpression cell systems should most certainly be undertaken to help identify mechanisms of differential Type I IFN induction between mam- and mos-RRV.

3.3.5 Differential Type I IFN-associated promoter transcription

Having gathered substantial evidence that elements of the Type I IFN signalling pathway were less responsive to mos-RRV than to mam-RRV infection, we determined whether the last step of the signalling pathway prior to gene expression, namely target sequence transcription, of IFN-

associated regulatory sequences was different in mam- and mos-RRV-infected cells. As expected, mos-RRV failed to induce levels of ISRE and IFN-β promoter transcription similar to those observed in mam-RRV-infected cells. Additionally, as observed throughout this chapter, differences were eliminated at 24 hpi.

Observations of differential luciferase activity signify that mam-RRV induced higher transcriptional activity than mos-RRV for the promoter sequences for ISRE and IFN-β used in this study. Such promoter sequences are based on homologous target binding sites for transcription factors, such as STAT-1, IRF-3 and NF-κB. The fact that mos-RRV induces less transcriptional activity suggests that the transcription factors involved are reduced. In conjunctions with findings that pSTAT-1 activation and IRF-3 translocation were reduced following mos-RRV infection, it is clear that mos-RRV fails to induce normal levels of i) IFN-β message; ii) transcription factor activation and iii) IFN-induced transcriptional activity compared to mam-RRV. The findings that the restoration of mam-RRV phenotype depends solely on a single passage in Vero cells reinforces the conjecture that the membrane coat acquired following one passage into mosquito cells is most likely to be responsible for the differential effects observed so far, and that a single further passage of mos-RRV in mammalian cells entirely abolishes its phenotype.

Our observations were consistent with findings recently published by Shabman and co-workers (2007), who used primary, bone marrow-derived dendritic cells and report differential infectivity and Type I IFN induction by mos-RRV. We were hereby able to translate published observations obtained *ex vivo* in primary dendritic cells in our *in vitro* macrophage and dendritic cell line system. Another study reports that West Nile virus (WNV) passaged in mosquito cells fails to induce Type I IFN levels in plasmacytoid DC (pDC) compared to mammalian-cell derived WNV (Silva et al., 2007). This suggests that it is plausible for a virus to avoid the host's Type I IFN system after acquiring a different cell surface membrane following replication in vector or mosquito cells, in the case of arboviruses such as RRV and WNV. In the present study, we also showed that mos-RRV failed to induce normal levels of activated PKR, suggesting that besides Type I IFN-induced transcription factors, independent viral recognition systems were being affected following mos-RRV infection.

The relevance of such findings lies in the increasing importance of arboviruses as emerging disease threats. This raised the question as to whether mosquito-derived viruses, due to their ability to evade some aspects of immune surveillance, can induce the required conditions for the development of disease. Namely, the infection of cells such as macrophages, and the higher infectivity of mos-RRV observed at early time points suggest that in humans, RRV administered following a mosquito bite would be able to avoid an early antiviral Type I IFN system and precede highly protective antiviral responses from specialised cells such as macrophages or dendritic cells. Mos-RRV would thus be able to delay Type I IFN-associated viral detection systems and replicate virtually unhindered before antiviral mechanisms are triggered at later time points, where differences in infectivity and Type I IFN induction between mam- and mos-RRV are no longer observed.

4.1. Introduction

Pathogen-induced arthritis is a common form of arthropathy, as viruses such as HIV, Hepatitis C virus (HCV), Epstein-Barr virus (EBV), Rubella virus, Dengue and Influenza viruses, as well as parasites like *Listeria monocytogenes* have been reported to cause a broad range of arthritic conditions (Calabrese et al., 1991; Levy, 1993; Ellis et al., 1995; Wendling and Herbein, 2006; Galossi et al., 2007). Often, chronic viral infections like HIV of HCV infections are seen to exacerbate chronic rheumatoid arthritis (RA) in convalescent patients (Wendling and Herbein, 2006). Alphaviruses are known causes of significant inflammatory pathologies, ranging form arthritis to encephalitis (Johnston and Peters, 1996; Harley et al., 2001). Importantly, emerging alphaviruses such as CHIKV, MAYV and ONNV viruses are now considered as significant public health threats by the World Health Organisation (WHO), with reports of severe cases of debilitating arthritis and arthralgia in various regions of the world (Suhrbier and Linn, 2004). For instance, a recent CHIKV epidemic caused more than 240,000 cases of polyarthritis and 250 deaths in the French island of La Réunion, and is emerging as an important pathogen in the Indian subcontinent with more than 1.25 million cases reported (Laharyia and Pradhan, 2006; WHO, 2006; Renault et al., 2007).

4.1.1. *RRV-induced disease: role of cells and soluble host factors*

As alluded to in the introduction, RRV is a major cause of arthritis and arthralgia in humans. However, the pathogenesis of the disease was until recently poorly understood due to the lack of a suitable animal model of the disease. To dissect the mechanisms of RRV infection *in vivo*, a mouse disease model was established by Lidbury and Hapel, who proposed that macrophages were essential in RRV-induced muscle inflammation (Lidbury et al., 2000b). Recently, *in vivo* studies carried out in C57BL/6J mice further confirmed that RRV targets the skeletal tissue, in particular the muscle, bone and joint of RRV-infected mice, and contributes to macrophage-driven inflammation of these tissues (Morrisson et al., 2007a; Lidbury et al., 2008). A recent study by Lidbury and co-workers reports that depletion of macrophages using macrophage-specific inhibitor clodronate significantly reduced joint and muscle inflammation in RRV-infected mice. The inflammatory response was associated with high levels of pro-inflammatory cytokine expression, such as TNF-α, CCL-2/MCP-1 and IFN-γ. The authors carried out a preliminary trial of a monoclonal antibody against TNF-α showing a significant reduction of symptoms severity in

RRV-infected mice, suggesting tha TNF-α plays an important role in RRVD pathogenesis. Additionally, the authors showed that sulfasalazine, a NF-κB inhibitor in RRV-infected mice, not only ameliorated RRVD symptoms, but also significantly reduced muscle and joint tissue destruction (Lidbury et al., 2008).

RRV studies *in vivo* were carried out using this model and allowed the identification of important mediators of RRVD. For example, Morrison and co-workers established a role for complement molecule C3 in the development of RRV-induced pathology in mice (Morrisson et al., 2007a). The establishment of a mouse model of RRV disease allowed extensive characterisation of disease pathogenesis and cellular factors implicated in the disease. The reproducibility of this model lies in the use of 18-21 day-old (do) C57BL/6J mice, which show obvious symptoms of hind limb dysfunction following the inoculation of 10^3 PFU purified RRV per mouse by subcutaneous route. Consistent observations of mild ruffled fur and mild to moderate lethargy can be made as early as 6-7 days post-infection (dpi). The most severe disease signs, including complete loss of hind-limb function and extreme lethargy, can generally be observed at 10 dpi. Death is not expected in 18-21 day-old C57BL/6J mice infected with 10^3 PFU RRV, and complete recovery is normally observed at 25-30 dpi.

Several studies aimed at characterising cellular and soluble factors involved in both rheumatoid and pathogen-induced arthritis have identified mononuclear cells and T cells as the main effector cells. In RA, CD4+ T cells are believed to initiate inflammation in the synovium flowing detection of an antigen. Interplay between infiltrating T-cells and synoviocytes is believed to contribute to the development of RA symptoms (Weyand, 2000). In the case of pathogen-induced arthritis, the identification of alphaviruses able to replicate in skeletal tissue paved the way for further investigations. In a murine model, Sindbis virus replication was localised in the periosteum of long bone, and RRV was found to replicate in periosteum and skeletal muscle tissue (Heise et al., 2000; Morrisson et al., 2007b). These studies reported macrophages, T cells and NK cells as the primary infiltrating cell types in muscles and joints of RRV-infected mice.

4.1.2. *Cytokines in arthritis: a focus on TNF-α*

Other than the essential requirement for cells such as macrophages, T cells and NK cells as effector cells in inflammation, cytokines have been strongly implicated in the pathogenesis of

RA. Cytokines such as tumor necrosis factor-α (TNF-α), interleukin-6 (IL-6), IL-1β and macrophage-colony stimulating factor (MCSF), as well as associated transcription factors such as NF-κB were found to have a regulatory effect on inflammatory processes and tissue destruction (Schett, 2008). Therapeutic trials of anti-IL-6 and anti-IL-1β antibodies have been carried out in patients with RA and other inflammatory conditions, and showed that depletion of such cytokines could, in some cases, reduce disease severity (Kishimoto, 2005; Maini et al., 2006). However, several anti-TNF-α compounds have been designed and tested in patients with RA, and were found to significantly improve the patients' health and reduce disease symptoms (Garrison and McDonnell, 1999; Bathon et al., 2000). Despite the new generation of neutralising antibodies against IL-6 and IL-1β which have generated promising results in patients with RA, the most efficient treatment remains anti-TNF-α therapy (Nishimoto et al., 2000).

In this study, we attempted to determine the effect of TNF-α inhibition in the RRV mouse model using a validated, commercialised anti-TNF-α recombinant antibody, Enbrel (Etanercept®, Amgen & Wyeth). A qualitative assessment of disease and symptom manifestations between RRV-infected and Enbrel-treated, RRV-infected mice (designated RRV-Enbrel) was performed. Mice were monitored daily for clinical signs of disease and body mass changes. Muscle and joint tissue was analysed by histology in untreated and Enbrel-treated, RRV-infected mice. Differences in inflammatory infiltrates were assessed and the expression of key host cytokines in Enbrel-treated and untreated tissue was compared using quantitative RT-PCR.

4.2 Results

4.2.1 Effect of Enbrel treatment on RRV disease

Mice were inoculated with 10^3 PFU of RRV by subcutaneous route, whereas Enbrel-treated, RRV-infected mice were inoculated intraperitoneally with 400 μg/g Enbrel every second day following inoculation with RRV. Enbrel-treated, RRV-infected mice will be referred to as RRV-Enbrel, and uninfected control mice that received Enbrel as a control will be referred to as Enbrel-uninfected.

Weight change **(Fig. 4.1A)** and disease signs **(Fig 4.1B)** were monitored daily. RRV-infected mice were gaining significantly less weight than uninfected controls *($p<0.001$)* by 7 dpi, and showed

clear signs of musculo-skeletal disease by 10 dpi. Moderate hind limb dragging and lethargy were the most prominent disease signs observed in RRV-infected mice. After 10 dpi, mice started recovering and exhibited consistent weight gain until full recovery of limb function **(Fig 4.1B)**. RRV-infected mice showed an average clinical score of mild to moderate disease hind limb dysfunction [2.6 (±0.678)] at 7 dpi, and reached a maximum score of 2.750 (±0.250) at 10 dpi. In untreated, RRV-infected mice, the highest individual score was 4. Mock-infected animals, which were given PBS only, did not show any weight change or disease signs.

RRV-Enbrel mice displayed similar pathological signs, however disease was observed as early as 4 dpi, ranging from lethargy to mild hind limb dysfunction **(Fig 4.1B)**. By 7 dpi, RRV-Enbrel mice were showing symptoms ranging from moderate to severe hind-limb dysfunction. By 10 dpi, the average clinical score in the RRV-Enbrel group was 3.750 (±0.479). Disease symptoms gradually worsened and by 10 dpi, RRV-Enbrel mice were showing severe to extreme signs of disease, including death. Only 2 mice out of 5 survived and recovered from infection, at a much slower pace than untreated mice. **Figure 4.2A** shows that by 12 dpi, 60% of the animals had died in the RRV-Enbrel group, whereas untreated, RRV-infected and uninfected controls survived throughout the experiment. Enbrel-uninfected mice did not show

Figure 4.1: RRV disease in RRV-infected (■) and Enbrel-treated, RRV-infected (designated RRV-Enbrel) (▲) C57BL/6J mice. 21 day-old C57BL/6J mice were inoculated with 10^3 PFU of RRV by subcutaneous route. Uninfected mice (▼) received PBS alone. Enbrel-treated, RRV-infected mice received 400 μg/g Enbrel intraperitoneally every second day after infection. Uninfected-Enbrel (◇) mice were injected with 400 μg/g Enbrel every two days. **(A)** Average percent weight change (±standard error of the mean; SEM) compared to starting body mass at Day 0. **(B)** Mean clinical disease score (±SEM) (0, no disease signs; 1, very mild lethargy and/or ruffled fur; 2, mild lethargy and mild hind limb dysfunction; 3 established lethargy with moderate to severe hind limb dysfunction; 4, extreme lethargy, loss of limb function and/or total paresis; 5, death.). Each data point represents the mean (and SEM) clinical score for each group (n=5). Data is representative of 3 experiments. Statistical significance of differences between RRV-infected and RRV-Enbrel mice was determined by 2-way ANOVA followed by Bonferroni's post-test.

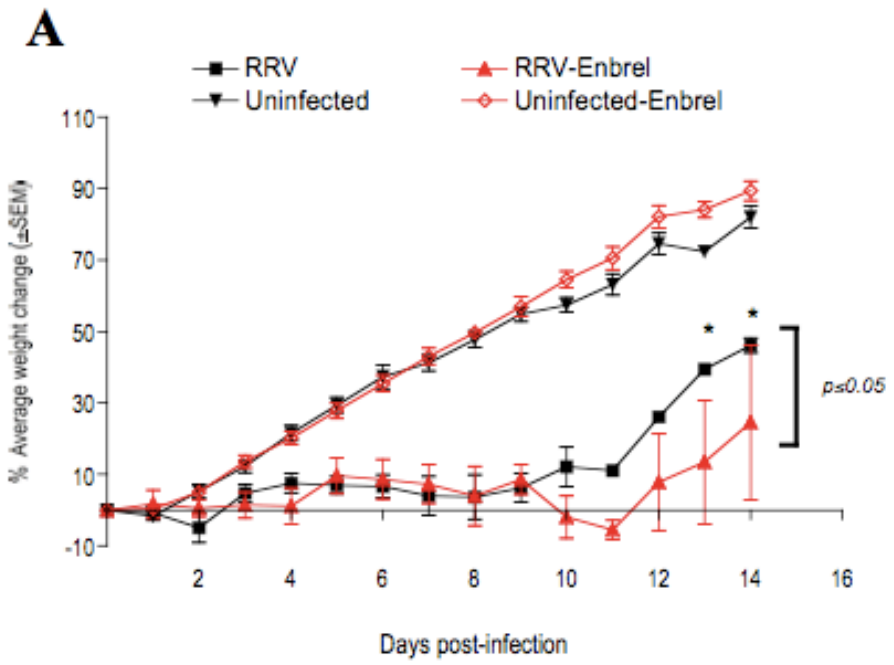
A
RRV
Uninfected
RRV-Enbrel
Uninfected-Enbrel
% Average weight change (±SEM)
110
90
70
50
30
10
-10
2
4
6
8
10
12
14
16
p≤0.05
Days post-infection

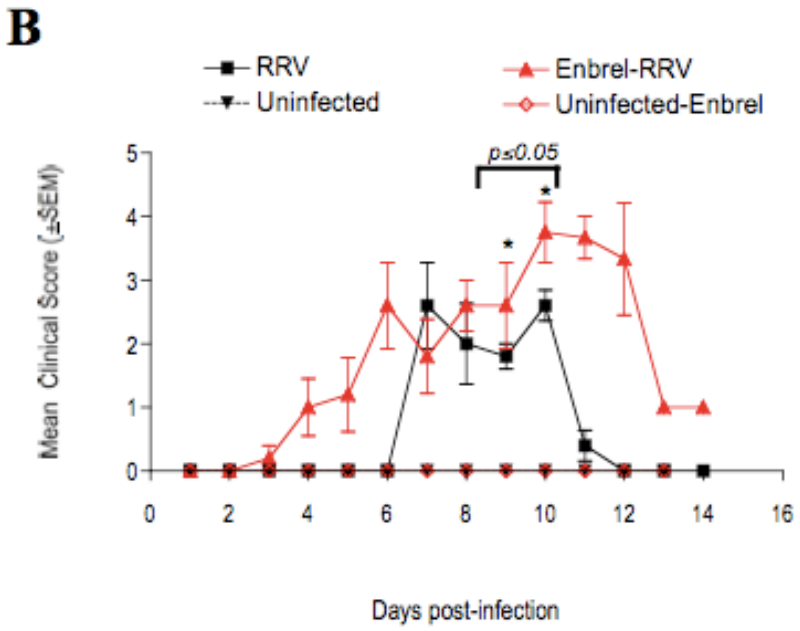
B
RRV
Uninfected
Enbrel-RRV
Uninfected-Enbrel
Mean Clinical Score (±SEM)
5
4
3
2
1
0
0
2
4
6
8
10
12
14
16
p≤0.05
Days post-infection

any difference in weight change nor did they develop any disease sign when compared to uninfected control mice.

At 13 and 14 dpi, the differences in mean percent weight change between RRV-infected and RRV-Enbrel mice were significant ($p \leq 0.05$). Differences in average clinical score between RRV-infected and RRV-Enbrel mice were significant at 9 and 10 dpi ($p \leq 0.05$).

4.2.2 Viral titres in tissue of RRV-infected mice

Next, we investigated whether Enbrel treatment of RRV-infected mice had any effect on RRV replication in muscle and joint tissues. We harvested quadriceps and ankle tissue at 10 dpi and processed them for viral titration by plaque assay. Mean RRV titre in muscle and joint tissue of RRV-infected and RRV-Enbrel mice, expressed in PFU per mg tissue, is shown in **Figure 4.2B**.
There were no significant differences in RRV titres between RRV-infected and RRV-Enbrel mice at 10 dpi. No significant differences were observed between muscle and joint viral titres.

4.2.3 Histological analysis of muscle and joint tissue

We next examined muscle and joint tissue and visually assessed morphological changes and tissue inflammation in RRV-infected and RRV-Enbrel mice. This was assessed by histological analysis. At 10 dpi, quadriceps muscle and ankle joint were dissected, sectioned and stained with H&E. **Figure 4.3** shows quadriceps muscle histology, and **Figure 4.4** shows ankle joint synovium histology at 10 dpi.
Mock-infected animals displayed a homogenous muscle structure with little or no cell infiltrates. However, RRV-infected and RRV-Enbrel mice showed substantial inflammation and muscle fibre damage at 10 dpi **(Fig 4.3)**. Infiltrating cells can be seen in the interstitial space, and cross-sectional histology shows an eroded, irregular muscle fibre structure and condensed interstitial space.
Synovial cavities in the joint of mock-infected animals showed a regular synovial tissue structure with sparse peripheral mononuclear cells. At 10 dpi, RRV-infected mice showed substantial infiltration of mononuclear cells in the synovial tissue. In

Figure 4.2: Survival and viral load. (A) Survival of RRV-infected (■), RRV-Enbrel (▲), uninfected (▼) and Enbrel-uninfected (◇) C57BL/6J mice. This data represents the survival in groups of 5 mice. **(B)** RRV titres in muscle and joint tissue at 10 dpi. Viral titre is expressed in Log_{10} PFU/mg tissue and was determined by plaque assay. Data is representative of 3 separate experiments.

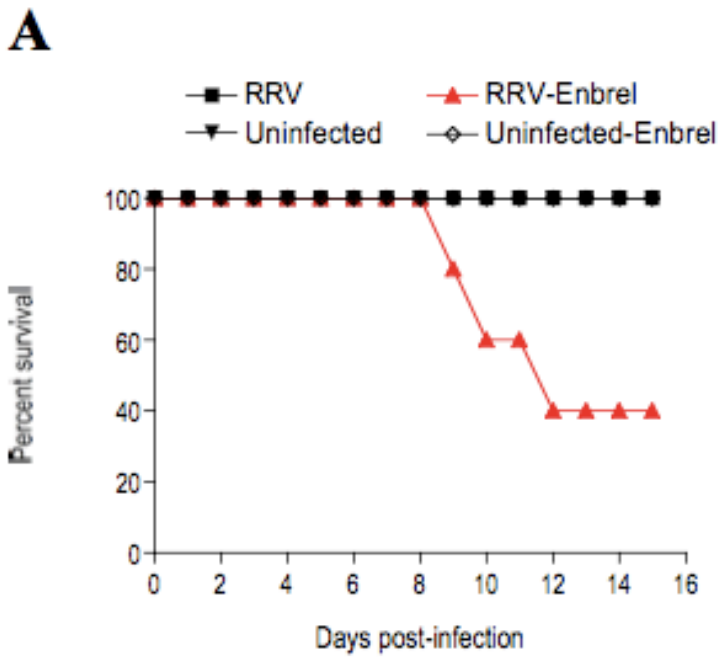
A
RRV
RRV-Enbrel
Uninfected
Uninfected-Enbrel
Percent survival
100
80
60
40
20
0
0
2
4
6
8
10
12
14
16
Days post-infection

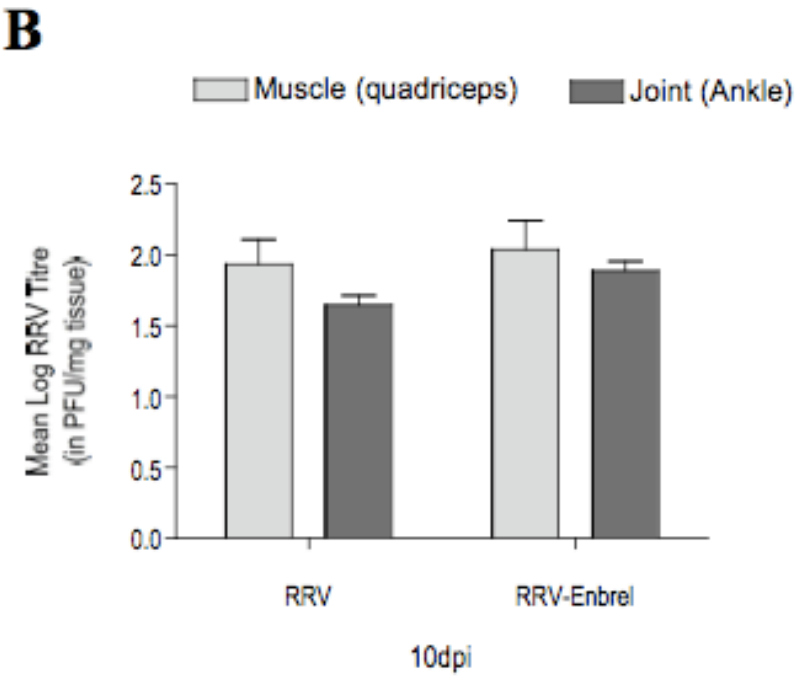
B
Muscle (quadriceps)
Joint (Ankle)
Mean Log RRV Titre
(in PFU/mg tissue)
2.5
2.0
1.5
1.0
0.5
0.0
RRV
RRV-Enbrel
10dpi

RRV-Enbrel mice, there was an extensive infiltration and congestion of the synovial space by inflammatory cells **(Fig 4.4)**. The extent of tissue damage and cellular infiltration correlated closely with high clinical disease scores (moderate to severe hind limb dysfunction and lethargy) in both RRV-infected and RRV-Enbrel mice. In summary, we observed that RRV-Enbrel mice clearly showed higher cellular inflammation in muscle and joint tissue compared to untreated, RRV-infected mice.

Figure 4.3: Histological analysis of muscle tissue of RRV-infected and RRV-Enbrel C57BL/6J mice at 10 dpi. 21 day-old mice were inoculated subcutaneously with 10^3 PFU of RRV. RRV-Enbrel animals were inoculated with 400 μg/g Enbrel every two days following RRV infection. Control animals were inoculated with 100μL PBS. Quadriceps muscle tissue was collected at 10 dpi and fixed in formalin and imbedded in paraffin. 10 μm-thick, longitudinal and transversal sections were performed and stained with Hematoxylin and Eosin (H&E). (Images were taken at 100x magnification). Data is representative of 5 animals per group.

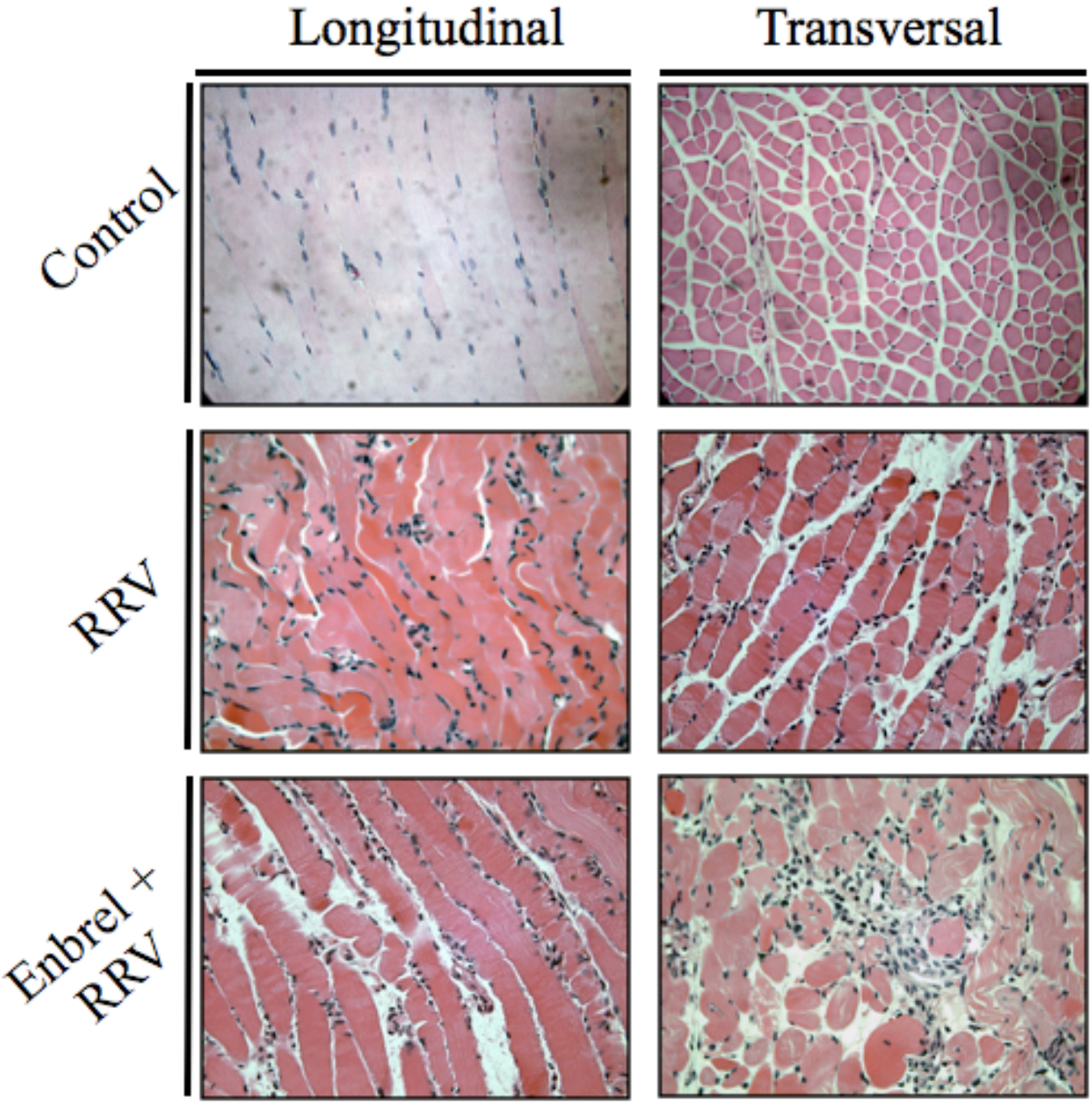
Longitudinal
Transversal
Control
RRV
Enbrel +
RRV

Figure 4.4: Histological analysis of joint synovium in RRV-infected and RRV-Enbrel C57BL/6J mice. 21 day-old mice were inoculated subcutaneously with 10^5 PFU of RRV. RRV-Enbrel animals were inoculated with 400 μg/g Enbrel every two days following RRV infection. Control animals were inoculated with 100μL PBS. Ankle joints were collected at 10 dpi and fixed in formalin. Ankles were imbedded in paraffin and sectioned longitudinally in 10μm-thick section Hematoxylin and Eosin (H&E) staining. (Images were taken at 10x and 100x magnification). Data is representative of 5 animals per group.

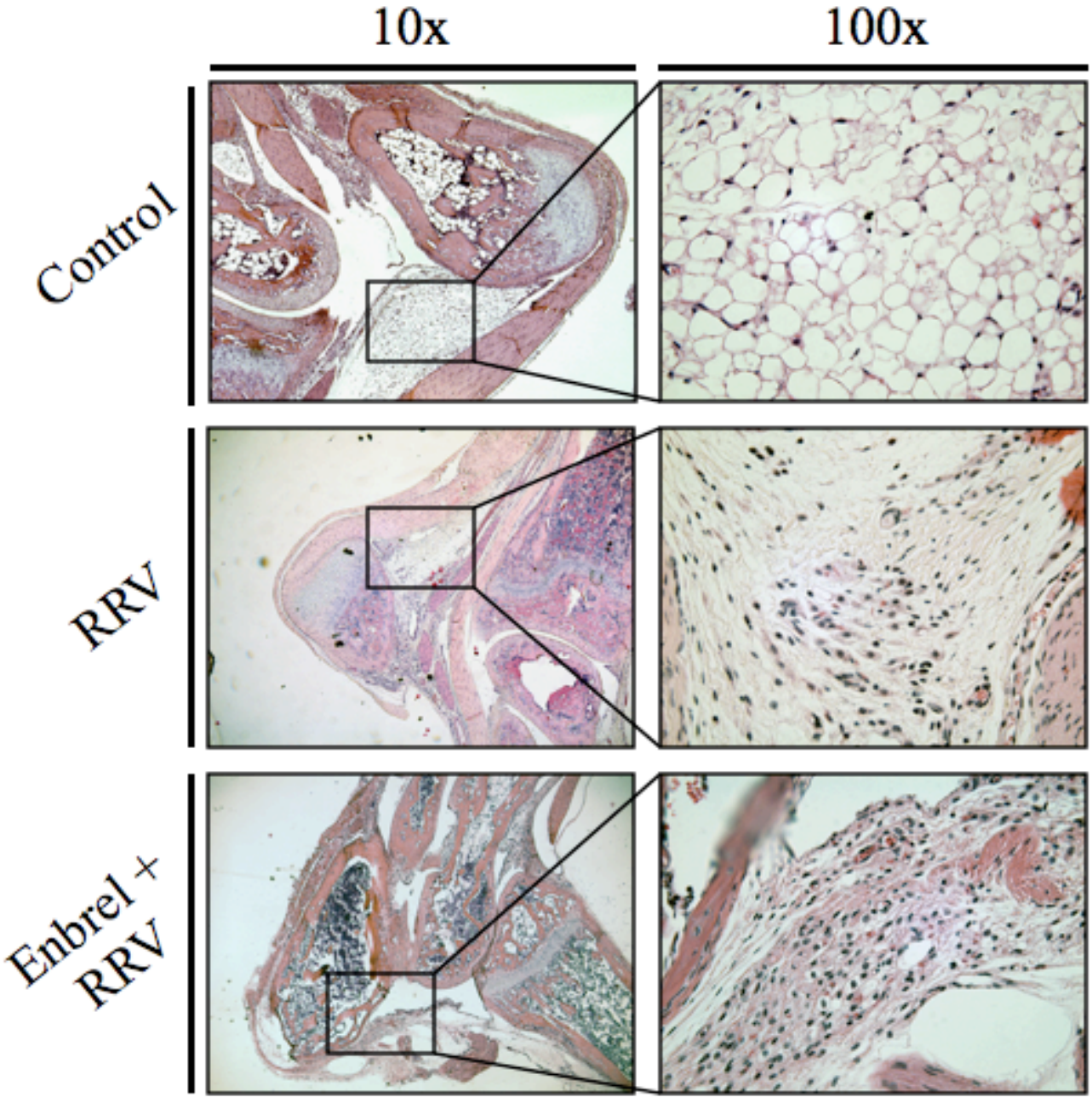
10x
100x
Control
RRV
Enbrel +
RRV

4.2.4 Quantitation of inflammatory cell infiltrates

Next, we attempted to determine whether Enbrel treatment had an effect on the type of infiltrating cell observed by microscopical analysis in the muscle and joints of RRV-infected mice. Muscle and joint (quadriceps and ankle, respectively) were taken at 10 dpi, homogenised and infiltrating leukocytes were stained with Giemsa/May-Grumwald stain. Leukocytes were counted and the composition of inflammatory infiltrates in muscle and joints is shown in **Figure 4.5A** and **Figure 4.5B**, respectively.

In the quadriceps muscle, macrophages were found in significantly higher proportions ($p=0.005$) in RRV-Enbrel mice compared to untreated, RRV-infected mice **(Fig. 4.5A)**. Lymphocyte, eosinophil and neutrophil numbers were not significantly different between treated and untreated groups. In the ankle joint, a higher number of macrophages ($p=0.0178$) were found in RRV-Enbrel mice compared to untreated, RRV-infected mice **(Fig 4.5B)**. In contrast, eosinophils and neutrophils were found in significantly higher proportions in the joints of untreated, RRV-infected mice. Differences were statistically significant for eosinophils ($p=0.0144$) and neutrophils ($p=0.0221$) in RRV-infected mice compared to RRV-Enbrel mice.

Figure 4.5 : Differential leukocyte cell count of muscle and joint tissue in RRV-infected and RRV-Enbrel C57BL/6J mice at 10 dpi. **(A)** Quadriceps muscle was homogenised and leukocyte cell suspensions were collected on a slide by cytospin. Cells were counterstained with Giemsa-Grunwald stain and differential cell count was performed over 10 mid-power fields (40x). **(B)** Ankle joints were collected and processed as described above for differential leukocyte staining. Data represents the mean (±SEM) of 10 mid-power fields. Statistical analysis (unpaired, two-tailed Student *t*-test) was performed using Prism GraphPad software.

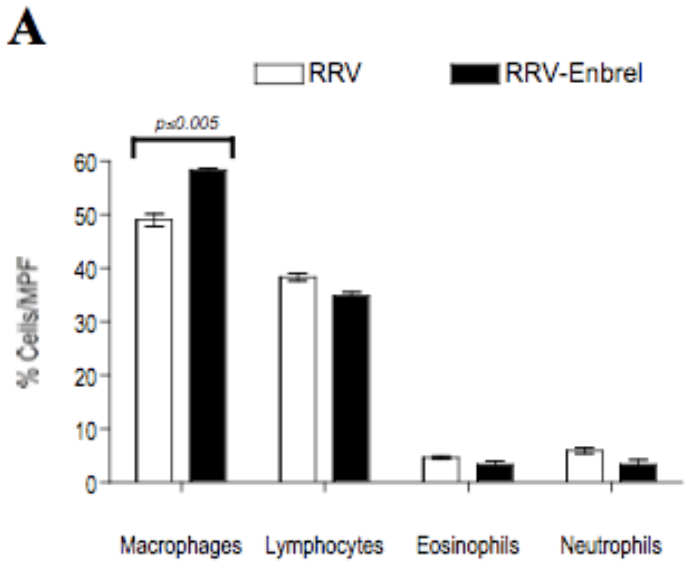
A
RRV
RRV-Enbrel
p≤0.005
% Cells/MPF
60
50
40
30
20
10
0
Macrophages
Lymphocytes
Eosinophils
Neutrophils

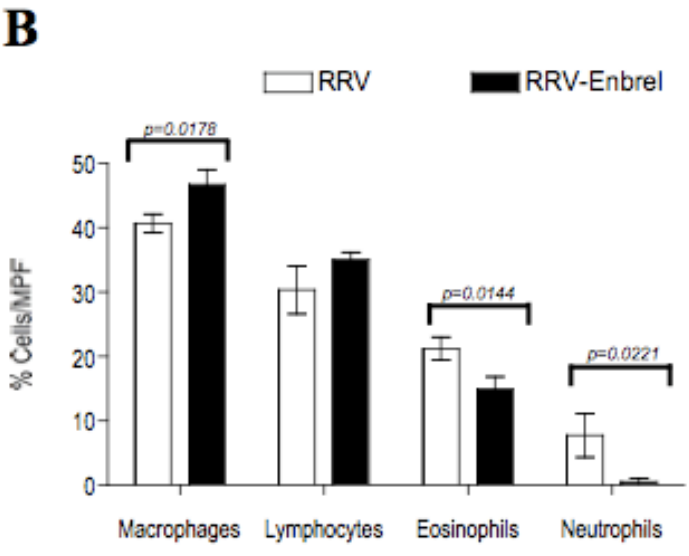
B
RRV
RRV-Enbrel
p=0.0178
p=0.0144
p=0.0221
% Cells/MPF
50
40
30
20
10
0
Macrophages
Lymphocytes
Eosinophils
Neutrophils

4.2.5 Differential analysis of host factor expression

The expression pattern of pro-inflammatory cytokines following infection can determine the outcome of the disease. We investigated the differences in cytokine expression profile in the muscle and joint tissue of RRV-infected and RRV-Enbrel mice at 10 dpi. Briefly, mice were sacrificed at 10 dpi and quadriceps or ankle tissues were processed for total RNA extraction. cDNA was generated and relative levels of cytokine messenger RNA was determined by quantitative, real-time PCR. Relative levels of mRNA expression are shown for muscle **(Fig. 4.6A)** and joint **(Fig 4.6B)**.

In the quadriceps muscle **(Fig 4.6A)**, RRV-Enbrel mice were found to express higher levels of RANTES and IFN-γ mRNA compared to untreated, RRV-infected mice. MCP-1 and IP-10 mRNA levels were found to be significantly up-regulated in the muscle of both Enbrel-treated and untreated, RRV-infected mice at 10 dpi. Levels of RANTES and TNF-α mRNA were significantly down-regulated in the muscle of RRV-infected mice. In the joint tissue **(Fig 4.6B)**, MCP-1 and TNF-α mRNA levels were found to be significantly up-regulated in RRV-Enbrel mice, whereas untreated, RRV-infected mice displayed basal expression levels of these cytokines.

Figure 4.6: Expression of pro-inflammatory cytokines in muscle (A) and joint (B) tissue of RRV-infected and RRV-Enbrel mice at 10 dpi. 21 day-old C57BL/6J mice were inoculated subcutaneously with 10^5 PFU of RRV. RRV=Enbrel mice received 400 μg/g Enbrel every second day following infection with RRV. Uninfected mice received PBS. Muscle (quadriceps) and joint (ankle) were collected at 10 dpi and total mRNA was extracted and processed for quantitative, real-time PCR. Data shown represents the average fold change in mRNA expression compared to uninfected samples. Statistically significant up- or down-regulation ($p \leq 0.05$) is marked with an asterisk. Statistically significant differences in mRNA levels were determined by two-tailed, unpaired *t*-test with Welch's correction.

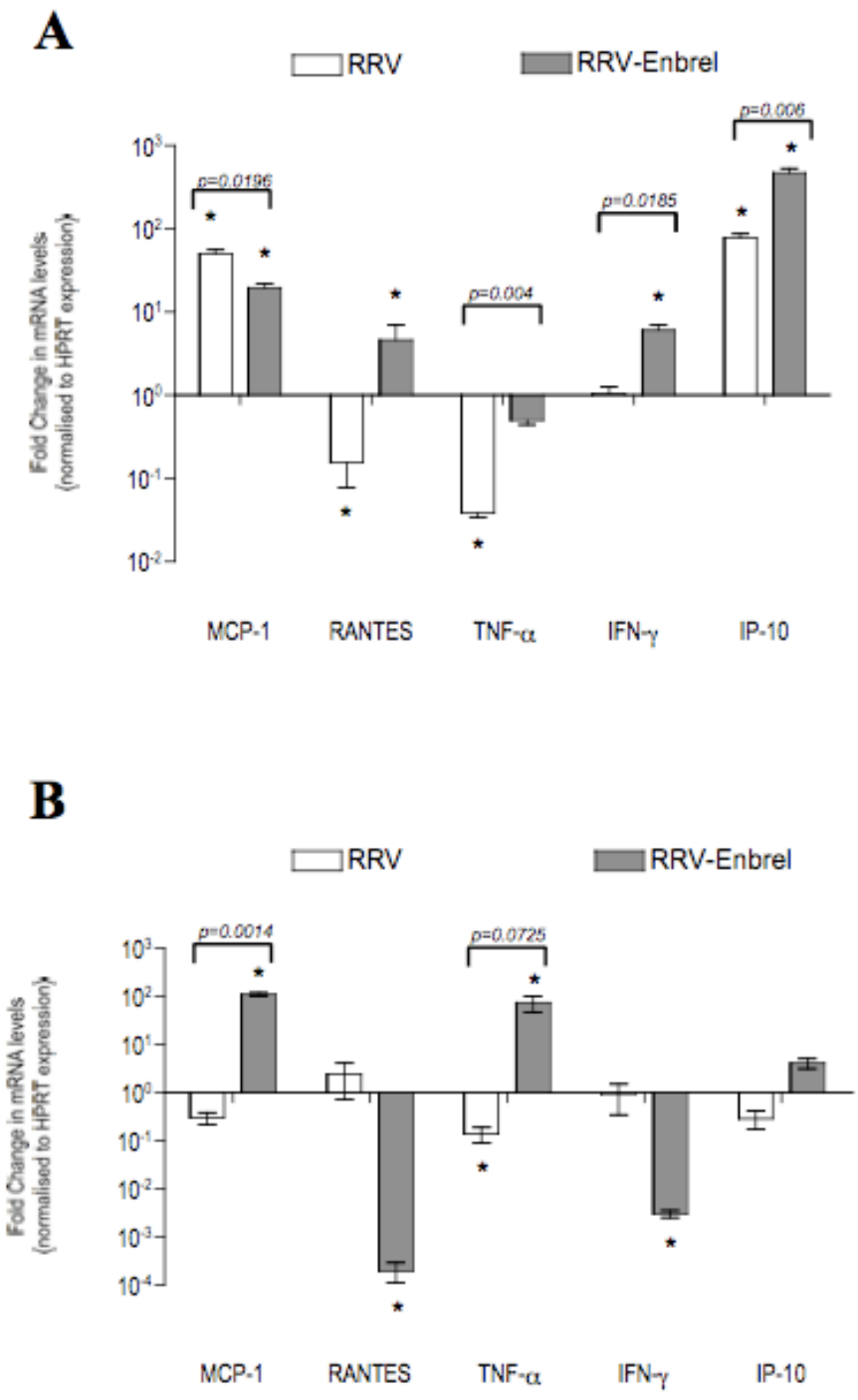
A
RRV
RRV-Enbrel
Fold Change in mRNA levels (normalised to HPRT expression)
p=0.0196
p=0.004
p=0.0185
p=0.006
MCP-1
RANTES
TNF-α
IFN-γ
IP-10
B
RRV
RRV-Enbrel
Fold Change in mRNA levels (normalised to HPRT expression)
p=0.0014
p=0.0725
MCP-1
RANTES
TNF-α
IFN-γ
IP-10

4.3 Discussion

The aim of this chapter was to assess the effect of Enbrel, a validated compound used to treat chronic RA, in the treatment of RRV-induced disease in mice. Drawing on analogous inflammatory processes in viral and rheumatoid arthritis, and the findings that RRV-infected mice and humans show prominent levels of TNF-α in the joint synovium (Lidbury et al., 2008), we hypothesised that the use of Enbrel, an anti-TNF-α fusion molecule, could prevent or ameliorate disease symptoms caused by RRV. Using a mouse model of RRV disease, we administered Enbrel intraperitoneally to C57BL/6J mice every second day following RRV infection and monitored the mice for signs of disease.

4.3.1 Enbrel treatment in RRV-induced disease

In this study, RRV-infected mice treated with Enbrel developed disease signs corresponding to the well-characterised signs of RRVD in the C57BL/6J mouse model. At 7 dpi, untreated, RRV-infected mice started showing characteristic signs of disease, namely mild to moderate hind limb dysfunction. In contrast, RRV-Enbrel mice started showing signs of disease three days earlier, with an average clinical score gradually matching that of untreated, RRV-infected mice at 7 dpi. Both treated and untreated mice had ceased to increase in body weight, whereas PBS and Enbrel-mock treated animals did not show any signs of disease or weight loss throughout the entire observation period. Clearly, Enbrel treatment alone in the absence of RRV infection did not have a detrimental effect on mouse weight and health.

Between 7 and 10 dpi, RRV-infected mice in both groups experienced moderate illness, however symptoms in untreated mice were gradually decreasing in intensity, as animals were slowly beginning to use their hind limbs for locomotion. In contrast, RRV-Enbrel mice experienced increasing disease severity, with average clinical scores showing extreme paresis or moribund states, most animals being unable to walk. Sixty percent of Enbrel-treated animals died by 14 dpi, following acute systemic illness. By days 10 and 11 post-infection, untreated RRV-infected mice were recovering steadily, resumed normal weight gain and increased activity, while the surviving RRV-Enbrel mice were slowly recovering from symptoms, which lasted until 14 dpi. These animals eventually fully recovered after 30 dpi.

Our studies also showed that Enbrel did not have any effect on RRV replication. We harvested muscle and joint tissue from RRV-Enbrel and RRV-infected, untreated mice and compared RRV titres. Similar RRV titres were recovered from muscle and joint homogenates of RRV-Enbrel and untreated mice. This suggests that a correlation between viral titres and disease pathogenesis would not be accurate, since severe symptoms leading to death in RRV-Enbrel mice were dependent on cellular and molecular events rather than viral replication. However, it is possible that significantly higher virus titres may be recovered from other tissue sites (other organs or blood) of RRV-Enbrel mice compared to untreated, RRV-infected mice, and perhaps provide an explanation for increased susceptibility of Enbrel-treated mice to RRV infection.

The possible physiological causes of disease - or death - following RRV infection in Enbrel-treated C57BL/6J mice were investigated by histological analysis. Quadriceps muscle and ankle joint sections were stained and revealed the extent of inflammation in tissue at 10 dpi. Muscle tissue of RRV-Enbrel mice displayed characteristic features of mononuclear cell infiltration observed in the RRV disease model, and showed extensive muscle fibre damage. Likewise, synovial cavities of RRV-Enbrel mice showed high cellular infiltration and periosteal congestion, which are clear signs of RRV-induced inflammation. This data provided rigorous evidence that contrary to expectations, Enbrel did not attenuate muscle and joint inflammation in RRVD.

4.3.2. TNF-α inhibition therapy in rheumatic diseases

The presence of TNF-α in synovial tissue of RA patients prompted investigations into the effects of TNF-α inhibition in inflammatory arthritis. TNF-α inhibitors first appeared in 1981, with the release of Enbrel (Etanercept), a fusion protein of murine anti-TNF-α epitope and human Fc receptor. Enbrel is the most commonly used anti-TNF-α compound and the most widely characterised, as many large-cohort, randomised trials have been performed to assess its efficacy as a therapy for RA and other arthritic conditions, such as psoriatic arthritis and spondylarthritis (Moreland et al., 1999; Caramaschi et al., 2006; Takeuchi, 2006). Studies have showed that Enbrel efficiently reduced arthritic symptoms and joint damage compared to methotrexate, an anti-inflammatory drug used in RA treatment (Garrison and McDonnell, 1999; Bathon et al., 2000; Takeuchi, 2006). Currently, anti-TNF-α therapy is the single most effective treatment against RA and several other inflammatory conditions, such as inflammatory bowel syndrome, spondylarthritis and juvenile rheumatoid arthritis.

The most efficient treatment available for symptoms caused by RRV disease consists of non-steroidal anti-inflammatory drugs, such as aspirin or ibuprofen (Mylonas et al., 2002). Considering both the possible extent of disease symptoms (up to 6 months), and the debilitating nature of the disease, a specific anti-inflammatory drug would certainly benefit up to 8,000 people infected with RRV each year. Additionally, the use of biologic therapies targeting other cytokines involved in inflammatory disease (eg. TNF-α, IL-1β, IL-6) could be extended to other infectious arthritides such as Chikungunya, Rubella and Leishmania-induced diseases.

In our attempt to assess the efficacy of Enbrel in treating RRV disease symptoms, we found that in the context of RRV-induced arthritis, Enbrel does not reduce clinical symptoms in the mouse disease model. Furthermore, we show that Enbrel treatment exacerbates inflammation and disease, leading to acute systemic illness followed by death in 60% of animals. Having established that administration of Enbrel alone does not cause any symptoms in mice, we propose that in light of studies associating Enbrel treatment with pathological complications, Enbrel treatment in RRV-infected mice may dysregulate immune response mechanisms resulting in aberrant inflammatory responses.

4.3.4. Possible mechanisms of RRVD pathogenesis: a role for TNF-α

In RRVD, several pro-inflammatory factors are at play in disease pathogenesis. Firstly, macrophages are potent TNF-α producers, chemokines such as MCP-1, which recruit macrophages towards to the tissue. Secondly, pro-inflammatory cytokines such as IL-1α/β, IL-6, IP-10 and TNF-α, have been implicated in a broad range of inflammatory disorders, including arthritis (De Rossi et al., 2000). Some studies have evoked the possibility that the recognition of viral RNA by host cells can trigger an inflammatory response leading to arthritis. A study by Zare and colleagues showed that dsRNA could be used to trigger arthritis in mice, suggesting that several receptors and immune system components, including those considered strictly as antiviral factors, could be involved in the development of dsRNA-induced arthritis (Zare et al., 2004). Arthritic symptoms were also reported in patients infected with Hepatitis C virus (Lovy et al., 1996). Other studies support the idea that antiviral response pathways maybe involved in arthritis. For example, IFN-β treatment was found to significantly reduce arthritic symptoms and slowed cartilage damage in RA patients in combination with methotrexate, an anti-inflammatory drug.

Such studies were first performed in mice, and were later carried out in large, double blind randomised cohorts (van Holten et al., 2004; van Holten et al., 2005). The authors report that levels of TNF-α, IP-10 and IL-6 were significantly reduced in mice with collagen-induced arthritis upon subcutaneous injection of IFN-β. Such studies reveal the possibility that some RNA viruses may interfere with host response and modulate TNFR-associated pathways, thus favouring the onset of excessive inflammation and tissue damage.

Recently, Lidbury and colleagues performed a qualitative assessment of TNF-α and NF-κB inhibition in RRV-induced disease in mice (Lidbury et al., 2008). NF-κB is one of the master regulators of gene expression in TNFR signalling as well as viral infection (Pfeffer et al., 2004). NF-κB is also involved in the regulation of several inflammatory disorders in humans, such as arthritis, asthma and inflammatory bowel syndrome (Karin and Ben-Neriah, 2000; Baldwin, 2001). NF-κB is a key coordinator of TNF-α induced signalling, as several studies targeting NF-κB reported physiological effects corresponding to diminished TNFR signalling (Tomita et al., 1999; Tomita et al., 2000). The study found that inhibition of TNF-α or NF-κB reduced disease symptoms in mice, which were exhibiting lower clinical scores. In the Lidbury et al. study, the intrinsic relationship between NF-κB and TNFR signalling has been shown in RRV-infected mice treated with NF-κB and TNF-α inhibitors. Elevated levels of TNF-α seen in RRV-infected humans were found to correlate with observations in the RRV mouse model. Specific inhibition of NF-κB was found to prevent disease, whereas TNF-α blockade was found to reduce disease symptoms in mice (Lidbury et al., 2008).

However, in the present study, the administration of Enbrel to RRV-infected mice led to the exacerbation of RRV-induced disease, and the subsequent death of 60% of RRV-infected, treated animals. Our data also suggests a higher degree of cellular inflammation in muscle and joint tissue of RRV-Enbrel mice at the peak of the disease. We also observed that Enbrel treatment correlated with higher levels of MCP-1, IFN-γ and IP-10 in tissue compared to untreated, RRV-infected mice.

The causes for aggravated symptoms following Enbrel treatment in RRV-infected mice could be independent of TNF-α signalling. There has been some reported side effects due to Enbrel treatment such as rheumatoid nodules (Kekow et al., 2002). In addition, dangerous side effects of

Enbrel were officially reported by the US health authorities, following the death of some Enbrel-treated patients as a result of severe sepsis (FDA, 1999). Interestingly, clinical reports have also associated Enbrel treatment with severe viral respiratory tract infections in humans, while an animal model of inflammatory cardiomyopathy induced by the parasite *Trypanozoma cruzii* found that Enbrel treatment aggravated disease symptoms (Moreland et al., 1999; Smith and Letendre, 2002; Bilate et al., 2007). The study by Bilate and colleagues investigated the effect of Enbrel treatment on *Trypanosoma cruzii*-induced Chronic Chagas Cardiomyopathy (CCC) in hamsters, and found that Enbrel treatment exacerbated CCC pathology. This suggests that in the context on pathogen-induced inflammation, Enbrel-mediated TNF-α inhibition may exhibit side effects for which the causes remain unknown. Based on our findings, we must consider the possibility that adverse reactions observed in Enbrel-treated humans may differ from reactions observed in RRV-infected, Enbrel-treated mice. Enbrel is a fusion protein carrying a human epitope, against which a prophylactic reaction could exacerbate pre-existing conditions, such as RRVD. Besides, such adverse reactions may only occur in an acute inflammatory context, since uninfected mice that were treated with Enbrel showed no signs of disease. The mechanisms by which Enbrel could exacerbate inflammatory symptoms remain unknown, and despite its widespread use, further studies are needed to characterise the effect of Enbrel therapy in patients susceptible to viral infections.

5.1 Introduction

Early clinical and physiological studies of RRV-infected EPA patients allowed the identification of infiltrating cell types in the synovium during RRV disease (Fraser et al., 1981; Fraser et al., 1983). As noted earlier in this thesis, macrophages have been identified as the main effector cell in RRV disease, being responsible for massive infiltration as well as release of cytotoxic compounds at the site of inflammation (Lidbury et al., 2008). However, a role of specialised cytotoxic cell subsets, such as T cells or Natural Killer cells was suggested by the presence of high levels of cytotoxic, CD8+ T cells, and the comparatively low levels of regulatory CD4+ T cells in the synovium of RRV-infected patients (Fraser et al., 1983). T cells have recently been shown to have a minimal role in RRV disease as mice deficient in T and B cells (RAG-1 -/- mice) developed similar signs of disease as their wild type congeners (Morrisson et al., 2007b). The role of NK cells in RRVD pathogenesis remains unclear and warrants further investigations.

The first study proposing a role of NK cells in RRVD was suggested by Aaskov and colleagues, who found that NK cell numbers were elevated in the blood of RRV-infected patients (Aaskov and Dalglish, 1981). Later, the same authors showed that while NK cells were able to kill autologous synovial cells, peripheral blood levels of NK cells were seen to rise shortly after RRV infection, then decline during symptom manifestations, suggesting for NK cells as an accessory, rather than effector role regulated by monocytic cells, the main cell type involved in RRVD (Aaskov et al., 1986). Interestingly, similar patterns of NK cell activity were observed in RA. Analysis of synovial effusions from RA patients revealed decreased NK cell activity, suggesting a regulatory role during the development of disease symptoms and tissue inflammation (Dobloug et al., 1982).

Natural killer (NK) cells are a subset of lymphocytes discovered in the 1970's. Their cytotoxic and anti-tumour activity was first observed in animals and humans, which led to extensive characterisation studies. NK cells are lymphocytes which possess lymphocyte antigenic makers, but do not share any antigenic characteristics with either T or B cells (Herberman and Ortaldo, 1981). Since their discovery, NK cells were found to be involved at several stages of the immune response. For example, NK cells can trigger the differentiation of monocytes to dendritic cells, as well as respond to RNA viruses such as HIV and contribute to early clearance of Herpes Simplex virus (HSV) (Reading et al., 2006; Alter et al., 2007; Zhang et al., 2007). NK cells have the ability to target and lyse virus-infected cells, and have potent anti-tumour functions, and despite their

lymphocytic attributes, are considered part of the innate immune system (Herberman and Ortaldo, 1981). More specifically, NK cells and dendritic cells are involved in the mutual activation and regulation of T-cell mediated immune responses, in particular following infection (Kamath et al., 2005).

NK cells have also been implicated in inflammatory disorders such as arthritis, and the Beige mutant mouse was initially used as a disease model for Chediak-Higashi syndrome, a rare autosomal recessive disorder in humans (Kelly, 1957; Brandt and Swank, 1976). Other than minor neurological defects such as retinal degeneration, Beige mice display a defect in NK cell lysosomal activity, resulting in increased susceptibility against pathogens (Kelly, 1957; Saxena et al., 1982; Kaplan et al., 2008). This defect primarily affects cytoplasmic transport of cytotoxic granules by defective microtubules, which renders NK cells unable to secrete cytolytic granules upon target cells, whereas other cell types, such as macrophages and T cells, remain functional (Roder, 1979; Roder and Duwe, 1979). Beige mice have been used in studies examining the requirement of NK cells in the development of inflammatory conditions, such as those observed in severe acute respiratory syndrome-coronavirus (SARS-CoV) and SFV infection (Gates et al., 1984; Glass et al., 2004).

In this chapter, we examined RRV disease pathogenesis in C57BL/6J-Lyst^{bg}/Arc or Lyst^{bg} mice, a mouse strain with deficient NK cell function, and compared disease features with those observed in the C57BL/6J background. We infected 20 day-old Lyst^{bg} and C57BL/6J mice with 10^3 PFU of RRV subcutaneously, and monitored for weight change and disease signs daily. We assessed inflammation by histological analysis and compared types of cell infiltrates by flow cytometry. Differences in cytokine expression between Lyst^{bg} and C57BL/6J mice were determined by real-time PCR. We also sought to determine the effect of NK cell depletion on RRVD pathogenesis using a monoclonal, anti-NK1.1 antibody in RRV-infected C57BL/6J mice.

5.2 Results

5.2.1 RRV-induced disease in 20 day-old Lyst^{bg} mice

Mice were inoculated with 10^3 PFU of RRV and mock controls were injected with PBS alone. Animals were weighed and monitored for disease signs daily. Lyst^{bg} mice showed early

symptoms of RRV-induced weight loss compared to C57BL/6J mice **(Fig 5.1A)**. Both groups of RRV-infected mice showed signs of disease at the expected time points. Interestingly, uninfected Lyst^{bg} mice showed substantial variation in weight gain compared to uninfected C57BL/6J mice. RRV-induced disease was more severe in Lyst^{bg} mice compared to C57BL/6J mice **(Fig 5.1B)**. At 6 dpi, Lyst^{bg} mice showed an average disease score of 3.4 (±0.245), whereas C57BL/6J mice only reached a similar score at 9 dpi. Lyst^{bg} mice consistently showed high disease scores, ranging from moderate to severe hind limb dysfunction and paresis. By 9 dpi, symptoms in C57BL/6J mice started to decline, whereas Lyst^{bg} mice were suffering severe illness **(Fig 5.1B)**. At 8 dpi, 20% of RRV-infected Lyst^{bg} mice had died, and by 12 dpi, all Lyst^{bg} mice had succumbed to the disease **(Fig 5.2)**.

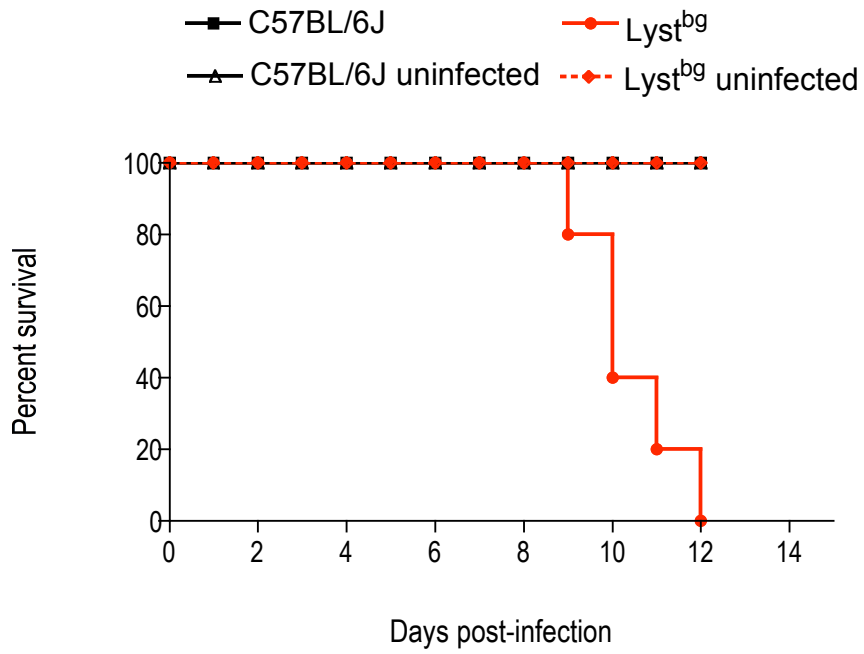

Figure 5.2: Survival plot for RRV-infected Lyst^{bg} and C57BL/6J mice. Mice were inoculated with 10^3 PFU RRV and monitored daily for signs of disease or mortality. Mock-infected animals were administered diluent (PBS) alone. Each data point is representative of 5 mice per group.

Figure 5.1: RRV disease in 20 day-old Lyst^{bg} and C57BL/6J mice. Mice were inoculated with 10^3 PFU of RRV subcutaneously and monitored daily for weight change and disease signs. **(A)** Average percent weight change (±standard error of the mean; SEM) in RRV-infected Lyst^{bg} (■) and C57BL/6J (▼) mice. Uninfected controls were inoculated with PBS. **(B)** Average clinical score (±SEM) (0, no disease signs; 1, very mild lethargy and/or ruffled fur; 2, mild lethargy and mild hind limb dysfunction; 3 established lethargy with moderate to severe hind limb dysfunction; 4, extreme lethargy, loss of limb function and/or total paresis; 5, death). Each data point shows the mean and standard deviation (n=5) for each group. Statistically significant differences (* $p<0.05$) were assessed by a 2-way ANOVA followed by a Bonferroni's post-test.

A

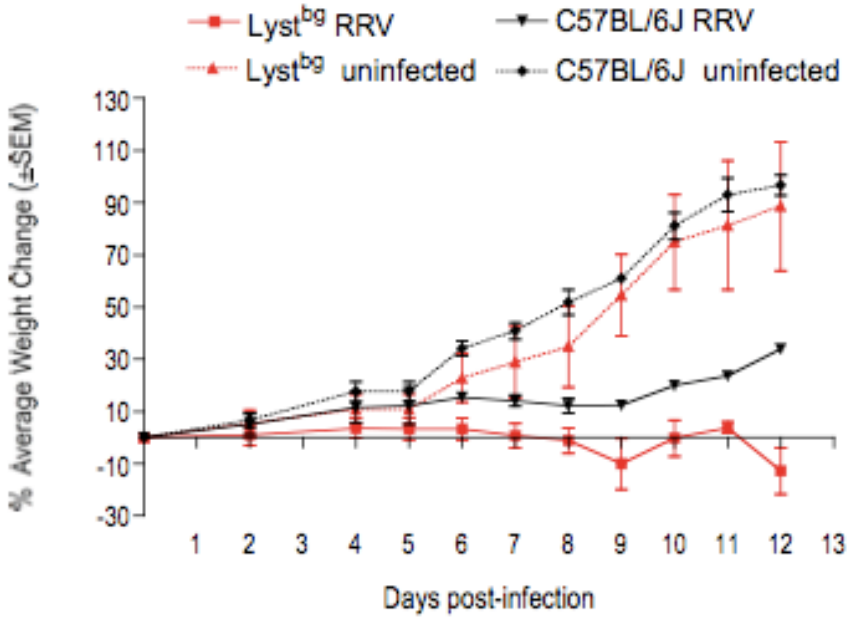
Lyst^bg RRV
C57BL/6J RRV
Lyst^bg uninfected
C57BL/6J uninfected
% Average Weight Change (±SEM)
130
110
90
70
50
30
10
-10
-30
1
2
3
4
5
6
7
8
9
10
11
12
13
Days post-infection

B

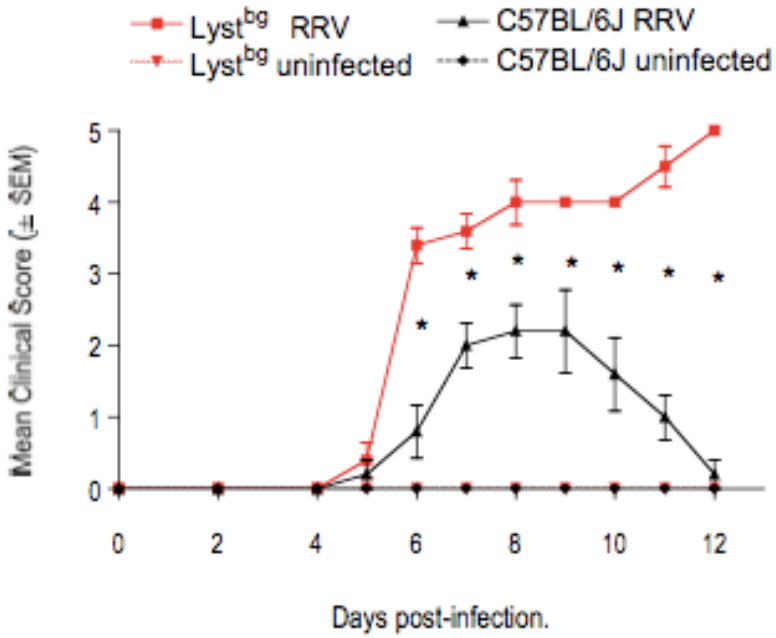
Lyst^bg RRV
C57BL/6J RRV
Lyst^bg uninfected
C57BL/6J uninfected
Mean Clinical Score (± SEM)
5
4
3
2
1
0
0
2
4
6
8
10
12
Days post-infection.

From 6 dpi onwards, differences in clinical score between RRV-infected C57BL/6J and Lyst^{bg} mice were found to be significant ($p<0.001$) as determined by 2-way ANOVA followed by Bonferroni's post-test.

5.2.2 Viral replication in muscle and joint tissue

We next determined whether there were any differences in RRV replication between Lyst^{bg} and C57BL/6J mice. Viral titres were determined in muscle and joint samples of C57BL/6J and Lyst^{bg} mice at 10 dpi. **Figure 5.3** shows the differences in RRV titre per mg of tissue. There was no significant difference in viral titres between the two groups, noting only a marginally higher titre recovered in the muscle of C57BL/6J mice. There were no differences in RRV titre between muscle and joint homogenates.

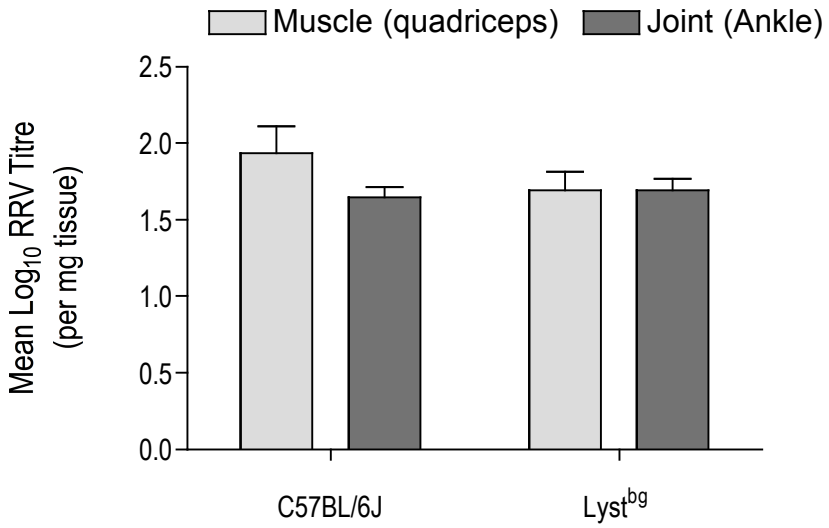

Figure 5.3: RRV titres in tissue of RRV-infected Lyst^{bg} and C57BL/6J mice at 10 dpi. At 10 dpi, muscle and joints were dissected, snap-frozen and weighed. Tissue was homogenised and RRV titres were determined by plaque assay on Vero cells. Data (mean ± standard deviation) is representative of 3 separate experiments.

Additionally, we attempted to localise sites of RRV replication in the muscle and joint tissue of RRV-infected Lyst^{bg} and C57BL/6J mice. A 441 bp digoxigenin-labelled riboprobe was used to detect RRV antigen by *in situ* hybridisation on paraffin sections of quadriceps muscle and ankle joint. **Figure 5.4** shows sites of RRV replication in the muscle tissue of RRV-infected C57BL/6J and Lyst^{bg} mice at 10 dpi. In C57BL/6J, RRV antigen was detected along long myofibres at

specific sites. In contrast, a higher RRV antigen signal was detected all throughout muscle tissue surface of Lyst^{bg} mice, while uninfected controls showed a pale shade of Fast Green counterstain. RRV antigen was also detected in the ankle joint of RRV-infected mice **(Figure 5.5)**. In C57BL/6J, RRV antigen was detected primarily within the synovial tissue, whereas in Lyst^{bg} mice, RRV antigen was localised within the periosteal muscle, and could not be detected in the synovium.

5.2.3 Histological analysis of RRV-infected muscle and joint tissue

Next, we sought to examine the degree of muscle and joint inflammation in Lyst^{bg} mice. In the previous chapter, we showed that C57BL/6J mice exhibited extensive cellular infiltration in muscle and synovial tissue at 10 dpi. Quadriceps muscle and ankle joint tissue were dissected at 10 dpi and stained in Hematoxylin & Eosin (H&E). **Figure 5.6** shows longitudinal and transversal sections of muscle in RRV-infected Lyst^{bg} mouse at 10 dpi. Compared to uninfected Lyst^{bg} control, RRV-infected Lyst^{bg} muscle shows extensive inflammation and tissue damage. Heavy cellular infiltrates can be seen in the congested interstitial space. **Figure 5.7** shows H&E staining of ankle joint tissue of a RRV-infected Lyst^{bg} mouse at 10x and 100x magnification. Some cellular infiltrates can be noted in the synovium of RRV-infected animals, with localised inflammation around the periosteum.

5.2.4 Composition of cellular infiltrates in RRV-infected Lyst^{bg} and C57BL/6J mice

We next investigate the nature of cellular infiltrates in muscle (quadriceps) and joint (ankle) tissue of RRV-infected Lyst^{bg} and C57BL/6J mice that showed clear disease signs by flow cytometry. At 8 dpi, tissue was collected, homogenised and processed for flow cytometry. Antibodies against CD11b and Pan-NK/DX5 cell surface antigens were used to differentiate between monocytic/macrophage (CD11b+) and natural killer (NK) (Pan-NK/DX5+) cell infiltrates. **Figure 5.8** shows differences in average percent CD11b-positive **(Fig. 5.8A)** and Pan-NK-positive **(Fig. 5.8B)** cells in muscle tissue.

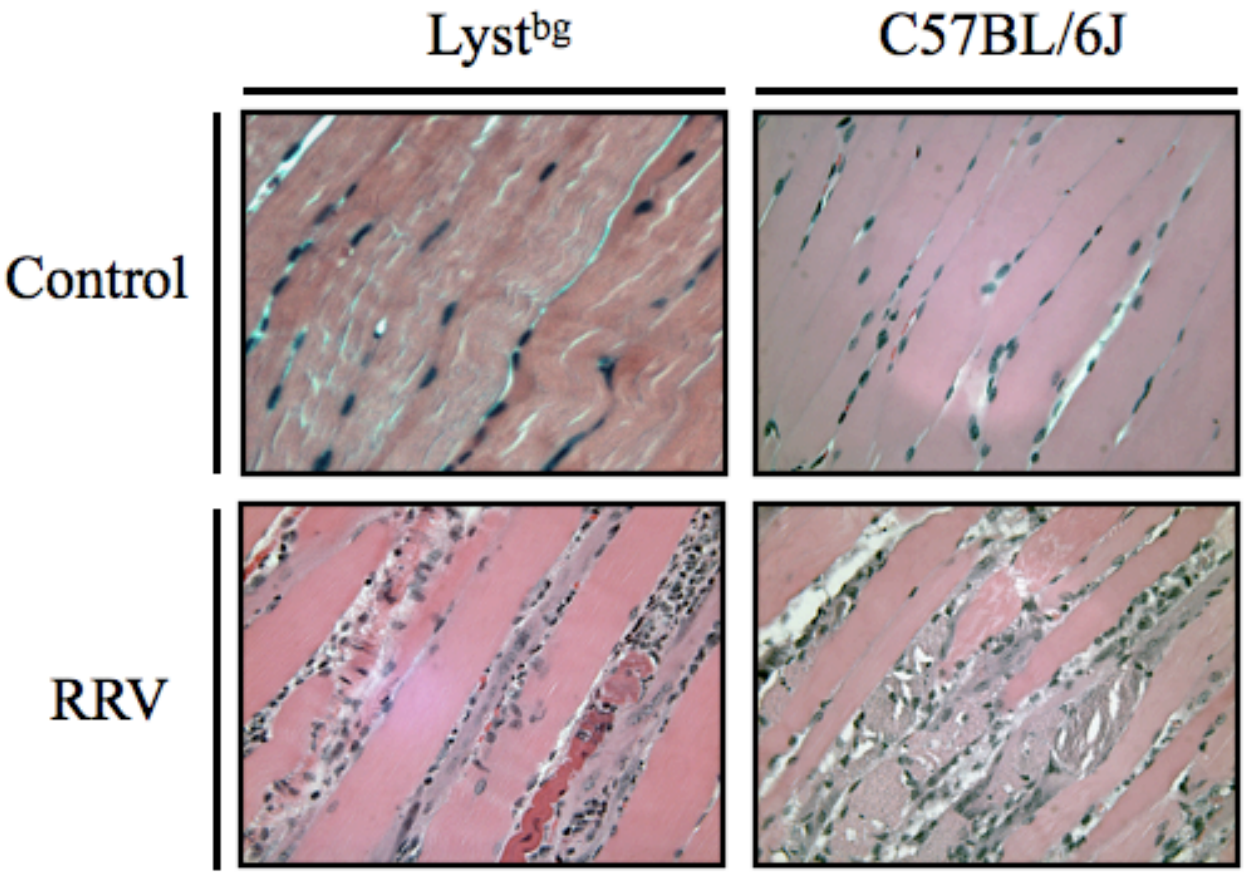

Figure 5.6: Histological sections of RRV-infected muscle in 20 day-old Lyst^{bg} and C57BL/6J mice at 10 dpi. Lyst^{bg} mice were inoculated with 10^{6} PFU of RRV subcutaneously. Uninfected mice received PBS alone. At 10 dpi, quadriceps muscle was collected and processed for histological staining with Hematoxylin & Eosin. Images were taken at 100 x magnification.

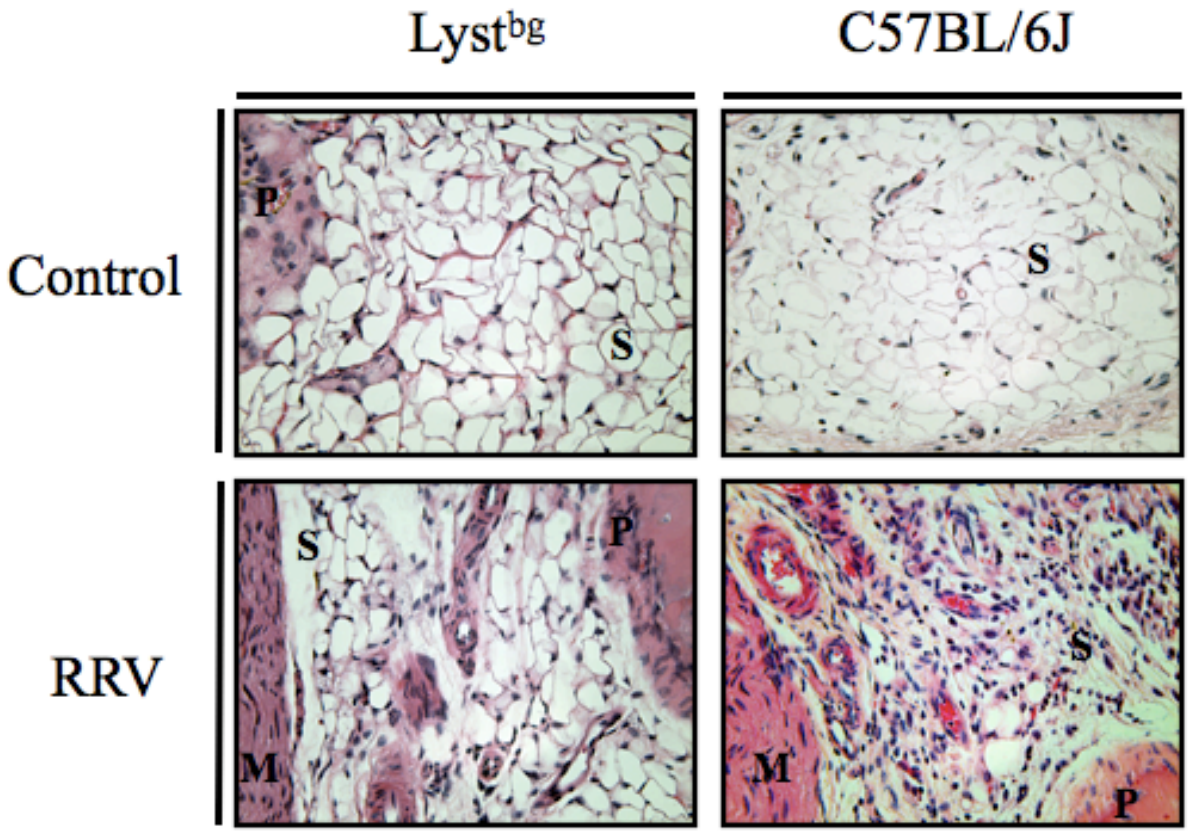

Figure 5.7: Histological sections of joint tissue of RRV-infected in 20 day-old Lyst^{bg} and C57BL/6J mice at 10 dpi. Lyst^{bg} mice were inoculated with 10^{5} PFU of RRV subcutaneously. At 10 dpi, ankle joint was collected and processed for histological staining with Hematoxylin & Eosin. Longitudinal and transversal tissue sections were performed, and images were taken at 100 x magnification. **M** muscle; **P** periosteum; **S** synovium.

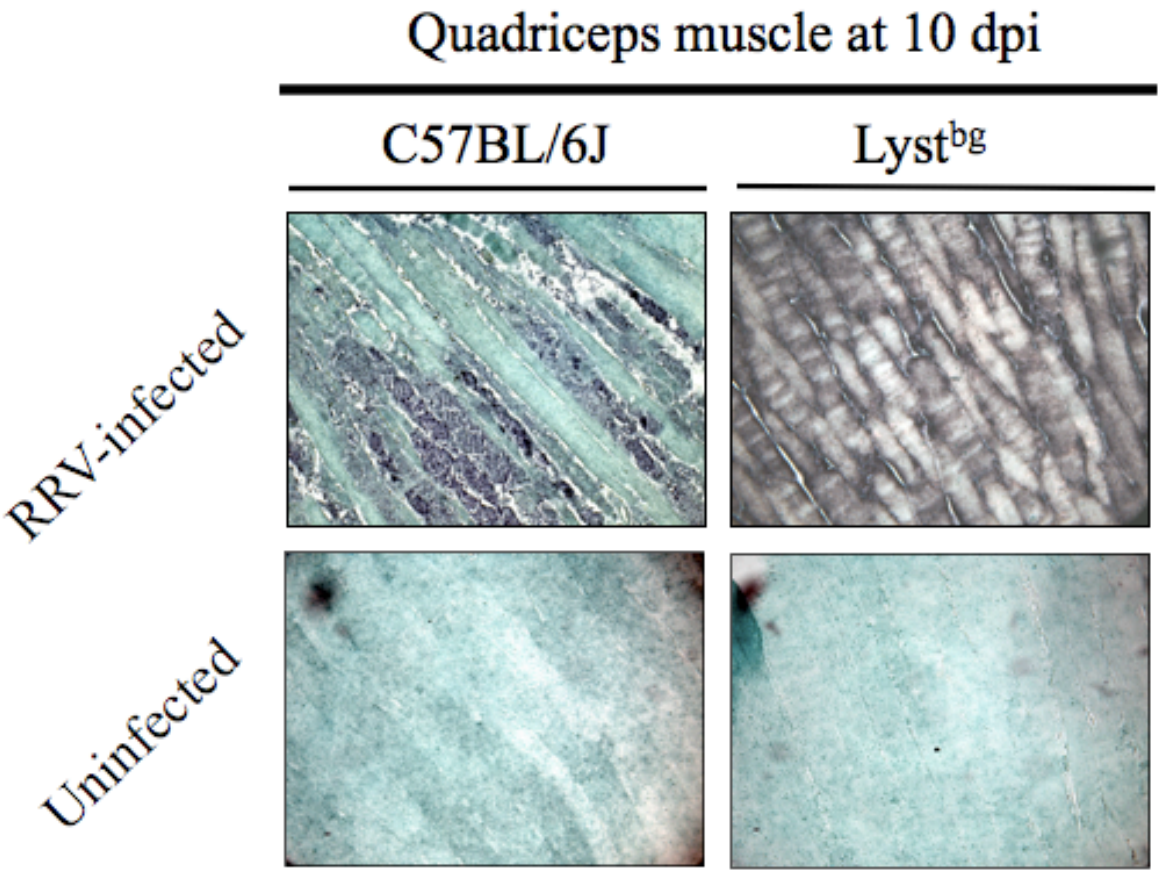

Figure 5.4: *In situ* hybridisation of RRV antigen in the quadriceps muscle of C57BL/6J and Lyst^{bg} mice at 10 dpi. C57BL/6J and Lyst^{bg} mice were inoculated with 10^3 PFU of RRV subcutaneously. At 10 dpi, quadriceps muscle was collected and embedded in paraffin (4 µm sections). RRV antigen was detected by *in-situ* hybridisation using a 441 bp DIG-labelled riboprobe specific to a conserved region of the E2 glycoprotein. The riboprobe was detected by alkaline phosphatase and tissue was counterstained with 0.01% Fast Green. Images were taken at 100x magnification.

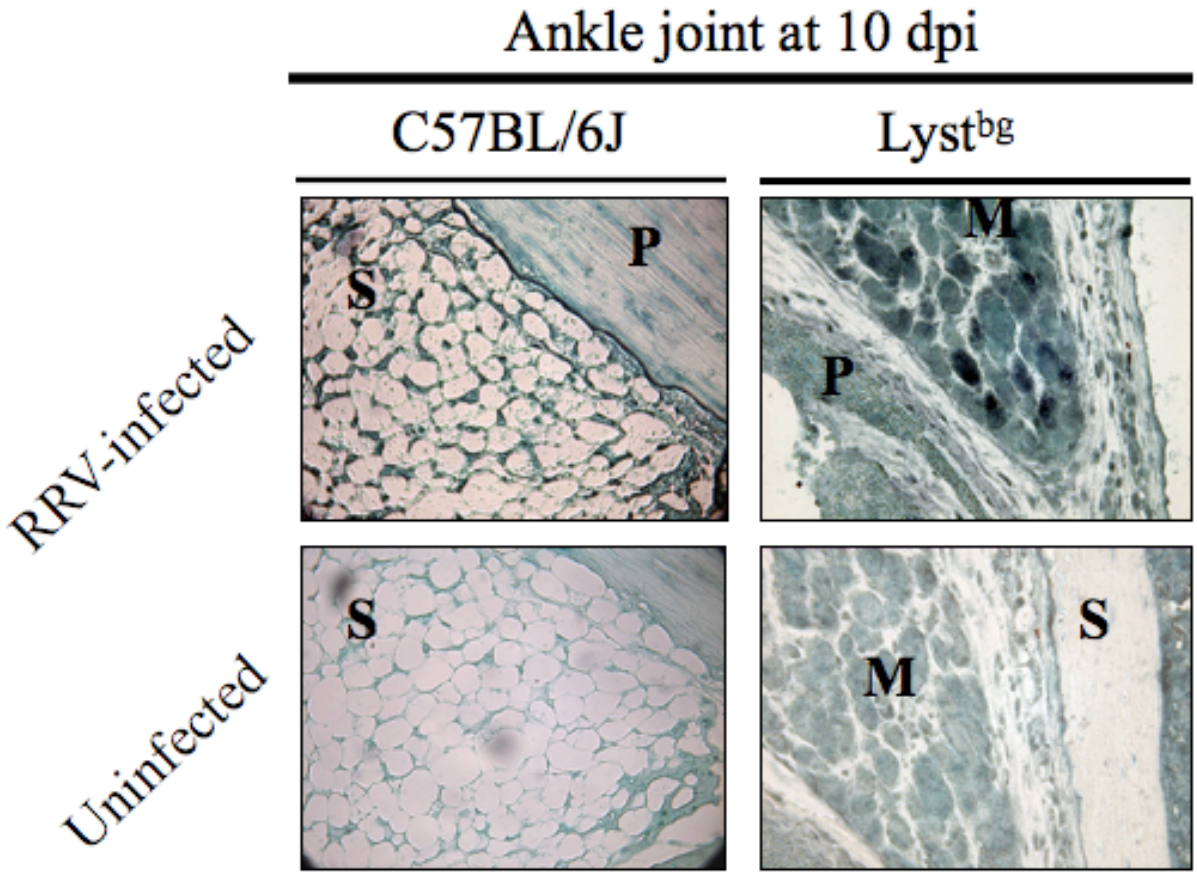

Figure 5.5: *In situ* hybridisation of RRV antigen in the ankle joint of C57BL/6J and Lyst^{bg} mice at 10 dpi. C57BL/6J and Lyst^{bg} mice were inoculated with 10^{3} PFU of RRV subcutaneously. At 10 dpi, ankle joints were collected and embedded in paraffin (4 µm sections). RRV antigen was detected in the synovial cavity of C57BL/6J mice and in the periosteal muscle of Lyst^{bg} mice by *in-situ* hybridisation using a 441 bp DIG-labelled riboprobe specific to a conserved region of the E2 glycoprotein. The riboprobe was detected by alkaline phosphatase-conjugated anti-DIG antibody and tissue was counterstained with 0.01% Fast Green. Images were taken at 100x magnification.

There were no differences in CD11b-positive cells in muscle infiltrates of Lyst^{bg} and C57BL/6J mice at 8 dpi. There was a 4-fold increase in percent CD11b-positive cells in RRV-infected mice compared to uninfected controls, and differences between RRV-infected mice (Lyst^{bg} and C57BL/6J) and uninfected controls were significant ($p \leq 0.05$) **(Fig 5.8A)**. The proportion of Pan-NK-positive cells **(Fig 5.8B)** was found to be significantly higher in the muscle ($p=0.0015$) of RRV-infected Lyst^{bg} mice compared to C57BL/6J mice. Our attempts to recover sufficient cell numbers from most joint tissue samples from RRV-infected mice for flow cytometry analysis were unsuccessful and inconclusive.

5.2.5 Expression of host factors in RRV-infected Lyst^{bg} and C57BL/6J mice

Next, we determined the cytokine expression profile in the muscle and joint tissue of RRV-infected C57BL/6J and Lyst^{bg} mice. The expression of key inflammatory and regulatory cytokines was determined by quantitative real-time PCR in muscle and joint tissue of RRV-infected mice at 8 dpi **(Figure 5.9)**. Relative expression of mRNA
levels was compared between the tissue of Lyst^{bg} and C57BL/6J mice that were exhibiting clear signs of RRV disease at the time of sample collection. There was a significant up-regulation of IFN-γ expression (10^6-fold) in the muscle of Lyst^{bg} mice compared to wild-type C57BL/6J mice. In contrast, no significant differences in the expression of chemokines such as MCP-1, MIP-1a and RANTES were observed between the two mouse strains. IFN-γ-inducible protein IP-10 and inducible nitric oxide synthase (iNOS-2) were only marginally up-regulated in the muscle of Lyst^{bg} mice at 10 dpi.

Figure 5.8: Flow cytometry analysis of cellular infiltrates in the muscle of 20-day-old RRV-infected C57BL/6J and Lyst^{bg} mice at 8 dpi. Lyst^{bg} mice were inoculated with 10^3 PFU of RRV subcutaneously. At 8 dpi, quadriceps muscle was collected and processed for for flow cytometry analysis. Plots represent the average percentage of **(A)** CD11b and **(B)** PanNK/DX5-positive cells in quadriceps muscle of RRV-infected Lyst^{bg} and C57BL/6J mice. Mock controls were inoculated with PBS. Statistically significant differences (* $p=0.0141$; ** $p=0.004$) were assessed by unpaired, two-tailed *t*-test with Welch's correction.

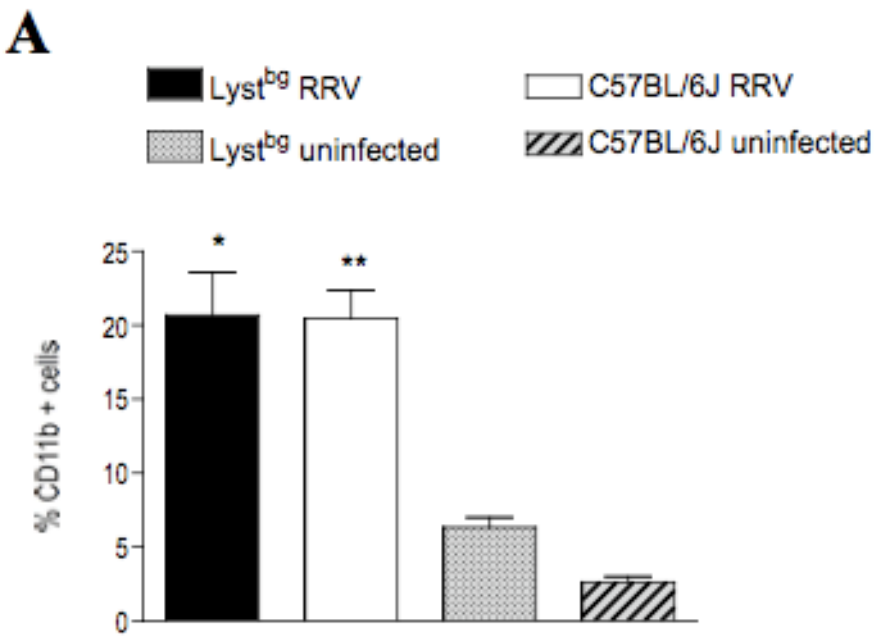
A
Lyst^bg RRV
C57BL/6J RRV
Lyst^bg uninfected
C57BL/6J uninfected
% CD11b + cells
25
20
15
10
5
0
*
**

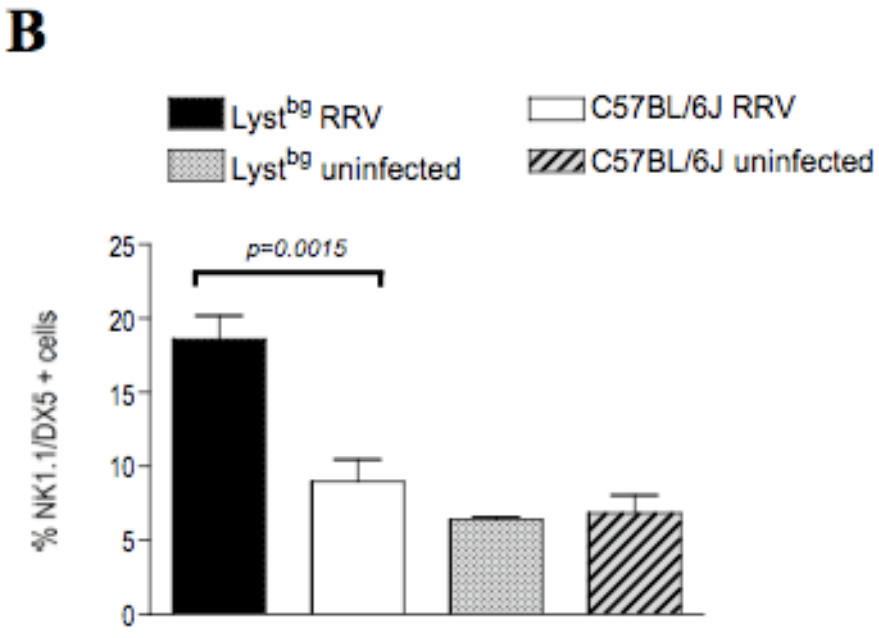
B
Lyst^bg RRV
C57BL/6J RRV
Lyst^bg uninfected
C57BL/6J uninfected
% NK1.1/DX5 + cells
25
20
15
10
5
0
p=0.0015

Figure 5.9: Expression of pro-inflammatory cytokines in muscle and joint of RRV-infected C57BL/6J and Lyst^{bg} mice at 10 dpi. C57BL/6J and Lyst^{bg} mice were inoculated with 10^3 PFU of RRV subcutaneously. At 10 dpi, quadriceps muscle and ankle joint were collected and processed for total mRNA extraction and cDNA synthesis by reverse transcription. Significant up- or down-regulation ($p<0.05$) of cytokine expression compared to uninfected controls is marked with an asterisk (*). Statistically significant differences and *p*-values between C57BL/6J and Lyst^{bg} mRNA levels were determined by unpaired, two-tailed *t*-test with Walch's correction.

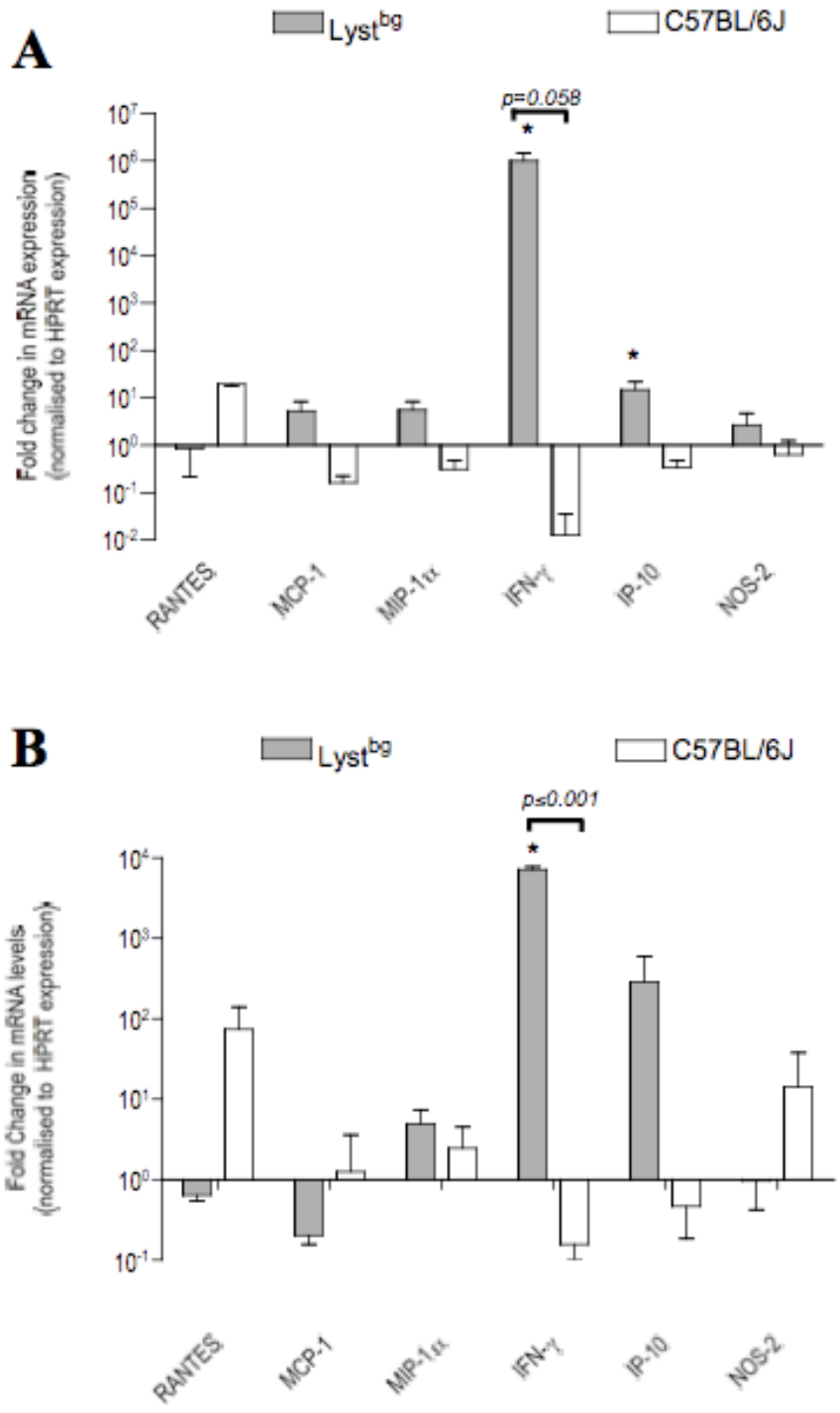
A
Lyst^bg
C57BL/6J
p=0.058
Fold change in mRNA expression (normalised to HPRT expression)
RANTES
MCP-1
MIP-1α
IFN-γ
IP-10
NOS-2
B
Lyst^bg
C57BL/6J
p≤0.001
Fold Change in mRNA levels (normalised to HPRT expression)
RANTES
MCP-1
MIP-1α
IFN-γ
IP-10
NOS-2

5.2.6 Depletion of NK cells using NK1.1 antibody (PK136)

We next sought out to further assess the role of NK cells in RRVD by means of cell depletion. 21 day-old C57BL/6J mice were inoculated with 10^3 PFU of RRV as previously described, and PK136, a monoclonal antibody raised against NK1.1 antigen was administered one day prior to, and every second day following RRV infection by intraperitoneal route. Mice were monitored daily for signs of disease and average weight change **(Figure 5.10)**. Mock animals included a PK136 group only, a PBS group, and a control IgG group. RRV-infected mice showed classical signs of disease, with a progressive disease score between 7 and 10 dpi that included mild to moderate hind limb dysfunction, and a steady recovery after 11 dpi. In contrast, RRV-infected mice treated with PK136 antibody showed higher average weight loss and more severe signs of clinical disease, shown in **Figure 5.10A** and **Figure 5.10B**, respectively.

In contrast, PK136-mock controls, which were administered PK136 antibody at the same dose and frequency as PK136-treated, RRV-infected animals, showed no signs of disease. Likewise, IgG control mice and PBS control mice did not show any signs of illness. In addition, we observed that by 10 dpi, 60% of PK136-treated, RRV-infected mice had succumbed to RRV disease, while untreated, RRV-infected mice survived and recovered from disease symptoms **(Figure 5.11)**.

Figure 5.10: Effect of NK cells depletion on RRV disease in 21 day-old C57BL/6J mice using a NK1.1 monoclonal antibody. Mice were inolculated with 10^3 PFU of RRV subcutaneously and monitored daily for weight change and disease signs. **(A)** Average percent weight change (±SEM) in PK136-treated, RRV-infected (■) and untreated (●) C57BL/6J mice. Mice in the CON group were inoculated with PBS, PK136 mice received 200 μg/g PK136 antibody one day before, then every two days following RRV infection. IgG control mice received 200 μg/g purified goat anti-rabbit IgG on an identical schedule. **(B)** Average (±SEM) clinical score (0, no disease signs; 1, very mild lethargy and/or ruffled fur; 2, mild lethargy and mild hind limb dysfunction; 3 established lethargy with moderate to severe hind limb dysfunction; 4, extreme lethargy, loss of limb function and/or total paresis; 5, death). Each data point shows the mean and standard deviation (n=5) for each group. Statistically significant differences (* $p<0.05$) were assessed by a 2-way ANOVA followed by a Bonferroni's post-test.

A

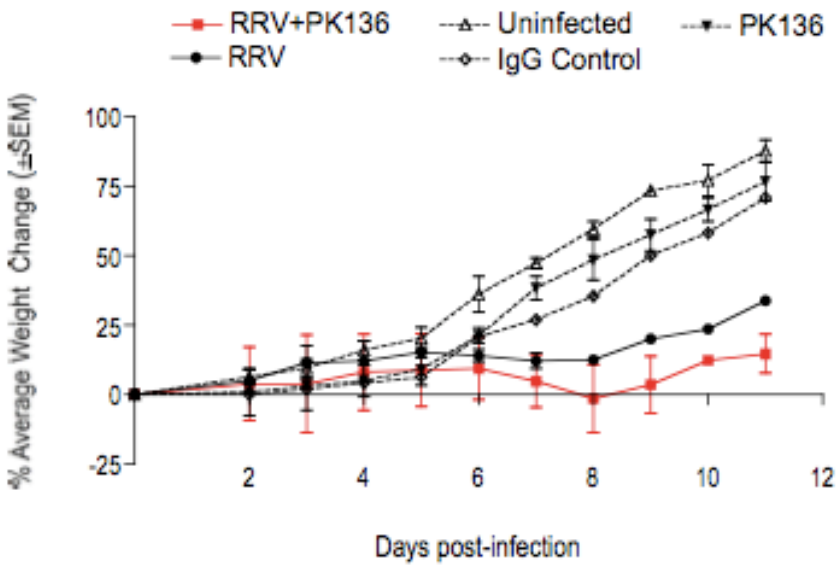
RRV+PK136
Uninfected
PK136
RRV
IgG Control
% Average Weight Change (±SEM)
100
75
50
25
0
-25
2
4
6
8
10
12
Days post-infection

B

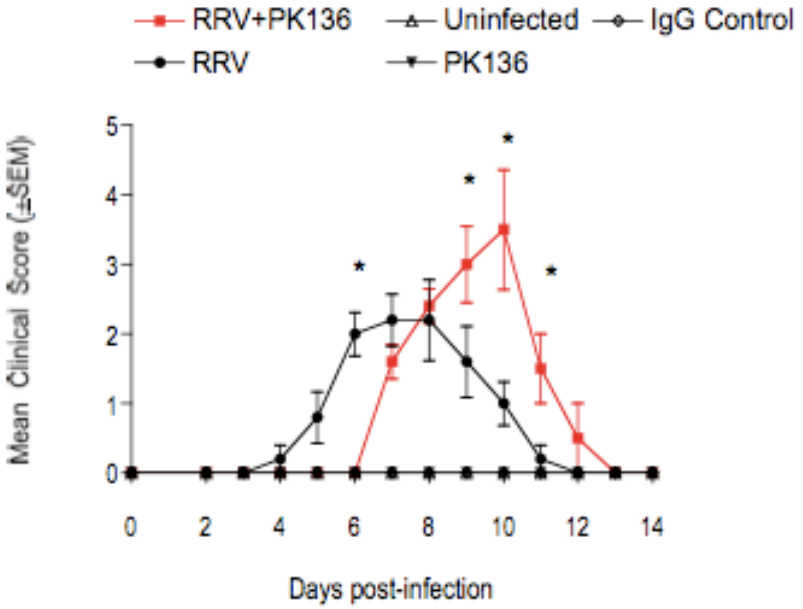
RRV+PK136
Uninfected
IgG Control
RRV
PK136
Mean Clinical Score (±SEM)
5
4
3
2
1
0
*
*
*
0
2
4
6
8
10
12
14
Days post-infection

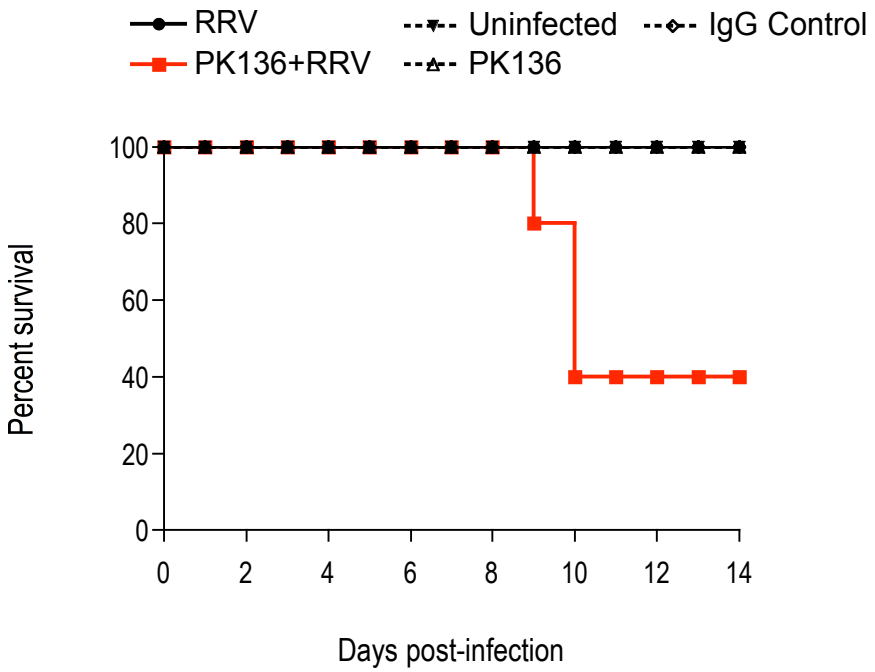

Figure 5.11: Survival plot of RRV-infected, PK136-treated C57BL/6J mice. Mice were inoculated with 10^3 PFU of RRV subcutaneously and administered 200 mg PK136 antibody. Data is representative of 3 mice per group. Uninfected mice received PBS as a negative control, PK136 mice received PK136 antibody every two days, and IgG control mice received 200 mg purified goat anti-rabbit IgG every two days.

We also determined viral titres in muscle and joint tissue of PK136-treated, RRV-infected mice and untreated, RRV-infected mice **(Fig. 5.12)**. No significant differences in viral titres were observed between PK136-treated and untreated RRV-infected mice. We did not observe any significant diffrences in RRV titres between muscle and joint tissue.

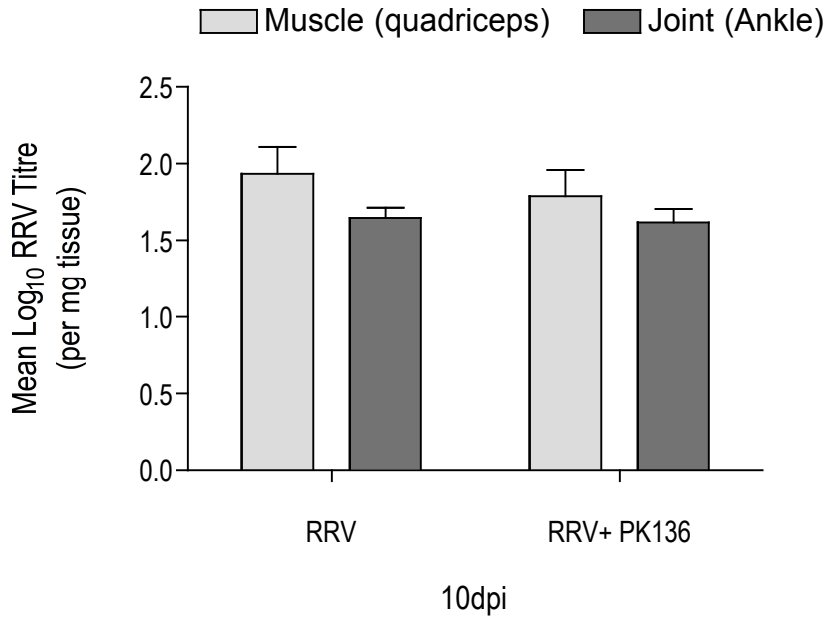

Figure 5.12: RRV titres in tissue of RRV-infected and RRV-infected, PK136-treated mice at 10 dpi. 21 day-old C57BL/6J mice were inoculated with 10^3 PFU of RRV subcutaneously, and muscle and joint tissue were collected at 10 dpi and snap-frozen. PK136-treated mice received 200 mg/g of the neutralising antibody intraperitoneally one day before, and every second day after infection. RRV titres were determined by plaque assay on Vero cells as described earlier. Data represents the mean ± standard deviation Log_{10} titre per mg tissue, representative of 3 mice per group.

5.3 Discussion

In this chapter, we sought to determine the requirement for NK cells during RRV-induced arthritis in mice using a mouse strain that exhibits deficient NK cell function, known as $Lyst^{bg}$ or Beige. This study was prompted by findings that NK cells are found in high numbers in the synovial effusions of RRV patients (Aaskov et al., 1986). Furthermore, NK cells were found in high numbers in the muscle of RRV-infected mice (Morrisson et al., 2007b). Such observations suggest that NK cells play a role in the RRV disease. The data in this chapter shows that a deficient NK cell system contributes to aggravated disease symptoms following RRV infection, leading to death in $Lyst^{bg}$ mice.

Lyst^{bg} mice showed typical signs of RRV disease, with significant loss of hind limb function, however none survived RRV infection. Muscle histology sections show clear signs of cellular infiltration and muscle damage. Virus was detected in the muscle and joint of RRV-infected Lyst^{bg} and C57BL/6J mice at the peak of disease symptoms. Cellular infiltrates were also found in the joint of RRV-infected Lyst^{bg} mice, and correlate with typical physiological signs of RRV disease in the C57BL/6J mouse model. Flow cytometry analysis revealed that macrophages were found in high numbers in the muscle and joint tissue of both Lyst^{bg} and C57BL/6J mice, however NK cells were more abundant in the tissue of RRV-infected Lyst^{bg} compared to C57BL/6J mice. We also carried out NK-depletion experiments in RRV-infected C57BL/6J mice with anti-NK.1.1 monoclonal antibody, PK136. We observed that treatment with PK136 resulted in the death of 60% of RRV-infected animals, while RRV-infected, untreated mice survived. PK136-treated, RRV-infected mice showed more severe disease signs than untreated, RRV-infected mice, in line with our observations in RRV-infected Lyst^{bg} mice. PK136 is a hybridoma-derived monoclonal antibody that has been used in NK cell depletion studies (Koo et al., 1986; Asea and Stein-Streilein, 1998; Figueiredo et al., 2007). The depletive effect of this antibody has been widely characterised and has helped elucidate aspects of NK cell ontogeny and function in inflammatory diseases such as uveitis and autoimmune uveoretinitis in mice, as well as in human papillomavirus-associated carcinogenesis (Kitaichi et al., 2002; Simova et al., 2004).

The data presented in this thesis suggests that with a deficient NK cell system, macrophages remain the main cellular infiltrate in the tissue of RRV-infected mice. This corroborates findings in a study by Lidbury and colleagues, who found that macrophage depletion abrogated RRV-induced disease in mice, thus confirming the essential requirement of macrophages (Lidbury et al., 2000b). However in our study, we observed that in the absence of functional NK cells, disease symptoms were aggravated, leading to high mortality in RRV-infected mice. Besides, we observed that while there was no difference in RRV titres between Lyst^{bg} and C57BL/6J mice, RRV antigen was detected at higher levels in the muscle of Lyst^{bg} mice by *in situ* hybridisation. This may indicate that plaque assay titration is not sensitive enough to detect tissue titres. Nevertheless, it would be sensible to hypothesise that in the absence of cytotoxic NK cells, RRV-infected muscle cells fail to be detected and cleared, which would explain the difference in RRV antigen staining observed between Lyst^{bg} and C57BL/6J muscle tissue. *In situ* hybridisation may indeed provide a more sensitive approach than plaque assay titration. A study by Soden and colleagues (2000) describes attempts at detecting RRV viral antigen in the synovium of RRV-

infected patients. The authors claim that despite using a sensitive approach such as RT-PCR, RRV may not be detected in RRV patients with evident synovial inflammation (Soden et al., 2000). This suggests that a relationship between viral titres and viral antigen detection are independent of disease pathogenesis, and our data supports this idea.

Additionally, higher levels of IFN-γ were found in the muscle of RRV-infected $Lyst^{bg}$ mice compared to C57BL/6J mice. NK cells are major producers of IFN-γ, which plays an important role in their activation, proliferation and cytotoxicity as well as cross-talk mechanisms with antigen-presenting cells, such as macrophages and dendritic cells (DCs) (Vivier et al., 2008).

IFN-γ is produced in response to IL-12 and IL-15, secreted by DCs and macrophages, following recognition of pathogen-infected or cancer cells. IFN-γ is known to be a potent inducer of chemokines RANTES, MCP-1 and IP-10, to which monocytes and lymphocytes respond to by migrating towards the source of IFN-γ (Boehm et al., 1997). Abnormally high levels of IFN-γ found in the muscle of RRV-infected $Lyst^{bg}$ mice suggest that lysis-deficient NK cells may be unable to respond to paracrine cytokine signals following RRV-dependent activation of macrophages and DCs, leading to an imbalance in cytokine signalling within the inflamed tissue. The high levels of IFN-γ may be attributed to the high numbers of NK cells found in the muscle of Lystbg mice. IFN-γ has been shown to be responsible for the development of some diseases, and that ablation of IFN-γ signalling can protect animals from virus-induced disease. For example, IFN-γ was found to be essential for the development of lupus disease in a mouse model (Balomenos et al., 1998). Similar observations were made with collagen-induced arthritis, where several groups observed that depletion of IFN-γ can reduce the severity of arthritic symptoms in mice and rats,, whereas the administration of IFN-γ often exacerbated the disease in mice (Mauritz et al., 1988; Boissier et al., 1995).

The role of IFN-γ in arthritis is still poorly defined, however studies involving depletion and/or exogenous IFN-γ suggest an important regulatory role during tissue inflammation (Jacob et al., 1989; Wiesenberg et al., 1989). Recently, Lidbury and co-workers showed that mice that were depleted of macrophages using clodronate showed less severe arthritic symptoms following RRV infection. Interestingly, IFN-γ was found at higher levels in the muscle and joint of untreated, RRV-infected mice compared to macrophage-depleted, RRV-infected mice at 10 dpi (Lidbury et al., 2008). Preliminary studies in RRV-infected C57BL/6J mice suggest that IFN-γ-/- mutants

exhibit milder arthritic symptoms than their wild-type congeners, further corroborating the idea that despite having important regulatory properties, IFN-γ can contribute to increased disease severity in RRVD (Mahalingam and Lidbury, personal communication). We were unable to find high levels of IFN-γ expression in the tissue of RRV-infected C57BL/6J mice, and this could be explained by the correlation between NK cell infiltration at 8 dpi and IFN-γ mRNA levels at 10 dpi. Lyst^{bg} mice showed higher NK cell infiltration at 8 dpi, and considering that NK cells are potent IFN-γ producers, we propose that IFN-γ mRNA detected in the tissue of Lyst^{bg} mice was produced by infiltrating NK cells. No significant NK cell infiltration was found in RRV-infected C57BL/6J mice, which could partially explain why two days later IFN-γ mRNA levels were lower than those found in Lyst^{bg} mice. Detection of IFN-γ protein by various immunotechniques (ELISA, Western Blotting) would have been more appropriate to conclude on the relationship between IFN-γ levels and RRVD severity. This also raises the question as to which aspect of the IFN-γ signalling pathway constitutes a trigger for tissue inflammation and damage.

Similar observations were made in mice infected with VEEV, an encephalitic New World alphavirus, which has been associated with high IFN-γ production *in vivo*, compared to mice infected with an attenuated, non pathogenic VEEV strain (Grieder et al., 1997). Abnormally high levels in IFN-γ were found in the airways of respiratory syncytial virus (RSV)-infected mice during pulmonary eosinophilia, as authors suggest that an excessive influx of T cells in response to high IFN-γ levels possibly contributed to a dysregulated cytokine milieu, ultimately leading to an aberrant inflammatory response (Spender et al., 1998).

In addition, we found that IFN-γ-inducible protein-10, (IP-10) was expressed at significantly higher levels, in accordance with high levels of IFN-γ in the muscle and joints of RRV-infected Lyst^{bg} mice compared to C57BL/6J mice. Chemokines are involved in leukocyte recruitment during inflammatory response and have been implicated in inflammatory arthropathies, including RA (Kunkel et al., 1996). A study by Hanaoka and colleagues showed high levels of IP-10 in the synovial tissue of RA patients (Hanaoka et al., 2003). The authors report that high IP-10 levels were associated with leukocyte binding, suggesting that IP-10 secretion by synoviocytes may contribute to the recruitment of T cells to the synovium, further enhancing inflammation. This hypothesis may partially explain our findings in the muscle tissue of RRV-infected Lyst^{bg} mice, which harboured a higher number of infiltrating NK cells compared to RRV-infected C57BL/6J mice. Therefore, the possibility that IP-10, under the induction of abnormally high IFN-γ signals

contributes to the recruitement of inflammatory cells in the muscle and joint tissue of Lyst^{bg} mice should be further explored.

A study by Morrisson and colleagues (2006) revealed that the effector phase in RRVD pathogenesis was independent of the adaptive immune system. The authors used RAG-1 -/- mice, which exhibit deficient T and B cells, to show that RRV-induced arthritis was due to the massive influx of macrophages to muscle and joint tissue, and that the absence of T and B lymphocytes did not affect the development of RRV-induced pathology in mice (Morrisson et al., 2007b). Such findings indeed rule out the involvement of T-cell-mediated inflammation and cytotoxicity in RRVD, yet provide little information as to the role of T-cell-associated cytokines such as IFN-γ.

Taken together, our findings indicate that the absence of a functional NK cell system exacerbates RRV-induced disease symptoms, suggesting a regulatory role for infiltrating NK cells in the tissue of RRV-infected mice. We hypothesise that molecular interactions between RRV-infected synoviocytes and infiltrating NK cells help regulate macrophage-driven inflammation and tissue damage via cytokine-dependent pathways. Our data establishes a correlation between NK cell deficiency, disease severity and high IFN-γ mRNA levels in RRV-infected mice. Further studies are thus needed to understand the interplay between NK cells and RRV-infected synoviocytes in humans.

6. Discussion

The objectives of this thesis were to characterise molecular and physiological processes associated with RRV infection and disease. The first aim of this study was to investigate the differences in infectivity and antiviral induction between mammalian cell- and mosquito cell-derived RRV. Studies have shown that arthropod-derived arboviruses gained facilitated entry into host cells. In addition, mosquito cell-derived RRV (mos-RRV) was recently reported to exhibit higher infectivity in myeloid dendritic cells (mDC) compared to mammalian cell-derived RRV (mam-RRV) (Shabman et al., 2007). Differential infectivity, in particular enhanced binding and entry of mosquito cell-derived arboviruses in dendritic cells (DCs) has been shown with DENV and WNV (Klimstra et al., 2003; Lozach et al., 2005; Davis et al., 2006). We showed that mos-RRV replicated to higher titres and showed higher infectivity than mam-RRV in RAW264.7 macrophage and JAWSII dendritic cell lines *in vitro*. We attempted to identify what antigenic determinants underlined the observed effects, and passaged mos-RRV once in a mammalian cell line.

In accordance with findings in the Shabman et al., study, we found that one passage of mos-RRV through a mammalian cell line abrogated differential infectivity of macrophages and dendritic cells. This confirmed that the observed effect is not due to a genetic mutation in the viral glycoprotein, since a single passage through a different cell is rather unlikely to cause an adaptive mutation. Thus, our data further strengthens the hypothesis elaborated in the Shabman et al. study, which suggests that differences in cell surface glycosylation, such as those observed between mammalian and mosquito cells, are acquired by budding RRV virions following one passage in these cell lines (Shabman et al., 2007; Shabman et al., 2008). In addition, the abovementioned study found that mosquito cell-derived Venezuelan equine encephalitis and Barmah Forest viruses showed higher infectivity of mDCs, and provided evidence that cell surface N-linked glycans of mosquito cells conferred these viruses with enhanced entry.

Thus far, our data corroborates findings of differential infectivity between mammalian and mosquito-cell derived arboviruses observed in studies mentioned earlier. However, few studies addressed the effect of differential activity on Type I IFN activity. Our study showed that differential infectivity required the presence of a functional antiviral Type I IFN system. We infected Vero and L929 cells, which do not respond to Type I IFN and observed no differences,

suggesting that differential infectivity is specific to Type I IFN responsive, and perhaps, Type I IFN-producing cells. We observed that Vero cells were not susceptible to differential infectivity by mam- and mos-RRV, despite treatment with Type I IFN, suggesting that mos-RRV requires a functional, responsive Type I IFN system to establish a putative interfering mechanism. We next set out to investigate whether mos-RRV was able to induce Type I IFN in macrophages and dendritic cell lines. The Shabman et al. study reported that mos-RRV induced a much lower Type I IFN response in mDCs than mam-RRV at early time points after infection. In this study, we showed that mos-RRV failed to induce antiviral Type I IFN responses compared to mam-RRV.

We further investigated the differential activation of early antiviral transcription factors STAT-1 and IRF-3, and Type I IFN-associated PKR, involved in dsRNA recognition. We showed that mos-RRV induced significantly lower levels of PKR activation and pStat-1 and IRF-3 nuclear translocation than mam-RRV at early time points, suggesting that several independent signal transduction pathways may be involved in antiviral responses following RRV infection. We were also able to show that mos-RRV induces less transcriptional activity of Type I IFN-associated genes than mam-RRV, indicating that evidence of lower Type I IFN induction is consistent at both cytoplasmic and nuclear levels. Our findings complement the Shabman et al. study, which did not investigate the expression profile of antiviral transcription factors and Type I IFN associated proteins. We hypothesise that mos-RRV fails to induce early IFN-associated components at early time points following infection, while mam-RRV is normally detected and elicits a substantial antiviral response. While we were unable to show evidence of direct interference between mos-RRV and antiviral mechanisms, this indicates that signalling mechanisms most likely to be avoided by mos-RRV are located upstream of the signalling cascade. Furthermore, preliminary findings from Shabman and Heise suggest that the nature of mos-RRV – DC interaction upon entry may contribute to a lower induction of a Type I IFN-associated antiviral system, due to a particular carbohydrate composition of the mosquito cell-derived virion membrane (Shabman and Heise, personal communication).

However, our data does not exclude the possibility that a receptor, such as DC-SIGN, shown to enhance DENV, WNV, SINV and HCV entry, may be involved in mos-RRV binding and entry (Lozach et al., 2003; Tassaneetrithep et al., 2003; Cambi et al., 2004; Lozach et al., 2005). Studies focussing on DC-SIGN-mediated entry used a monocytic cell line expressing DC-SIGN, and showed that these cells were more permissive to infection with some of the abovementioned

viruses. Such techniques allowed the Lozach et al. team to observe that while DENV uses DC-SIGN to bind the host cell membrane, the function of DC-SIGN is merely to concentrate viral particles at the surface (Lozach et al., 2005). The authors hypothesise that following DC-SIGN-mediated concentration of viral particles, an unknown pH-dependent virion-cell fusion mechanism contributes to internalisation of DENV virion. Incidentally, we conducted preliminary, pilot studies using the THP-1-DC-SIGN cell line and tested the hypothesis that DC-SIGN mediates differential infectivity of mam- and mos-RRV. Our data did not show clear evidence of differential infectivity or replication, however this may be due to the nature of the cell system tested. Early RRV studies have established that monocytic cell lines are not as permissive to RRV infection as macrophages and DC cell lines are, therefore the cell line used in DENV and WNV studies may not be appropriate for our in vitro RRV model.

The possibility that one receptor, such as DC-SIGN, could be involved in differential infectivity and possibly Type I IFN induction, raises the eventuality that other receptors known to mediate viral entry could be involved. For example, a carbohydrate receptor has been identified as an antigenic determinant for a novel subset of myeloid DC. The mannose receptor (MR) was found to internalise mannosylated ligands and regulate migration of macrophages and dendritic cells (McKenzie et al., 2007; Sturge et al., 2007). A study by Reading et al. found that MR was able to enhance internalisation of Influenza virus particles in murine macrophages, and cells expressing high MR levels were found to be more permissive to Influenza infection (Reading et al., 2000). Interestingly, DENV, which has been shown to utilise DC-SIGN for virion binding and entry, also appears to bind MR on macrophage cells (Miller et al., 2008). Moreover, the authors show that MR preferentially binds DENV passaged in C6/36 mosquito cells, which is the cell line used to generate mos-RRV in our studies. Incidentally, we performed preliminary experiments aimed at determining the role of MR in mam- and mos-RRV infection of macrophages, however results thus far do not indicate that MR acts as a binding receptor for RRV.

Linn and Suhrbier identified a collagen receptor capable of mediating RRV binding and entry. The α1β1 integrin collagen IV receptor was found to bind a highly conserved region of RRV E2 glycoprotein, which shares amino acid homology with collagen IV sequences known to bind α1β1 integrin receptors (Linn et al., 2005). The authors hypothesis that binding of RRV to α1β1 integrins could possibly lead to inflammatory symptoms, since antibodies specific to α1β1 integrins were found to reduce disease in animal models of inflammation (de Fougerolles et al.,

2000). However, no mechanism of differential induction of antiviral response mediated by a putative receptor to which mos-RRV would preferentially bind has been proposed, henceforth further studies aimed at characterising i) antigenic determinants responsible for differential infectivity and Type I IFN induction, ii) mechanisms of Type I IFN evasion by mos-RRV and iii) possible host cell receptor-mediated signalling pathways used by mos-RRV are needed.

The early interactions between the arthropod-derived arbovirus and initially infected dendritic cells is a significant event and likely to be important in determining whether a virus is able to successfully establish infection. Characterising these early events are likely to expand our knowledge of how arboviruses cause disease. Since viral vectors are being used extensively as vaccine delivery platforms, understanding how modifications of the virion affect the host immune response may provide valuable information toward optimising these vaccine systems. The first part of this thesis provides insights into the pathogenesis of RRV, and has the potential to provide clues as to a general mechanism employed by arthropod-borne alphaviruses, and possibly other arboviruses, to evade the early interferon response within the host.

The second part of this thesis addressed questions related to the pathogenesis of RRV-induced disease in a recently established murine model using C57BL/6J mice. We and others (Morrison et al., 2006; Lidbury et al., 2008) have established the first mouse model of RRV-induced inflammatory disease, which represents one of the first experimental models of viral arthritis using C57BL/6J mice. Infection of C57BL/6J mice resulted in severe disease signs, including hind limb dysfunction, paresis and lethargy. Disease was transient and the mice regained healthy symptoms by 28 days post infection (dpi). The ankle joint and skeletal muscles were the sites of enhanced viral replication. RRV infection elicited an inflammatory response that was first detectable in joint and muscle tissues at 5 dpi and peaked at 7-10 dpi. Inflammatory cells were observed within the synovial tissues and joint-associated connective tissue (periosteum, tendons). The peak inflammatory response corresponded with muscle fibre destruction (7-10 dpi), with inflammation and tissue destruction resolving by 30 dpi. Infection of skeletal muscle tissue by RRV in humans has not been directly demonstrated, although 60% of RRVD patients experience myalgia (Harley et al., 2002). Mouse inflammatory infiltrates predominantly comprise macrophages, NK cells, CD4 and CD8 T cells with no B cells detected (Morrison et al., 2006; Morrisson et al., 2006). The mouse model thus recapitulates many aspects of RRVD in humans and thus provides one of the first mouse models to study the pathogenesis of viral arthritis/

arthralgia. In the second and third part of this thesis, this mouse model will be exploited to determine the role of TNF-α, and NK cells in RRV-induced inflammatory disease.

Based on findings by Lidbury and colleagues (Lidbury et al., 2008) that RRVD was caused by a massive infiltration to the muscle and joint tissue of macrophages stimulated by high levels of pro-inflammatory factors, we attempted to characterise the effect of host cytokine depletion on disease symptoms in RRV-infected mice. TNF-α was identified as a major pro-inflammatory cytokine in RRVD, and antibody-mediated blocking of TNF-α appeared to reduce disease symptoms in the mouse model (Lidbury et al., 2008). In our study, we tested the ability of a commercially available anti-TNF-α compound to reduce RRVD symptoms in mice. Enbrel is a USFDA-validated biologic compound that has been used to treat symptoms of rheumatoid arthritis (RA) and psoriasis for over 15 years. The efficacy of Enbrel has been shown in randomised trials using large cohorts of patients, and its use has been extended to a range of inflammatory conditions.

The mouse model of RRVD is characterised by a short onset (7 days) and disease signs very similar to those observed in RRV-infected EPA patients, namely arthritic pain, myalgia, lethargy and limb dysfunction. We based our hypothesis on the findings by Lidbury et al. that if both TNF-α and NF-κB inhibitors are able to reduce disease symptoms independently of one another, neutralisation of TNFR signalling using Enbrel should help diminish disease severity. Our results indicate that treatment of RRV-infected mice with Enbrel not only exacerbates symptoms, but can lead to acute systemic illness, which resulted in a 60% fatality, whereas untreated, RRV-infected animals recover after showing hind limb dysfunction and lethargy. RRV-Enbrel did show typical disease symptoms and muscle and joint histology data was consistent with previous findings describing massive macrophage infiltration. However, symptoms persisted in RRV-Enbrel mice until death (60% of animals), whereas survivors recovered from the disease, albeit at a slower pace than untreated, RRV-infected animals.

Although these findings are contrary to the TNF-α inhibition data presented in the Lidbury et al. (2008) study, several factors can account for an adverse effect of Enbrel in viral-induced arthritis. Firstly, Lidbury et al., used a laboratory-generated monoclonal antibody against TNF-α, whereas Enbrel is a fusion of the extracellular domain of human p_{75}TNFR and human Fc receptor-binding portions (Scallon et al., 2002). Secondly, the possibility that species cross-reactivity caused an

adverse reaction to Enbrel in RRV-infected mice cannot be ruled out, although our study shows clearly that Enbrel does not induce symptoms in uninfected mice, and carries no obvious physiological effect. It is also possible that Enbrel may only exert its effect in an inflammatory milieu resulting from an autoimmune condition, which may exhibit essential yet unknown differences compared to virus-induced macrophage inflammation. Another explanation is that Enbrel treatment may in fact be associated with high RRV titres at alternate tissue sites (eg. Blood, brain, other organs) that were not analysed in the present study.

However, several studies have associated the use of Enbrel with negative side effects. The USFDA issued warnings in 1999 following the deaths of patients undertaking Enbrel treatment (FDA, 1999), and this prompted several studies investigating complications in Enbrel-treated patients. A study by Smith and Letendre (2002) associated Enbrel treatment with severe respiratory complications in a patient diagnosed with RA. The study reports that no bacterial pathogens were identified, however respiratory virus parainfluenza virus type 3 was detected, prompting the authors to suggest that TNF-α inhibition by Enbrel may hamper TNF-α signalling processes initially aimed at inhibiting viral progression (Smith and Letendre, 2002). Similarly, Kekow and colleagues (2002) report the formation of rheumatoid nodules in the lungs of an RA patient undertaking Enbrel therapy (Kekow et al., 2002). The authors do not formulate any hypothesis as to whether rheumatoid nodules were the result of Enbrel treatment, but indicate that further studies investigating autoimmune reactions during Enbrel treatment should be carried out.

We were not able to find any published work describing Enbrel treatment in an animal model of viral-induced arthritis, however a study on parasite *Trypanosoma cruzii*-induced cardiomyopathy did describe adverse effects of Enbrel on disease symptoms. Bilate and co-workers (2007) used a hamster model of Chagas Chronic Cardiomyopathy (CCC) to examine the effect of Enbrel following *T. cruzii* infection (Bilate et al., 2007). While the authors were able to show that Enbrel reduced TNF-α bioactivity *in vivo*, Enbrel-treated animals showed aggravated disease symptoms characterised by enhanced left ventricular dysfunction.

Our study does not provide any evidence regarding the possibility of Enbrel-induced cardiomyopathy or respiratory failure, since muscle and joint tissue were the only organs analysed. Based on our findings, we can only conclude that Enbrel can potentially lead to acute systemic illness in RRV-infected mice, however the role of TNF and TNFR signalling in RRVD

pathogenesis remains to be elucidated. TNFR signalling is likely to be implicated in RRV-induced inflammation, based on the findings by Lidbury et al. (2008) that sulfasalazine, an NF-κB inhibitor, is able to prevent disease in mice (Lidbury et al., 2008). TNF-α binds to a specific, but non-exclusive TNF-α receptor (TNFR), to induce a signalling cascade through the activation of transcription factor NF-κB (Hayden and Ghosh, 2008).

In RA, TNF-α is believed to enhance the formation of osteoclasts, precursor cells involved in bone remodelling during development, as well as bone erosion during inflammatory arthritis (Gravallese, 2002; Bradley, 2008). This provides the basis for future studies investigating mechanisms of TNFR signalling in RRVD, in light of recent findings that showed a strong link between TNFR1 signaling and acute inflammation in a murine disease model. Two successive studies by Mazzon and colleagues (2008) found that TNFR1 gene knock-out and Enbrel treatment produced very similar effects during experimental inflammation, suggesting that Enbrel modulates upstream processes of TNFR1-dependent signal transduction, and possibly reduces airway tight junction permeability, believed to facilitate macrophage infiltration in carrageenan-induced acute inflammation in mice (Mazzon and Cuzzocrea, 2007; Mazzon et al., 2008). Hence, the role of TNF-α in skeletal muscle and bone/joint remodelling is worth being investigated in rheumatoid arthritis, particularly if applied to the RRVD mouse model, as it would provide a reference basis for further studies on other important viral arthritides such as Chikungunya virus-induced disease.

The third and final objective of this thesis was to investigate the requirement of Natural Killer (NK) cells in RRV-induced disease. NK cells are known to be involved in viral infections, and early studies report high numbers of NK cell infiltrates in the synovial effusions of RRV-infected EPA patients (Aaskov and Dalglish, 1981; Aaskov et al., 1986; Orange et al., 1995; Biron et al., 1999). Using the RRV mouse model, we compared RRV disease development between C57BL/6J mice and Lyst^{bg} mice, which possess lysis-deficient NK cells (Kelly, 1957; Brandt and Swank, 1976; Roder and Duwe, 1979). In order to minimise the possibility of strain-dependent outcomes of RRV infection, we used Lyst^{bg} mice on a C57BL/6J background, which is the strain in which the RRVD mouse model is currently established (Morrisson et al., 2007b; Lidbury et al., 2008). Lyst^{bg} mice have been used to characterise the role of NK cells in various pathological conditions, including experimental arthritis, severe acute respiratory syndrome coronavirus (SARS-CoV) and Herpes Simplex virus HSV infection (Schalkwijk et al., 1988; Schalkwijk et al., 1990; Carr et al.,

1997; Glass et al., 2004). We also carried out a qualitative assessment of the requirement of NK cells in RRVD using a NK-specific monoclonal antibody, PK136. PK136 has been described in NK cell depletion experiments as an effective means of inhibiting NK cell-mediated action (Asea and Stein-Streilein, 1998; Kitaichi et al., 2002; Simova et al., 2004).

We found that in the absence of a functional NK cell system, RRV-infected mice succumbed to RRV infection at the peak of RRV disease symptoms. We observed a 100% lethality rate in RRV-infected Lyst^{bg} mice, while uninfected Lyst^{bg} mice showed no symptom or signs of illness throughout the experiment. We also tested the requirement of NK cells in RRVD by depleting NK cells using a specific monoclonal antibody (PK136), and found that NK-depleted mice were susceptible to RRVD. Histological analysis showed significant infiltration of monocytic cells in muscle and joint tissue, consistent with typical observations of RRV-induced inflammation in C57BL/6J mice. We compared the proportions of cellular infiltrates in the muscle of RRV-infected Lyst^{bg} and C57BL/6J mice, and found that there was no difference in the number of macrophages between the two strains. This confirms initial findings by Morrison and colleagues, who used T and B cell-deficient mice to prove that RRVD was essentially, of not exclusively, caused by infiltrating macrophages (Morrison et al., 2006; Morrisson et al., 2007b). However, we found significantly higher numbers of infiltrating NK cells in the muscle of RRV-infected Lyst^{bg} mice compared to C57BL/6J mice, suggesting that a deficiency in cytotoxic function does not prevent NK cells from responding to chemokines and migrating to inflamed tissue. Infiltrating NK cells were found in the muscle of RRV-infected mice in the Morrison et al. (2006) study, however we were unable to assess NK cell infiltration in joint tissue by flow cytometry due to low cell recovery from infected animals.

We also investigated the differences in pro-inflammatory cytokine expression in the muscle and joint tissue of RRV-infected Lyst^{bg} and C57BL/6J mice during RRV disease. We found that Lyst^{bg} mice consistently displayed abnormally high levels of IFN-γ expression in muscle and joint, while only basal IFN-γ expression was detected in tissue of RRV-infected C57BL/6 mice. High IFN-γ levels were associated with high IFN-γ-inducible protein (IP-10) expression, which has been associated with RA symptoms (Hanaoka et al., 2003). Observations that IFN-γ expression was associated with RRVD symptoms have been made in the Lidbury et al. (2008) study that showed reduced levels of IFN-γ following treatment macrophage-depleting compounds,

suggesting that macrophages may be involved in eliciting high levels of IFN-γ via the activation of NK and T cells.

In our studies, we showed that Lyst^{bg} mice express higher levels of IFN-γ mRNA, which correlates with higher NK cell infiltrates compared to C57BL/6J mice, suggesting that the majority of IFN-γ mRNA species detected by PCR were most likely produced by infiltrating NK cells. T cells may also be a major source of IFN-γ, but our attempts at detecting T cells in synovium and muscle of RRV-infected mice was unsuccessful. However, the role of T cells was ruled out following an in depth comparative study between RRV-infected, T and B cell-deficient RAG-1 -/- mice and immunocompetent C57BL/6J mice, showed that the adaptive immune response is not required for RRV-induced inflammatory disease (Morrison et al., 2006). We therefore hypothesise that in a NK cell-deficient system, macrophages remain the principal effector cell in inflammation and tissue damage, and that 'unresponsive' NK cells which are unable to detect, bind to and lyse RRV-infected cells could be responsible for high IFN-γ signals observed. NK cells are potent IFN-γ producers, and macrophages respond to IFN-γ by eliciting pro-inflammatory responses, thus creating an environment that favours host tissue damage. The possibility that dysfunctional NK cells secrete large quantities of IFN-γ and are then unable to effectively lyse cells can result in aberrant macrophage-dependent inflammation and tissue destruction should be further investigated.

Conclusions

In this thesis, we showed that mosquito cell-derived RRV was able to display higher infectivity in macrophage and dendritic cell lines compared to mammalian cell-derived RRV. In addition, we showed that mos-RRV induced significantly lower levels of Type I IFN in macrophage and dendritic cell lines. Our study also showed that treatment with Enbrel, a rheumatoid arthritis therapeutic drug that inhibits pro-inflammatory cytokine TNF-α, contributed to aggravated disease symptoms in RRV-infected mice. Finally, we showed that the absence of a functional NK cell system resulted in extreme severity of RRV-induced disease in mice, suggesting that NK cell may exert a regulatory function in RRV-induced inflammatory disease.

Our findings contribute to current knowledge of RRV infection mechanisms and disease pathogenesis. However, further studies are necessary to elucidate viral evasion mechanisms

displayed by mos-RRV, and to determine antigenic determinants responsible for differential infectivity. The role of TNF-α in RRV-induced disease, in particular TNFR signalling should be further investigated in order to evolve towards potential therapies that could be used to treat symptoms caused by other viral arthritides. Additionally, more research is needed to completely characterise the function of NK cells in RRVD and their role in macrophage-mediated inflammation.

Aaskov J, Dalglish D (1981) Regulation in vitro of human natural killer (NK) cell activity. Medical Microbiology and Immunology **170:** 109-116
Aaskov J, Dalglish D, Harper J, Douglas J, Donaldson M, Hertzog P (1986) Natural Killer Cells in Viral Arthritis. Clinical & Experimental Immunology **68:** 23-32
Aaskov J, Mataika J, Lawrence G, Rabukawaqa V, Tucker M, Miles J, Dalglish D (1981) An epidemic of Ross River virus infection in Fiji, 1979. The American Journal of Tropical Medicine and Hygiene **30:** 1053-1059
Aaskov J, Ross P, Harper J, Donaldson M (1985) Isolation of Ross River virus from epidemic polyarthritis patients in Australia. The Australian Journal of Experimental Biology and Medical Science **63:** 587–597
Akira S, Takeda K, Kaisho T (2001) Toll-like Receptors: Critical Proteins Linking Innate and Acquired Immunity. Nature Immunology **2:** 675-680
Alter G, Suscovich T, Teigen N, Meier A, Streeck H, Brander C, Altfeld M (2007) Single-Stranded RNA Derived from HIV-1 Serves as a Potent Activator of NK Cells. The Journal of Immunology **178:** 7658-7666
Andersen J, VanScoy S, Cheng T, Gomez D, Reich N (2007) IRF-3-dependent and augmented target genes during viral infection. Genes and Immunity **9:** 168-175
Arjona A, Ledizet M, Anthony K, Bonafe N, Modis Y, Town T, Fikrig E (2007) West Nile Virus Envelope Protein Inhibits dsRNA-Induced Innate Immune Responses. The Journal of Immunology **179:** 8403-8409
Asea A, Stein-Streilein J (1998) Signalling through NKI.1 triggers NK cells to die but induces NK T cells to produce interleukin-4. Immunology **93:** 296-305
Azuolas J, Wishart E, Bibby S, Ainsworth C (2003) Isolation of Ross River virus from Mosquitoes and from Horses with Signs of Musculo-Skeletal Disease. Australian Veterinary Journal **81:** 344-347
Bach E, Aguet M, Schreiber R (1997) The IFN-gamma receptor: A paradigm for cytokine receptor signaling. Annual Reviews of Immunology **15:** 563-591
Baldwin AS, Jr. (2001) Series Introduction: The transcription factor NF-{{kappa}}B and human disease. The Journal of Clinical Investigation **107:** 3-6
Balomenos D, Rumold R, Theofilopoulos A (1998) IFN-gamma is Required for Lupus-like Disease and Lymphoaccumulation in MRL lpr Mice. Journal of Clinical Investigation **101:** 364-372
Bathon JM, Martin RW, Fleischmann RM, Tesser JR, Schiff MH, Keystone EC, Genovese MC, Wasko MC, Moreland LW, Weaver AL, Markenson J, Finck BK (2000) A Comparison of Etanercept and Methotrexate in Patients with Early Rheumatoid Arthritis. The New England Journal Of Medicine **343:** 1586-1593
Bell J, Kinney R, Trent D, Strauss E, Strauss J (1984) An evolutionary tree relating eight alphaviruses, based on amino-terminal sequences of their glycoproteins. Proceedings of the National Academy of Sciences **81:** 4702-4706
Bhatia M, Ramnath R, Chevali L, Guglielmotti A (2005) Treatment with bindarit, a blocker of MCP-1 synthesis, protects mice against acute pancreatitis. American Journal of Physiology. Gastrointestinal and Liver Physiology **288:** G1259-1265
Bielefeldt-Ohmann H, Barclay J (1998) Pathogenesis of Ross River virus-induced diseases: a role for viral quasispecies and persistence. Microbial Pathogenesis **24:** 373-383
Bilate A, Salemi V, Ramires F, de Brito T, Russo M, Fonseca S, Fae K, Martins D, Silva A, Mady C, Kalil J, Cunha-Neto E (2007) TNF blockade aggravates experimental chronic Chagas disease cardiomyopathy. Microbes and Infection **9:** 1104-1113
Billecocq A, Spiegel M, Vialat P, Kohl A, Weber F, Bouloy M, Haller O (2004) NSs protein of Rift Valley Fever virus blocks interferon production by inhibiting host gene transcription. Journal of Virology **78:** 9798-9806
Biron C, Nguyen K, Pien G, Cousens L, Salazar-Mather T (1999) Natural Killer cells in antiviral defense: Function and regulation by innate cytokines. Annual Review of Immunology **17:** 189-220
Blobel C (1997) Metalloprotease-Disintegrins: Links to Cell Adhesion and Cleavage of TNF[alpha] and Notch. Cell **90:** 589-592
Boehm U, Klamp T, Groot M, Howard J (1997) Cellular responses to interferon gamma. Annual Review of Immunology **15:** 749-795
Boissier M, Chiocchia G, Bessis N, Hajna J, Garotta G, Nicoletti F, Fournier C (1995) Biphasic effect of IFN-gamma in murine collagen-induced arthritis. European Journal of Immunology **25:** 1184-1190
Bondeson J, Wainwright S, Lauder S, Amos N, Hughes C (2006) The Role of Synovial Macrophages and Macrophage-produced Cytokines in driving Aggrecanases, Matrix Metalloproteinases, and Other Destructive and Inflammatory Responses in Osteoarthritis. Arthritis Research and Therapy **8:** R187
Bour S, Perrin C, Akari H, Strebel K (2001) The Human Immunodeficiency Virus Type 1 Vpu Protein Inhibits NF-kappa B Activation by Interfering with beta TrCP-mediated Degradation of Ikappa B. The Journal of Biological Chemistry **276:** 15920-15928
Bradley J (2008) TNF-mediated inflammatory disease. The Journal of Pathology **214:** 149-160
Brandt E, Swank R (1976) The Chediak-Higashi (beige) mutation in two mouse strains: Allelism and similarity in lysosomal dysfunction. The American Journal of Pathology **82:** 573-288
Brault A, Powers A, Medina G, Wang E, Kang W, Salas R, De Siger J, Weaver S (2001) Potential Sources of the 1995 Venezuelan Equine Encephalitis Subtype IC Epidemic. Journal of Virology **75:** 5823-5832
Brokenshire T, Symonds S, Reynolds R, Doggett S, Geary M, Russell R (2000) A cluster of locally-acquired Ross River virus infection in outer western Sydney. NSW Public Health Bulletin **11:** 132-134
Burdeinick-Kerr R, Griffin DE (2005) Gamma Interferon-Dependent, Noncytolytic Clearance of Sindbis Virus Infection from Neurons In Vitro. Journal of Virology **79:** 5374-5385

Calabrese L, Kelley D, Myers A, O'Connell M, Easley K (1991) Rheumatic symptoms and human immunodeficiency virus infection. The influence of clinical and laboratory variables in a longitudinal cohort study. Arthritis & Rheumatism **34:** 257-263

Cambi A, de Lange F, van Maarseveen N, Nijhuis M, Joosten B, van Dijk E, de Bakker B, Fransen J, Bovee-Geurts P, van Leeuwen F, Van Hulst N, Figdor C (2004) Microdomains of the C-type lectin DC-SIGN are portals for virus entry into dendritic cells. Journal of Cell Biology **164:** 145-155

Camelo S, Lafage M, Lafon M (2000) Absence of the p55 Kd TNF- receptor promotes survival in rabies virus acute encephalitis. Journal of Neurovirology **6:** 507-518

Cantell K, Pyhala L, Strander H (1974) Circulating levels of human interferon after intramuscular injection in animals and man. Journal of General Virology **22:** 453-455

Caramaschi P, Biasi D, Colombatti M, Pieropan S, Martinelli N, Carletto A, Volpe A, Pacor L, Bambara L (2006) Anti-TNF therapy in rheumatoid arthritis and autoimmunity. Rheumatology International **26:** 209-214

Carr J, Rogerson J, MJ M, Roberts N, Booth R (1997) Interleukin-12 exhibits potent antiviral activity in experimental herpesvirus infections. Journal of Virology **71:** 7799-7803

Carroll M (2004) The complement system in regulation of adaptive immunity. Nature Immunology **5:** 981-986

Carswell E, Old L, Kassel R, Green S, Fiore N, Williamson B (1975) An endotoxin-induced serum factor that causes necrosis of tumors (activated macrophage). Proceedings of the National Academy of Sciences **72:** 3666-3670

Chan A, Filer A, Parsonage G, Kollnberger S, Gundle R, Buckley C, Bowness P (2008) Mediation of the pro-inflammatory cytokine response in rheumatoid arthritis and spondylarthritis by interactions between fibroblast-like synoviocytes and natural killer cells. Arthritis & Rheumatism **58:** 707-717

Chan C, Crafton E, Fan H, Flook J, Yoshimura K, Skarica M, Brockstedt D, Dubensky T, Stins M, Lanier L, Pardoll D, Housseau F (2006) Interferon-producing killer dendritic cells provide a link between innate and adaptive immunity. Nature Medicine **advanced online publication**

Chen G, Goeddel D (2002) TNF-R1 Signaling: A Beautiful Pathway. Science **296:** 1634-1635

Chen W, Wu H, Chiou S (2003) E/NS1 modifications of Dengue 2 virus after serial passages in mammalian and/or mosquito cells. Intervirology **46:** 289-295

Cheng G, Zhong J, Chung J, Chisari F (2007) Double-stranded DNA and double-stranded RNA induce a common antiviral signaling pathway in human cells. Proceedings of the National Academy of Sciences **104:** 9035-9040

Cheng R, Kuhn R, Olson H, Rossmann M, Choi H, Smith T, Baker T (1995) Nucleocapsid and glycoprotein organization in an enveloped virus. Cell **80:** 621-630

Clarris B, Doherty R, Fraser J, French E, Muirden K (1975) Epidemic polyarthritis: a cytological, virological and immunochemical study. Australia New Zealand Journal of Medicine **5:** 450-457

Coccia E, Marziali G, Stellaci E, Perrotti E, Ilari R, Orsatti R, Battistini A (1995) Cells resistant to interferon-beta respond to interferon-gamma via the Stat1-IRF-1 pathway. Virology **211:** 113-122

Cutrone EC, Langer JA (2001) Identification of Critical Residues in Bovine IFNAR-1 Responsible for Interferon Binding. The Journal of Biological Chemistry **276:** 17140-17148

Daffis S, Samuel M, Keller B, Gale MJ, Diamond M (2007) Cell-specific IRF-3 responses protect against West Nile virus infection by interferon-dependent and -independent mechanisms. PLoS Pathogens **3:** e106

Dalbeth N, Callan M (2002) A subset of natural killer cells is greatly expanded within inflamed joints. Arthritis and Rheumatism **46:** 1763-1775

Dalbeth N, Gundle R, Davies RJO, Lee YCG, McMichael AJ, Callan MFC (2004) CD56bright NK Cells Are Enriched at Inflammatory Sites and Can Engage with Monocytes in a Reciprocal Program of Activation. The Journal of Immunology **173:** 6418-6426

Dalgarno L, Marshall I (1999) Ross River virus and Barmah Forest virus (Togaviridae). *In* A Press, ed, Encyclopedia of Virology, 2nd Edition, San Diego, USA

David M (2002) Signal Transduction by Type I Interferons. Bio Techniques **33:** S58-S65

Davies M, Chang H, Jacobs B, Kaufman R (1993) The E3L and K3L vaccinia virus gene products stimulate translation through inhibition of the double-stranded RNA-dependent protein kinase by different mechanisms. Journal of Virology **67:** 1688-1692

Davis C, Mattei L, Nguyen H, Ansarah-Sobrino C, Doms R, Pierson T (2006) The location of asparagin-linked glycans on West Nile virions controls their interactions with CD209 (dendritic cell-specific ICAM3 grabbing non-integrin). The Journal of Biological Chemistry **281:** 37183-37194

Davis C, Nguyen H, Hanna S, Sanchez M, Doms R, Pierson T (2006) West Nile Virus Discriminates between DC-SIGN and DC-SIGNR for Cellular Attachment and Infection. Journal of Virology **80:** 1290-1301

de Fougerolles A, Sprague A, Nickerson-Nutter C, Chi-Rosso G, Rennert P, Gardner H, Gotwals P, Lobb R, Koteliansky V (2000) Regulation of inflammation by collagen-binding integrins alpha1beta1 and alpha2beta1 in models of hypersensitivity and arthritis. Journal of Clinical Investigation **105:** 721-729

De Rossi M, Bernasconi P, Baggi F, de Waal Malefyt R, Mantegazza R (2000) Cytokines and chemokines are both expressed by human myoblasts: possible relevance for the immune pathogenesis of muscle inflammation. International Immunology **12:** 1329-1335

de Weerd N, Samarajiwa S, Hertzog P (2007) Type I Interferon Receptors: Biochemistry and Biological Functions. The Journal of Biological Chemistry **282:** 20053-20057

Dinarello C (1997) Proinflammatory and Anti-inflammatory Cytokines as Mediators in the Pathogenesis of Septic Shock. Chest **112:** 321S-329
Dinarello C (2007) Historical insights into cytokines. European Journal of Immunology **37:** S34-S45
Dobloug J, Forre O, Kvien T, Egeland T, Degre M (1982) Natural killer (NK) cell activity of peripheral blood, synovial fluid, and synovial tissue lymphocytes from patients with rheumatoid arthritis and juvenile rheumatoid arthritis. Annals of Rheumatic Diseases **41:** 490-494
Doherty R, Carley J, Best J (1972) Isolation of Ross River virus from man. The Medical Journal of Australia **1:** 1083-1084
Doherty R, Whitehead R, Gorman B, O'Gower A (1963) The isolation of a third group A arbovirus in Australia with preliminary observations on its relationship to epidemic polyarthritis. The Australian Journal of Science **26:** 183-184
Dowling P (1946) Epidemic polyarthritis. The Medical Journal of Australia **2:** 245-246
Elliott M, Maini R, Feldmann M, Long-Fox A, Charles P, Katsikis P, Brennan F, Walker J, Bijl H, Ghrayeb J, Woody J (1993) Treatment of rheumatoid arthritic with chimeric monocloanl antibodies to Tumour Necrosis Factor alpha. Arthritis & Rheumatism **36:** 1681-1690
Ellis L, Segreti J, Gitelis S, Huber J (1995) Joint infections due to Listeria monocytogenes: case report and review. Clinical Infectious Diseases **20:** 1548-1550
Faragher S, Meek A, Dalgarno L (1988) Genome sequence of a mouse avirulent and a mouse-virulent strain of Ross River virus. Virology **163:** 509-521
Fauquet C, Mayo M, Maniloff J, Desselberger U, Ball L (2005) Virus Taxonomy: Classification and Nomenclature of Viruses. *In* C Fauquet, M Mayo, J Maniloff, U Desselberger, L Ball, eds, International Union of Microbiological Societies
Virology Division, Vol Eighth Report of the International Committee on Taxonomy of Viruses. Elsevier Academic Press
FDA (1999) New warning for Arthritis Drug Enbrel. *In*. Food and Drug Administration, U.S. Department of Health and Human Services, Rockville, MD 20857
Feldmann M, Maini R (2001) Anti-TNFalpha therapy of Rheumatoid Arthritis: What have we learned? Annual Reviews of Immunology **19:** 163-196
Figueiredo F, Commodaro A, de Camargo M, Rizzo L, Belfort RJ (2007) NK1.1 cells downregulate murine endotoxin-induced uveitis following intraocular administration of interleukin-12. Scandinavian Journal of Immunology **66:** 329-334
Fitzgerald KA, Rowe DC, Barnes BJ, Caffrey DR, Visintin A, Latz E, Monks B, Pitha PM, Golenbock DT (2003) LPS-TLR4 Signaling to IRF-3/7 and NF-kB Involves the Toll Adapters TRAM and TRIF. The Journal of Experimental Medicine **198:** 1043-1055
Fraser J (1986) epidemic polyarthritis and Ross River virus disease. Clinics in Rheumatic Diseases **12:** 369-388
Fraser J, Becker G (1984) Mononuclear cell types in chronic synovial effusions of Ross River virus disease. Australia New Zealand Journal of Medicine **14:** 505-506
Fraser J, Cunningham A, Clarris B, Aaskov J, Leach R (1981) Cytology of synovial effusions in epidemic polyarthritis. Australia New Zealand Journal of Medicine **11:** 168-173
Fraser J, Ratnamohan V, Dowling J, Becker G, Varigos G (1983) The exanthem of Ross River virus infection: histology, location of virus antigen and nature of inflammatory infiltrate. Journal of Clinical Pathology **36:** 1256-1263
Fredericksen B, Gale MJ (2006) West Nile Virus Evades Activation of Interferon Regulatory Factor 3 through RIG-I-Dependent and -Independent Pathways without Antagonizing Host Defense Signaling. Journal of Virology **80:** 2913-2923
Funami K, Sasai M, Oshiumi H, Seya T, Matsumoto M (2008) Homo-oligomerization is essential for Toll/IL-1 receptor domain-containing adaptor molecule-1-mediated NF-kappa B and IRF-3 activation. The Journal of Biological Chemistry**:** M801013200
Gabriel S, Crowson C, O'Fallon M (1999) The epidemiology of rheumatoid arthritis in Rochester, Minnesota, 1955-1985. Arthritis & Rheumatism **42:** 415-420
Galossi A, Guarisco R, Bellis L, Puoti C (2007) Extrahepatic manifestations of chronic HCV infection. Journal of Gastrointestinal and Liver Diseases **16:** 65-73
Garrison L, McDonnell N (1999) Etanercept: therapeutic use in patients with rheumatoid arthritis. Annals of Rheumatic Diseases **58:** 165-169
Gates M, Sheahan B, Atkins G (1984) The Pathogenicity of the M9 Mutant of Semliki Forest Virus in Immunecompromised Mice. Journal of General Virology **65:** 73-80
Geijtenbeek T, van Kooyk Y (2003) DC-SIGN functions as a pathogen receptor with broad specificity. APMIS **111:** 698-714
Geiss G, Jin G, Guo J, Bumgarner R, Katze MG, Sen GC (2001) A Comprehensive View of Regulation of Gene Expression by Double-stranded RNA-mediated Cell Signaling. The Journal of Biological Chemistry **276:** 30178-30182
Glass W, Subbarao K, Murphy B, Murphy P (2004) Mechanisms of Host Defense following Severe Acute Respiratory Syndrome-Coronavirus (SARS-CoV) Pulmonary Infection of Mice. The Journal of Immunology **173:** 4030-4039
Goodbourn S, Didcock L, Randall R (2000) Interferons: Cell Signalling, Immune Modulation, Antiviral Responses and Virus Countermeasures. Journal of General Virology **81:** 2341-2364

Gosselin L, Martinez D (2004) Impact of TNF-alpha blockade on TGF-beta1 and type I collagen mRNA expression in dystrophic muscle. Muscle Nerve **30:** 244-246
Goswell G (1946) A further report of an epidemic of acute polyarthritis. The Medical Journal of Australia **2:** 861-862
Gotoh B, Komatsu T, Takeuchi K, Yokoo J (2002) Paramyxovirus Strategies for Evading the Interferon Response. Reviews in Medical Virology **12:** 337-357
Gravallese E (2002) Bone destruction in arthritis. Annals of Rheumatic Diseases **61:** 84ii-86
Grieder F, Davis B, Zhou X, Chen S, Finkelman F, Gause W (1997) Kinetics of Cytokine Expression and Regulation of Host Protection Following Infection with Molecularly Cloned Venezuelan Equine Encephalitis Virus. Virology **233:** 302-312
Grounds M, Torrisi J (2004) Anti-TNF{alpha} (Remicade(R)) therapy protects dystrophic skeletal muscle from necrosis. FASEB J. **18:** 676-682
Gubler D (2001) Human arbovirus infections worldwide. Annals of the New York Academy of Sciences **951:** 13-24
Gubler D, Reiter P, Ebi K, Yap W, Nasci R, Patz J (2001) Climate Variability and Change in the United States: Potential Impacts on Vector- and Rodent-Borne Diseases. Environmental Health Perspectives **109:** 223-233
Guglielmotti A, D'Onofrio E, Coletta I, Aquilini L, Milanese C, Pinza M (2002) Amelioration of rat adjuvant arthritis by therapeutic treatment with bindarit, an inhibitor of MCP-1 and TNF-a production. Inflammation Research **51:** 252-258
Hahn CS, Lustig S, Strauss EG, Strauss JH (1988) Western Equine Encephalitis Virus is a Recombinant Virus. Proceedings of the National Academy of Sciences **85:** 5997-6001
Hamerman J, Ogasawara K, Lanier L (2005) NK cells in innate immunity. Current Opinion in Immunology **17:** 29-35
Hanaoka R, Kasama T, Muramatsu M, Yajima N, Shiozawa F, Miwa Y, Negishi M, Ide H, Miyaoka H, Uchida H, Adachi M (2003) A novel mechanism for the regulation of IFN-gamma inducible protein-10 expression in rheumatoid arthritis. Arthritis Research and Therapy **5:** R74 - R81
Haque SJ, Harbor PC, Williams BRG (2000) Identification of Critical Residues Required for Suppressor of Cytokine Signaling-specific Regulation of Interleukin-4 Signaling. The Journal of Biological Chemistry **275:** 26500-26506
Harley D, Bossingham D, Purdie D, Pandeya N, Sleigh A (2002) Ross River virus disease in tropical Queensland: evolution of rheumatic manifestations in an inception cohort followed for six months. The Medical Journal of Australia **177:** 352-355
Harley D, Sleigh A, Ritchie S (2001) Ross River virus transmission, infection and disease: a cross-disciplinary review. Clinical Microbiology Reviews **14:** 909-932
Harris L (1944) Polyarthritis in the Northern Territory. The Medical Journal of Australia **1:** 546-547
Hata H, Sakaguchi N, Yoshitomi H, Iwakura Y, Sekikawa K, Azuma Y, Kanai C, Moriizumi E, T N, Nakamura T, Sakaguchi S (2004) Distinct contribution of IL-6, TNF-alpha, IL-1 and IL-10 to T-cell-mediated spontaneous autoimmune arthritis. Journal of Clinical Investigation **114:** 582-588
Hayden M, Ghosh S (2008) Shared principles in NF-kappaB signaling. Cell **132:** 344-362
Hayward M, Jones B, Saparov A, Hain H, Trillat A-C, Bunzel M, Corona A, Li-Wang B, Strenkowski B, Giordano C, Shen H, Arcamone E, Weidlick J, Vilensky M, Tugusheva M, Felkner R, Campbell W, Rao Y, Grass D, Buiakova O (2007) An Extensive Phenotypic Characterization of the hTNF-alpha Transgenic Mice. BMC Physiology **7:** 1-16
Heil F, Hemmi H, Hochrein H, Ampenberger F, Kirschning C, Akira S, Lipford G, Wagner H, Bauer S (2004) Species-Specific Recognition of Single-Stranded RNA via Toll-Like Receptor 7 and 8. Science **303:** 1526-1529
Heise M, Morrison T (2008) The host complement system and arbovirus pathogenesis. Current Drug Targets **9:** 165-172
Heise M, Simpson D, Johnston R (2000) Sindbis-Group Alphavirus Replication in Periosteum and Endosteum of Long Bones in Adult Mice. Journal of Virology **74:** 9294-9299
Herbein G, O'Brien W (2000) Tumor Necrosis Factor (TNF)-alpha and TNF Receptors in Viral Pathogenesis. Proceedings of the Society for Experimental Biology and Medicine **223:** 241-257
Herberman RB, Ortaldo JR (1981) Natural Killer Cells: Their Role in Defenses against Disease. Science **214:** 24-30
Hiscott J (2007) Triggering the Innate Antiviral Response through IRF-3 Activation. The Journal of Biological Chemistry **282:** 15325-15329
Hodgetts S, Radley H, Davies M, Grounds M (2006) Reduced Necrosis of Dystrophic Muscle by Depletion of Host Neutrophils, or Blocking TNFa Function with Etanercept in mdx mice. Neuromuscular Disorders **16:** 591-602
Honda K, Yanai H, Negishi H, Asagiri M, Sato M, Mizutani T, Shimada N, Ohba Y, Takaoka A, Yoshida N, Taniguchi T (2005) IRF-7 is the master regulator of type-I interferon-dependent immune responses. Nature **434:** 772-777
Hornung V, Ellegast J, Kim S, Brzozka K, Jung A, Kato H, Poeck H, Akira S, Conzelmann K-K, Schlee M, Endres S, Hartmann G (2006) 5'-Triphosphate RNA Is the Ligand for RIG-I. Science **314:** 994-997
Hoshino K, Takeuchi O., Kawai T., Sanjo H., Ogawa T., Takeda Y., Takeda K. and Akira S., (1999) Toll-Like Receptor-4 (TLR4)- Deficient Mice Are Hyporesponsive to Lipopolysaccharide: evidence for TLR4 as the *Lps* Gene Product. The Journal of Immunology **162:** 3749-3752

Howard J, Morris C, Emord D, Grayson M (1988) Epizootiology of eastern equine encephalitis virus in upstate New York, USA. VII. Virus surveillance 1978-85, description of 1983 outbreak, and series conclusions. The Journal of Medical Entomology **25:** 501-514
Hu W, Tong S, Mengersen K, Oldenbrug B (2007) Exploratory spatial analysis of social and enironmental factors associated with the incidence of Ross River virus in Brisbane, Australia. The American Journal of Tropical Medicine and Hygiene **76:** 814-819
Jacob C, Holoshitz J, van der Meide P, Strober S, McDevitt H (1989) Heterogenous effects of IFN-gamma in adjuvant arthritis. The Journal of Immunology **142:** 1500-1505
Jiang Z, Mak T, Sen G, Li X (2004) Toll-Like Receptor 3-Mediated Activation of NF-κB and IRF3 Diverges Toll-IL-1 Receptor Domain-Containing Adapter Inducing IFN-β. Proceedings of the National Academy of Sciences, USA **101:** 3533-3538
Johnston C, Jiang W, Chu T, Levine B (2001) Identification of genes involved in the host response to neurovirulent alphavirus infection. Journal of Virology **75:** 10431-10445
Johnston R, Peters C (1996) Alphaviruses, Vol 2. Lippincott-Raven, Philadelphia, PA
Joosten L, Helsen M, Saxne T, van de Loo F, Heinegard D, van den Berg W (1999) IL-1alpha/beta BlockadePrevents Cartilage and Bone Destruction in Murine Type II Collagen-Induced Arthritis, Whereas TNF-alpha Blockade Only Ameliorates Joint Inflammation. The Journal of Immunology **163:** 5049-5055
Journeaux SF, Brown WG, Aaskov JG (1987) Prolonged Infection of Human Synovial Cells with Ross River Virus. Journal of General Virology **68:** 3165-3169
Kamath AT, Sheasby CE, Tough DF (2005) Dendritic Cells and NK Cells Stimulate Bystander T Cell Activation in Response to TLR Agonists through Secretion of IFN-{alpha}{beta} and IFN-{gamma}. The Journal of Immunology **174:** 767-776
Kaplan J, de Domenico I, Ward D (2008) Chediak-Higashi syndrome. Current Opinion in Hematology **15:** 22-29
Kariko K, Ni H., Capodici J., Laphier M. and Weissman D., (2004) mRNA Is an Endogenous Ligand for Toll-Like Receptor 3. The Journal of Biological Chemistry **279:** 12542-12550
Karin M, Ben-Neriah Y (2000) Phosphorylation Meets Ubiquitination: The Control of NF-kB Activity. Annual Review of Immunology **18:** 621-663
Kato H, Sato S, Yoneyama M, Yamamoto M, Uematsu K, Matsui K, Tsujimura T, Takeda K, Fujita M, Takeuchi O, Akira S (2005) Cell Type-Specific Involvement of RIG-I in Antiviral Response. Immunity **23:** 19-28
Kato H, Takeuchi O, Sato S, Yoneyama M, Yamamoto M, Matsui K, Uematsu S, Jung A, Kawai T, Ishii K, Yamaguchi O, Otsu K, Tsujimura T, Koh C-S, e Sousa C, Matsuura Y, Fujita T, Akira S (2006) Differential roles of MDA5 and RIG-1 Helicases in the Recognition of RNA viruses. Nature **441:** 101-105
Kay B, Boyd A, Ryan P, Hall R (2007) Mosquito feeding patterns and natural infection of vertebrates with Ross River and Barmah Forest viruses in Brisbane, Australia. The American Journal of Tropical Medicine and Hygiene **76:** 417-423
Keffer J, Probert L, Cazlaris H, Georgopoulos S, Kaslaris E, Kioussis D, Kollias G (1991) Transgenic Mice Expressing Human Tumour Necrosis Factor: A Predictive Genetic Model of Arthritis. The EMBO Journal **10:** 4025-4031
Kekow J, Welte T, Kellner U, Pap T (2002) Development of rheumatoid nodules during anti-tumor necrosis factor alpha therapy with etanercept. Arthritis & Rheumatism **46:** 843-844
Kelly E (1957) Beige, bg. Mouse NewsLetter **16:** 36
Kishimoto T (2005) Interleukin-6: From Basic Science to Medicine - 40 Years of Immunology. Annual Review of Immunology **23:** 1-21
Kistner O, Barrett N, Bruhmann A, Reiter M, Mundt W, Savidis-Dacho H, Schober-Bendixen S, Dorner F, Aaskov J (2007) The Preclinical Testing of a Formaldehyde Inactivated Ross River virus Vaccine Designed for Use in Humans. Vaccine **25:** 4845-4852
Kitaichi N, Kotake S, Morohashi T, Onoe K, Ohno S, Taylor A (2002) Diminution of experimental autoimmune uveoretinitis (EAU) in mice depleted of NK cells. Journal of Leukocyte Biology **72:** 1117-1121
Klimstra W, Nangle E, Smith M, Yurochko A, Ryman K (2003) DC-SIGN and L-SIGN Can Act as Attachment Receptors for Alphaviruses and Distinguish between Mosquito Cell- and Mammalian Cell-Derived Viruses. Journal of Virology **77:** 12022-12032
Koo G, Dumont F, Tutt M, Hackett JJ, Kumar V (1986) The NK-1.1(-) mouse: a model to study differentiation of murine NK cells. The Journal of Immunology **137:** 3742-3747
Kunkel SL, Lukacs N, Kasama T, Strieter RM (1996) The role of chemokines in inflammatory joint disease. J Leukoc Biol **59:** 6-12
La Linn M, Gardner J, Warrilow D, Darnell GA, McMahon CR, Field I, Hyatt AD, Slade RW, Suhrbier A (2001) Arbovirus of Marine Mammals: a New Alphavirus Isolated from the Elephant Seal Louse, Lepidophthirus macrorhini. J. Virol. **75:** 4103-4109
LaBeaud AD (2008) Why Arboviruses Can Be Neglected Tropical Diseases. PLoS Neglected Tropical Diseases **2:** e247
Laemmli U (1970) Cleavage of structural proteins during the assembly of the head of bacteriophage T4. Nature **227:** 680-685
Laharyia C, Pradhan S (2006) Emergence of chikungunya virus in Indian subcontinent after 32 years: a review. Journal of Vector Borne Diseases **43:** 151-160
Lanier L (2008) Evolutionary struggles between NK cells and viruses. Nature Reviews Immunology **8:** 259-268

Lawlor K, Campbell I, O'Donnell K, Wu L, Wicks I (2001) Molecular and Cellular Mediators of Interleukin-1-Dependent Acute Inflammatory Arthritis. Arthritis and Rheumatism **44:** 442-450

Lechner F, Vogt H, Seow H, Bertoni G, Cheevers W, von Bodungen U, Zurbriggen A, Peterhans E (1997) Expression of cytokine mRNA in Lentivirus-Induced arthritis. The American Journal of Pathology **151:** 1053-1065

Levy JA (1993) Pathogenesis of human immunodeficiency virus infection. Microbiol. Mol. Biol. Rev. **57:** 183-289

Lewthwaite J, Blake S, Hardingham T, Foulkes R, Stephens S, Chaplin L, Emtage S, Catterall C, Short S, Nesbitt A (1995) Role of TNF alpha in the induction of antigen induced arthritis in the rabbit and the anti-arthritic effect of species specific TNF alpha neutralising monoclonal antibodies. Annals of Rheumatic Diseases **54:** 366-374

Lidbury B, Rulli N, Suhrbier A, Smith P, McColl S, Cunningham A, Tarkowski A, van Rooijen N, Fraser R, Mahalingam S (2008) Macrophage-derived proinflammatory factors contribute to the develpoment of arthritis and myositis after infection with an arthrogenic alphavirus. The Journal of Infectious Diseases **197:** 1-9

Lidbury B, Simeonovic C, Maxwell G, Marshall I, Hapel A (2000b) Macrophage-Induced Muscle Pathology Results in Morbidity and Mortality for Ross River Virus-Infected Mice. The Journal of Infectious Diseases **181:** 27-34

Limesand K, Higgs S, Pearson L, Beaty B (2000) Potentiation of vesicular stomatitis New Jersey virus infection in mice by mosquito saliva. Parasite Immunology **22:** 461-467

Limesand K, Higgs S, Pearson L, Beaty B (2003) Effect of Mosquito Salivary Gland Treatment on Vesicular Stomatitis New Jersey Virus Replication and Interferon α/β Expression In Vitro. Journal of Medical Entomology **40:** 199–205

Linn M, Aaskov J, Suhrbier A (1996) Antibody-dependent enhancement and persistence in macrophages of an arbovirus associated with arthritis. Journal of General Virology **77:** 407-411

Linn M, Eble J, Lubken C, Slade R, Heino J, Davies J, Suhrbier A (2005) An arthritogenic alphavirus uses the alpha-1/beta-1 integring collagen receptor. Virology **336:** 229-239

Linn M, Gardner J, Warrilow D, Darnell G, McMahon C, Field I, Hyatt A, Slade R, Suhrbier A (2001) Arbovirus of Marine Mammals: a New Alphavirus Isolated from the Elephant Seal Louse, Lepidophthirus macrorhini. Journal of Virology **75:** 4103-4109

Liu W, Chen H, Wang X, Huang H, Khromykh A (2004) Analysis of Adaptive Mutations in Kunjin Virus Replicon RNA Reveals a Novel Role for the Flavivirus Nonstructural Protein NS2A in Inhibition of Beta Interferon Promoter-Driven Transcription. Journal of Virology **78:** 12225-12235

Liu Y-J (2005) IPC: Professional Type 1 Interferon-Producing Cells and Plasmacytoid Dendritic Cell Precursors. Annual Review of Immunology **23:** 275-306

Lovy M, Starkebaum G, Uberoi S (1996) Hepatitis C infection presenting with rheumatic manifestations: a mimic of rheumatoid arthritis. Journal of Rheumatology **23:** 979-983

Lozach P, Burleigh L, Staropoli I, Navarro-Sanchez E, Harriague J, Virelizier J, Rey F, Despres P, Arenzana-Seisdedos F, Amara A (2005) Dendritic Cell-specific Intercellular Adhesion Molecule 3-grabbing Non-integrin (DC-SIGN)-mediated Enhancement of Dengue Virus Infection Is Independent of DC-SIGN Internalization Signals. The Journal of Biological Chemistry **280:** 23698-23708

Lozach P-Y, Lortat-Jacob H, De Lacroix De Lavalette A, Staropoli I, Foung S, Amara A, Houles C, Fieschi F, Schwartz O, Virelizier J-L, Arenzana-Seisdedos F, Altmeyer R (2003) DC-SIGN and L-SIGN Are High Affinity Binding Receptors for Hepatitis C Virus Glycoprotein E2. J. Biol. Chem. **278:** 20358-20366

Luers A, Adams S, Smalley J, Campanella J (2005) A phylogenomic study of the genus alphavirus employing whole genome comparison. Comparative and Functional Genomics **6:** 217-227

Lund JM, Alexopoulou L., Sato, A., Karow M., Adams N.C., Gale N.W., Iwasaki A. and Flavell R.A., (2004) Recognition of Single-Stranded RNA Viruses by Toll-Like Receptor 7. Proceedings of the National Academy of Sciences, USA **101:** 5598-5603

Mageed R, Adams G, Woodrow D, Podhajcer O, Chernajovsky Y (1998) Prevention of Collagen-Induced Arthritis by Gene Delivery of Soluble p75 Tumour Necrosis Factor Receptor. Gene Therapy **5:** 1584-1592

Maggi L, Heitmeier M, Scheuner D, Kaufman R, Buller R, Corbett J (2000) Potential Role of PKR in Double-Stranded RNA-induced Macrophage Activation. The EMBO Journal **19:** 3630-3638

Maini R, Taylor P, Szechinski J, Pavelka K, Broll J, Balint G, Emery P, Raemen F, Petersen J, Smolen J, Thomson D, Kishimoto T, (2006) Double-blind randomized controlled clinical trial of the interleukin-6 receptor antagonist, tocilizumab, in European patients with rheumatoid arthritis who had an incomplete response to methotrexate. Arthritis & Rheumatism **54:** 2817-2829

Markiewski M, Lambris J (2007) The role of complement in inflammatory diseases from behind the scenes into the spotlight. The American Journal of Pathology **71:** 715-727

Marok R, Winyard P, Coumbe A, Kus M, Gaffney K, Blades S, Mapp P, Morris C, Blake D, Kaltschmidt C, Baeuerle P (1996) Activation of the transcription factor nuclear factor-κB in human inflamed synovial tissue. Arthritis & Rheumatism **39:** 583-591

Mateo L, Linn M, McColl S, Cross S, Gardner J, Suhrbier A (2000) An Arthrogenic Alphavirus Induces Monocyte Chemoattractant Protein-1 and Interleukin-8. Intervirology **43:** 55-60

Mauritz N, Holmdahl R, Jonsson R, van der Meide P, Scheynius A, Klareskog L (1988) Treatment with IFN-gamma triggers the onset of collagen arthritis in mice. Arthritis & Rheumatism **31**

Mazzon E, Cuzzocrea S (2007) Role of TNF-α in lung tight junction alteration in mouse model of acute lung inflammation. Respiratory Research **8:** 75-92
Mazzon E, Esposito E, Di Paola R, Mui C, Crisafulli C, Genovese T, Caminiti C, Meli R, Bramanti P, Cuzzocrea S (2008) Effect of tumour necrosis factor-alpha receptor 1 genetic deletion on carrageenan-induced acute inflammation: a comparison with etanercept. Clinical & Experimental Immunology **153:** 136-149
McKenzie EJ, Taylor PR, Stillion RJ, Lucas AD, Harris J, Gordon S, Martinez-Pomares L (2007) Mannose Receptor Expression and Function Define a New Population of Murine Dendritic Cells. The Journal of Immunology **178:** 4975-4983
Melton JV, Ewart GD, Weir RC, Board PG, Lee E, Gage PW (2002) Alphavirus 6K Proteins Form Ion Channels. The Journal of Biological Chemistry **277:** 46923-46931
Miagkov A, Kovalenko D, Brown C, Didsbury J, Cogswell J, Stimpson S, Baldwin A, Makarov S (1998) NF-κB activation provides the potential link between inflammation and hyperplasia in the arthritic joint
. Proceedings of the National Academy of Sciences **95:** 13859-13864
Miller JL, deWet BJM, Martinez-Pomares L, Radcliffe CM, Dwek RA, Rudd PM, Gordon S (2008) The Mannose Receptor Mediates Dengue Virus Infection of Macrophages. PLoS Pathogens **4:** e17
Mims C, Murphy F, Taylor W, Marshall I (1973) Pathogenesis of Ross River virus infection in mice: Ependymal infection, cortical thinning, and hydrocephalus. The Journal of Infectious Diseases **127:** 121-128
Mondotte J, Lozach P, Amara A, Gamarnik A (2007) Essential Role of Dengue Virus Envelope Protein N Glycosylation at Asparagine-67 during Viral Propagation. Journal of Virology **81:** 7136-7148
Moreland L, Schiff M, Baumgartner S, Tindall E, Fleischmann R, Bulpitt K, Weaver A, Keystone E, Furst D, Mease P, Ruderman E, Horwitz D, Arkfeld D, Garrison, Burge D, Blosch C, Lange M, McDonnell N, Weinblatt M (1999) Etanercept Therapy in Rheumatoid Arthritis: A Randomized, Controlled Trial. Annals of Internal Medicine **130:** 478-486
Morrison T, Whitmore A, Shabman R, Lidbury B, Mahalingam S, Heise M (2006) Characterization of Ross river Virus Tropism and Virus-Induced Inflammation in a Mouse Model of Viral Arthritis and Myositis. Journal of Virology **80:** 737-749
Morrisson T, Fraser R, Smith P, Mahalingam S, Heise M (2007a) Complement Contributes to Inflammatory Tissue Destruction in a Mouse Model of Ross River Virus-Induced Disease. Journal of Virology **81:** 5132-5143
Morrisson T, Whitmore A, Shabman R, Lidbury B, Mahalingam S, Heise M (2006) Characterization of Ross river Virus Tropism and Virus-Induced Inflammation in a Mouse Model of Viral Arthritis and Myositis. Journal of Virology **80:** 737-749
Morrisson T, Whitmore A, Shabman R, Lidbury B, Mahalingam S, Heise M (2007b) Characterization of Ross river Virus Tropism and Virus-Induced Inflammation in a Mouse Model of Viral Arthritis and Myositis. Journal of Virology **80:** 737-749
Moss M, Sklair-Tavron L, Nudelman R (2008) Drug Insight: tumor necrosis factor-converting enzyme as a pharmaceutical target for rheumatoid arthritis. Nature Clinical Practice Rheumatology **4:** 300-310
Mukhopadhyay S, Zhang W, Gabler S, Chipman P, Strauss E, Strauss J, Baker T, Kuhn R, Rossmann M (2006) Mapping the structure and function of the E1 and E2 glycoproteins in alphaviruses. Structure **14:** 63-73
Mylonas A, Brown A, Carthew T, McGrath B, Purdie D, Pandeya N, Vecchio P, Collins L, Gardner I, de Looze F, Reymond E, Suhrbier A (2002) Natural history of Ross River virus-induced epidemic polyarthritis. The Medical Journal of Australia **177:** 356-360
Mylonas A, Brown A, Carthew T, McGrath B, Purdie D, Pandeya N, Vecchio P, Collins L, Gardner I, de Looze F, Reymond E, Suhrbier A (2004) Corticosteroid therapy in an alphaviral arthritis. Journal of Clinical Rheumatology **10:** 326-330
Nimmo J (1928) An unsual epidemic. The Medical Journal of Australia **1:** 549-550
Ning S, Huye LE, Pagano JS (2005) Regulation of the Transcriptional Activity of the IRF7 Promoter by a Pathway Independent of Interferon Signaling. The Journal of Biological Chemistry **280:** 12262-12270
Nishimoto N, Kishimoto T, Yoshizaki K (2000) Anti-interleukin 6 receptor antibody treatment in rheumatic disease. Annals of Rheumatic Diseases **59:** 21-27
Old J, Deane E (2005) Antibodies to the Ross River Virus in Captive Marsupials in Urban Areas of Eastern New South Wales, Australia. Journal of Wildlife Diseases **41:** 611-614
Orange J, Wang B, Terhorst C, Biron C (1995) Requirement for natural killer cell-produced interferon gamma in defense against murine cytomegalovirus infection and enhancement of this defense pathway by interleukin 12 administration. Journal of Experimental Medicine **182:** 10445-11056
Ordemann R, Hutchinson R, J F, Burakoff S, Reddy P, Duffner U, Braun T, Liu C, Teshima T, Ferrara J (2002) Enhanced allostimulatory activity of host antigen-presenting cells in old mice intensifies acute graft-versus-host disease. The Journal of Clinical Investigation **109:** 1249-1255
Oshiumi H, Matsumoto M, Funami K, Akazawa T, Seya T (2003) TICAM-I, an Adaptor Molecule that Participates in Toll-like Receptor 3-mediated Interferon-b Induction. Nature Immunology **4:** 161-167
Paredes A, Heidner H, Thuman-Commike P, Venkataram Prasad B, Johnston R, Chiu W (1998) Structural localisation of the E3 glycoprotein in attenuated Sindbis virus mutants. Journal of Virology **72:** 1534-1541
Paun A, Pitha P (2007) The IRF family, revisited. Biochimie **89:** 744-753

Pestka S (2000) Human Interferon-alpha species and receptors. Biopolymers **55:** 254-287
Pestka S (2007) The Interferons: 50 Years after Their Discovery, There Is Much More to Learn. The Journal of Biological Chemistry **282:** 20047-20051
Pfaffl M, Tichopad A, Prgomet C, Neuvians T (2004) Determination of Stable Housekeeping Genes, Differentially Regulated Target Genes and Sample Integrity: BestKeeper - Excel-based Tool using Pair-Wise Correlations. Biotechnology Letters **26:** 509-515
Pfaffl MW, Horgan GW, Dempfle L (2002) Relative expression software tool (REST(C)) for group-wise comparison and statistical analysis of relative expression results in real-time PCR. Nucleic Acids Research **30:** e36-
Pfeffer L, Kim J-G, Pfeffer S, Carrigan D, Baker D, Homayouni R (2004) Role of Nuclear Factor-kappaB in the antiviral action of interferon and interferon-regulated gene expression. The Journal of Biological Chemistry **279:** 31304-31311
Pichlmair A, Schulz O, Tan C, Naslund T, Liljestrom P, Weber F, Sousa C (2006) RIG-I-Mediated Antiviral Responses to Single-Stranded RNA Bearing 5'-Phosphates. Science **314:** 997-1001
Platanias LC, Fish EN (1999) Signaling pathways activated by interferons. Experimental Hematology **27:** 1583-1592
Poppers J, Mulvey M, Perez C, Khoo D, Mohr I (2003) Identification of a Lytic-Cycle Epstein-Barr Virus Gene Product That Can Regulate PKR Activation. Journal of Virology **77:** 228-236
Powers A, Brault A, Shirako Y, Strauss E, Kang W, Strauss J, Weaver S (2001) Evolutionary relationships and systematics of the alphaviruses. Journal of Virology **75:** 10118-10131
Ravelli A (2002) Macrophage Activation Syndrome. Current Opinion in Rheumatology **14:** 548-552
Reading P, Whitney P, Barr D, Smyth M, Brooks A (2006) NK cells contribute to the early clearance of HSV-1 from the lung but cannot control replication in the central nervous system following intranasal infection. European Journal of Immunology **36:** 897-906
Reading PC, Miller JL, Anders EM (2000) Involvement of the Mannose Receptor in Infection of Macrophages by Influenza Virus. Journal of Virology **74:** 5190-5197
Renault P, Solet J-L, Sissoko D, Balleydier E, Larrieu S, Filleul L, Lassalle C, Thiria J, Rachou E, de Valk H, Ilef D, Ledrans M, Quatresous I, Quenel P, Pierre V (2007) A Major Epidemic of Chikungunya Virus Infection on Reunion Island, France, 2005 2006. Am J Trop Med Hyg **77:** 727-731
Rigby W (2007) Drug Insight: Different mechanisms of action of tumor necrosis factor antagonists: passive-aggressive behaviour? Nature Clinical Practice **3:** 227-233
Roder J (1979) The Beige mutation in the mouse: I. A Stem cell predetermined impairment in Natural Killer cell function. The Journal of Immunology **123:** 2168-2173
Roder J, Duwe A (1979) The beige mutation in the mouse selectively impairs natural killer cell function. Nature **278:** 451-453
Rulli N (2007) Ross River virus infection: Disease mechanisms and potential treatment. University of Canberra, Canberra, ACT2617
Rulli N, Melton J, Wilmes A, Ewart G, Mahalingam S (2007) The Molecular and Cellular Aspects of Arthritis Due to Alphavirus Infections: Lesson Learned from Ross River Virus. Annals of the New York Academy of Sciences **1102:** 96-108
Russell R (2002) Ross River virus: Ecology and Distribution. Annual Review of Entomology **41:** 1-31
Ryman K, Meier K, Nangle E, Ragsdale S, Korneeva N, Rhoads R, MacDonald M, Klimstra W (2005) Sindbis Virus Translation Is Inhibited by a PKR/RNase L-Independent Effector Induced by Alpha/Beta Interferon Priming of Dendritic Cells. Journal of Virology **79:** 1487-1499
Samuel C (2001) Antiviral Actions of Interferons. Clinical Microbiology Reviews **14:** 778-809
Samuel M, Whitby K, Keller B, Marri A, Barchet W, Williams B, Silverman R, Gale MJ, Diamond M (2006) PKR and RNase L Contribute to Protection against Lethal West Nile Virus Infection by Controlling Early Viral Spread in the Periphery and Replication in Neurons. Journal of Virology **80:** 7009-7019
Saxena R, Saxena Q, Adler W (1982) Defective T-cell response in beige mutant mice. Nature **295:** 240-241
Scallon B, Cai A, Solowski N, Rosenberg A, Song X, Shealy D, Wagner C (2002) Binding and Functional Comparisons of Two Types of Tumor Necrosis Factor Antagonists. Journal of Pharmacology and Experimental Therapeutics **301:** 418-426
Schalkwijk J, Joosten L, van den Berg W, van de Putte L (1988) Experimental arthritis in C57BL/6 normal and beige (Chediak-Higashi) mice: in vivo and in vitro observations on cartilage degradation. Annals of Rheumatic Diseases **47:** 940-946
Schalkwijk J, Joosten L, van den Berg W, van de Putte L (1990) Antigen induced arthritis in beige (Chediak-Higashi) mice. Annals of Rheumatic Diseases **49:** 607-610
Scherbik SV, Stockman BM, Brinton MA (2007) Differential Expression of Interferon (IFN) Regulatory Factors and IFN-Stimulated Genes at Early Times after West Nile Virus Infection of Mouse Embryo Fibroblasts. Journal of Virology **81:** 12005-12018
Schett G (2008) Review: Immune cells and mediators of inflammatory arthritis. Autoimmunity **41:** 224 - 229
Schneider B, Soong L, Zeidner N, Higgs S (2004) Aedes aegypti Salivary Gland Extracts Modulate Anti-Viral and TH1/TH2 Cytokine Responses to Sindbis Virus Infection. Viral Immunology **17:** 565-573
Seay A, Griffin D, Johnson R (1981) Experimental viral polymyositis: age dependency and immune responses to Ross River virus infection in mice. Neurology **31:** 656-660

Seay A, Wolinsky J (1983) Ross River virus-induced demyelination: II. Ultrastructural studies. Annals of Neurology **14:** 559-568
Semple S, Reynolds G, O'Leary M, Flower R (1998) Screening of Australian medicinal plants for antiviral activity. Journal of Ethnopharmacology **60:** 163-172
Seth R, Sun L, Chen Z (2006) Antiviral innate immunity pathways. Cell Research **16:** 141-147
Shabman R, Morrison T, Moore C, White L, Suthar M, Hueston L, Rulli N, Lidbury B, Ting J, Mahalingam S, Heise M (2007) Differential Induction of Type I Interferon Responses in Myeloid Dendritic Cells by Mosquito and Mammalian-Cell-Derived Alphaviruses. Journal of Virology **81:** 237-247
Sibree E (1944) Acute polyarthritis in Queensland. The Medical Journal of Australia **2:** 565-567
Silva M, Guerrero-Plata A, Gilfoy F, Garofalo R, Mason P (2007) Differential Activation of Human Monocyte-Derived Plasmacytoid Dendritic Cells by West Nile Virus Generated in Different Host Cells. Journal of Virology **81:** 13640-13648
Simova J, Bubenok J, Bieblov J, Jandlov T (2004) The Role of NK1.1+ Cells in the Protection against MHC Class I+ HPV16-Associated Tumours. Folia Biologica (Praha) **50:** 200-202
Smith D, Letendre S (2002) Viral Pneumonia as a Serious Complication of Etanercept Therapy. Annals of Internal Medicine **136:** 174-
Soden M, Vasudevan H, Roberts B, Coelen R, Hamlin G, Vasudevan S, La Brooy J (2000) Detection of viral ribonucleic acid and histologic analysis of inflamed synovium in Ross River virus infection. Arthritis & Rheumatism **43:** 365-369
Spender L, Hussell T, Openshaw P (1998) Abundant IFN-gamma production by local T cells in respiratory syncytial virus-induced eosinophilic lung disease. Journal of General Virology **79:** 1751-1758
Steinman RM (2000) DC-SIGN: A Guide to Some Mysteries of Dendritic Cells. Cell **100:** 491-494
Strauss JH, Strauss EG (1994) The alphaviruses: gene expression, replication, and evolution. Microbiol. Mol. Biol. Rev. **58:** 491-562
Sturge J, Todd SK, Kogianni G, McCarthy A, Isacke CM (2007) Mannose receptor regulation of macrophage cell migration. Journal of Leukocyte Biology **82:** 585-593
Suhrbier A, Linn M (2004) Clinical and pathological aspects of arthritis due to Ross River virus and other alphaviruses. Current Opinion in Rheumatology **16:** 374-379
Takasugi K, Yamamura M, Iwahashi M, Otsuka F, Yamana J, Sunahori K, Kawashima M, Yamada M, Makino H (2006) Induction of tumour necrosis factor receptor-expressing macrophages by interleukin-10 and macrophage colony-syimulating factor in rheumatoid arthritis. Arthritis Research and Therapy **8:** 126-139
Takeuchi T (2006) Treatment of inflammatory immunologic disease: Anti-TNF therapy in rheumatoid arthritis. *In* 103rd Annual Scientific Meeting of The Japanese Society of Internal Medicine. Internal Medicine, Tokyo, Japan
Tassaneetrithep B, Burgess T, Granelli-Piperno A, Trumpfheller C, Finke J, Sun W, Eller M, Pattanapanyasat K, Sarasombath S, Birx D, Steinman R, Schlesinger S, Marovich M (2003) DC-SIGN (CD209) Mediates Dengue Virus Infection of Human Dendritic Cells. The Journal of Experimental Medicine **197:** 823-829
Tellinghuisen TL, Hamburger AE, Fisher BR, Ostendorp R, Kuhn RJ (1999) In Vitro Assembly of Alphavirus Cores by Using Nucleocapsid Protein Expressed in Escherichia coli. Journal of Virology **73:** 5309-5319
Tomita T, Takano H, Tomita N, Morishita R, Kaneko M, Shi K, Takahi K, Nakase T, Kaneda Y, Yoshikawa H, Ochi T (2000) Transcription factor decoy for NF{kappa}B inhibits cytokine and adhesion molecule expressions in synovial cells derived from rheumatoid arthritis. Rheumatology **39:** 749-757
Tomita T, Takeuchi E, Tomita N, Morishita R, Kaneko M, Yamamoto K, Nakase T, Seki H, Kato K, Kaneda Y, Ochi T (1999) Suppressed severity of collagen-induced arthritis by in vivo transfection of nuclear factor kappaB decoy oligodeoxynucleotides as a gene therapy. Arthritis & Rheumatism **42:** 2532-2542
Tong S (2004) Ross River virus disease in Australia: epidemiology, socioecology and public health response. Internal Medicine Journal **34:** 58-60
Tong S, Bi P, Parton K, Hobbs J, McMichael A (1998) Climate variability and transmission of epidemic polyarthritis. The Lancet **351:** 1100
Tupanceska D, Zaid A, Rulli N, Thomas S, Lidbury B, Matthaei K, Ramirez R, Mahalingam S (2007) Ross River Virus: An Arthritogenic Alphavirus of Significant Importance in the Asia Pacific. *In* S Lal, ed, Emerging Viral Diseases of Southeast Asia, Vol 4. Issues Infect Dis, Basel, Karger, pp 94-111
van der Poll T, Opal S (2008) Host–pathogen interactions in sepsis. The Lancet Infectious Disease **8:** 32-43
van Holten J, Pavelka K, Vencovsky J, Stahl H, Rozman B, Genovese M, Kivitz AJ, Alvaro J, Nuki G, Furst DE, Herrero-Beaumont G, McInnes IB, Musikic P, Tak PP (2005) A multicentre, randomised, double blind, placebo controlled phase II study of subcutaneous interferon beta-1a in the treatment of patients with active rheumatoid arthritis. Annals of Rheumatic Diseases **64:** 64-69
van Holten J, Reedquist K, Sattonet-Roche P, Smeets T, Plater-Zyberk C, Vervoordeldonk M, Tak P (2004) Treatment with recombinant interferon-beta reduces inflammation and slows cartilage destruction in the collagen-induced arthritis model of rheumatoid arthritis. Arthritis Research and Therapy **6:** R239 - R249
van Kooyk Y, Engering A, Lekkerkerker A, Ludwig I, Geijtenbeek T (2004) Pathogens Use Carbohydrates to Escape Immunity Induced by Dendritic Cells. Current Opinion in Immunology **16:** 488-493
van Kooyk Y, Geijtenbeek T (2003) DC-SIGN: Escpae Mechanism For Pathogens. Nature Reviews Immunology **3:** 697-609

Veckman V, Osterlund P, Fagerlund R, Melen K, Matikainen S, Julkunen I (2006) TNF-alpha and IFN-alpha enhance influenza-A-virus-induced chemokine gene expression in human A549 lung epithelial cells. Virology **345:** 96-104

Villanueva J, Lee S, Giannini E, Graham T, Passo M, Filipovich A, Grom A (2005) Natural Killer cell dysfunction is a distinguishing feature of systemic onset Juvenile Rheumatoid Arthritis and Macrophage Activation Syndrome. Arthritis Research and Therapy **7:** 30-37

Vivier E, Tomasello E, Baratin M, Walzer T, Ugolini S (2008) Functions of natural killer cells. Nature Immunology **9:** 503-510

Vogel S, Fitzgerald K, Fenton M (2003) TLRs: Differential Adapter Utilization by Toll-Like Receptors Mediates TLR-Specific Patterns of Gene Expression. Molecular Interventions **3:** 466-477

Wajant H, Pfizenmaier K, Scheurich P (2003) Tumor necrosis factor signaling. Cell Death & Differentiation **10:** 45-65

Wang L, Chen R, Liu J, Yu H, Kuo H, Yang K (2007) Implications of Dynamic Changes among Tumor Necrosis Factor-alpha (TNF-alpha), Membrane TNF Receptor, and Soluble TNF Receptor Levels in Regard to the Severity of Dengue Infection. The American Journal of Tropical Medicine and Hygiene **77:** 297-302

Ware C (2003) The TNF superfamily. Cytokines and Growth Factor Reviews **14:** 181-184

Way S, Lidbury B, Banyer J (2002) Persistent Ross River virus infection of murine macrophages: an in vitro model for the study of viral relapse and immune modulation during long-term infection. Virology **301:** 281-292

Weaver S, Frey T, Huang H, Kinney R, Rice C, Roehrig J, Shope R, Strauss E (2005) Virus Taxonomy: Classification and Nomenclature of Viruses. *In* C Fauquet, M Mayo, J Maniloff, U Desselberger, L Ball, eds, International Union of Microbiological Societies

Virology Division, Vol Eighth Report of the International Committee on Taxonomy of Viruses. Elsevier Academic Press

Weaver S, Powers A, Brault A, Barrett A (1999) Molecular epidemiological studies of veterinary arboviral encephalitides. Veterinary Journal **157:** 123-138

Weaver S, Salas R, Rico-Hesse R, Ludwig G, Oberste M, Boshell J, Tesh R (1996) Re-emergence of epidemic Venezuelan equine encephalomyelitis in South America. The Lancet **348:** 436-441

Wendling D, Herbein G (2006) TNFa antagonist therapy in patients with joint disease and chronic viral infection. Joint Bone Spine **74:** 407-409

Weston J, Villoing S, Bremont M, Castric J, Pfeffer M, Jewhurst V, McLoughlin M, Rodseth O, Christie KE, Koumans J, Todd D (2002) Comparison of Two Aquatic Alphaviruses, Salmon Pancreas Disease Virus and Sleeping Disease Virus, by Using Genome Sequence Analysis, Monoclonal Reactivity, and Cross-Infection. Journal of Virology **76:** 6155-6163

Weyand CM (2000) New insights into the pathogenesis of rheumatoid arthritis. Rheumatology **39:** 3-8

White D, Fenner F (1994) Medical Virology, Ed 4th Academic Press, c1994, San Diego

WHO (2006) Disease Outbreak News: Chikungunya in India. *In*. http://www.who.int/csr/don/2006_10_17/en/index.html

Wiesenberg I, van der Meide P, Schellekens H, Alkan S (1989) Suppression and augmentation of rat adjuvant arthritis with monoclonal anti-interferon-gamma antibody. Clinical & Experimental Immunology **78:** 245-249

Williams A, Richards P, Thomas E, Carty, Nowell M, Goodfellow R, Dent C, Williams B, Jones S, Topley N (2007) Interferon-gamma protects against the development of structural damage in experimental arthritis by regulating polymorphonuclear neutrophil influx into disease joints. Arthritis & Rheumatism **56:** 2244-2254

Williams M, Woodall J, Gillett J (1965) O'Nyong-Nyong Fever: an epidemic virus disease in East Africa. Virus Isolation from man and serological studies up to July 1961. Transactions of the Royal Society of Tropical Medicine and Hygiene **59:** 186-197

Yoneyama M, Kikuchi M, Natsukawa T, Shinobu N, Imaizumi T, Miyagishi M, Taira K, Akira S, Fujita T (2004) The RNA Helicase RIG-1 Has an essential Function in Double-Stranded RNA-Induced Innate Antiviral Response. Nature Immunology **5:** 730-737

Young D, Didcock L, Goodbourn S, Randall R (2000) Paramyxoviridae Use Distinct Virus-Specific Mechanisms to Circumvent the Interferon Response. Virology **269:** 383-390

Yu S, Aaskov J (1994) Development of a candidate vaccine against Ross River virus infection. Vaccine **12:** 1118-1124

Zare F, Bokarewa M, Nenonen N, Bergstrom T, Alexopoulou L, Flavell R, Tarkowski A (2004) Arthritogenic Properties of Double-Stranded (Viral) RNA. The Journal of Immunology **172:** 5656-5663

Zhang AL, Colmenero P, Purath U, Teixeira de Matos C, Hueber W, Klareskog L, Tarner IH, Engleman EG, Soderstrom K (2007) Natural killer cells trigger differentiation of monocytes into dendritic cells. Blood **110:** 2484-2493

Zhang Y, Xu J, Levin J, Hegen M, Li G, Robertshaw H, Brennan F, Cummons T, Clarke D, Vansell N, Nickerson-Nutter C, Barone D, Mohler K, Black R, Skotnicki J, Gibbons J, Feldmann M, Frost P, Larsen G, Lin L (2004) Identification and characterization of 4-[[4-(2-butynyloxy)phenyl]sulfonyl]-N-hydroxy-2,2-dimethyl-(3S)thiomorpholinecarboxamide (TMI-1), a novel dual tumor necrosis factor-alpha-converting enzyme/matrix metalloprotease inhibitor for the treatment of rheumatoid arthritis. Journal of Pharmacology and Experimental Therapeutics **309:** 348-355

Zhao C, Fernandes M, Turgeon M, Tancrede S, Di Battista J, Poubelle P, Bourgoin S (2008) Specific and overlapping sphingosine-1-phosphate receptor functions in human synoviocytes: impact of TNF-alpha. Journal of Lipid Research**:** M800143-JLR800200

Zoja C, Corna D, Benedetti G, Morigi M, Donadelli R, Guglielmotti A, Pinza M, Bertani T, Remuzzi G (1998) Bindarit retards renal disease and prolongs survival in murine lupus autoimmune disease. Kidney International **53:** 726-734